MECHANISMS OF HEPATOTOXIC INTERACTION OF AMIODARONE WITH INFLAMMATORY STRESS

—A MODEL OF IDIOSYNCRATIC, DRUG-INDUCED LIVER INJURY

By

Jingtao Lu

A DISSERTATION

Submitted to
Michigan State University
In partial fulfillment of the requirements
For the degree of

DOCTOR OF PHILOSOPHY

Biochemistry & Molecular Biology

2012

ABSTRACT

Idiosyncratic, drug-induced liver injury is a type of adverse reaction that occurs in a small fraction of patients during drug therapy. Amiodarone (AMD) is a class III antiarrythmic drug that causes idiosyncratic hepatotoxicity in human patients. The mechanisms of AMD-induced hepatotoxicity are not understood, and inflammatory stress has been proposed to be one of the contributors to idiosyncratic, drug-induced hepatotoxicity. The inflammatory stress hypothesis is supported by the work presented in this thesis demonstrating that cotreatment with AMD and the inflammagen lipopolysaccharide (LPS) results in liver damage in rats.

The importance of several inflammatory factors was explored. AMD enhanced LPS-induced TNF production, coagulation system activation and fibrinolysis impairment. AMD/LPS cotreatment caused activation of neutrophils (PMNs) in the liver. Inhibition of TNF signaling, inhibition of activation of coagulation or inactivation of PMNs attenuated AMD/LPS-induced liver injury in rats, demonstrating the importance of each of these events to toxicity. The activation of PMNs in the liver after AMD/LPS cotreatment was dependent on the activation of coagulation system, suggesting interaction among these inflammatory pathways. TNF potentiated AMD-induced apoptotic cell death of Hepa1c1c7 cells, in which caspase activation and lipid peroxidation played important roles. These studies of the interaction between AMD and inflammatory responses in animals further our understanding of the mechanisms of AMD-induced idiosyncratic hepatotoxicity and provide potential targets for treatment or prevention of such reactions in human patients.

ACKNOWLEDGMENTS

During the first few days after I arrived at MSU as well as the US, I was told by my colleagues and friends that the lab of Dr. Roth and Dr. Ganey is really outstanding. Then I was further impressed by the brilliant work they published and beautiful posters hung on the hallway. So I immediately contacted Bob and Patti and expressed my interest, which turns out to be one of my best decisions for my career.

During more than five years learning and working in the lab, Bob and Patti give me tremendous training and help. As my mentor, Patti always tries her best to understand my not very fluent English plus gestures, teaches me how to make plans of my experiments, trains me how to analyze and understand the results and discuss with me to make the best decisions in each step of my research project. Patti is also very kind and patient to help me improve my writing and presentation skills throughout my graduate life. Bob always impresses me and enlightens me with his deep and thorough understanding of science. Every time I met a difficulty in my project, Bob can always see through the disturbance and reach the hidden problem and suggest a brilliant solution. I also appreciate the fun atmosphere in the lab, including Friday night happy hours, occasional parties at Bob and Patti's house and annual kayaking and camping trips.

I want to thank Dr. Jack Harkema and Dr. Mike Scott in the Department of Pathobiology and Diagnostic Investigation for their help in histological evaluation of my slides; Dr. Daniel Jones in the Department of Biochemistry and Molecular Biology, who trained me to operate the LC/MS/MS and Dr Melinda Frame in the Center for Advanced Microscopy, who helped me to do the confocal microscopy. I also want to thank all my

committee members, Dr. David DeWitt, Dr. Eric Hegg, Dr. John LaPres and Dr. Timothy Zacharewski for all the time and effort they put on my research and all the great advice they gave me during all these years' committee meetings.

I am so grateful that I can work with so many talented and warm-hearted people in our lab. Dr. Xiaomin (Shawn) Deng is the person I closely worked with during my rotation and first few months after I joined the lab. He taught me all kinds of lab techniques, especially in animal studies. Dr. Wei Zou is the person I asked the most questions in the lab. He is always smiling and ready to answer all my questions regarding every aspect of experiments, course works or everyday life. I also want to thank Dr. Jane Maddox, Dr. Jesus Olivero-Verbel, Dr. Sachin Devi, Dr. Rohit Sinhal, Dr. Pat Shaw, Dr. Erica Sparkenbaugh, Dr. Christine Dugan, Aaron Fullerton, Kevin Beggs, Kyle Poulsen, Kazuhisa Miyakawa and Ashley Maiuri, who have been great friends and coworkers. Nicole Crisp and Sandy Newport as research assistants, Allen Macdonald, Emily Evenson and Ryan Albee as undergraduates also helped a lot in my research work.

I am also grateful to the Department of Biochemistry and Molecular Biology, Department of Pharmacology and Toxicology and Center for Integrative Toxicology at MSU, who helped though all my course works, administrative processes, financial aid and travel arrangements. Thank you to College of Natural Science for a Dissertation Completion Fellowship. Many thanks to Society of Toxicology for providing me numerous opportunities to connect with so many excellent scientists and for my experience as a student representative in the Comparative and Veterinary Specialty Section.

Last but not least, I owe my great thanks to my parents and my wife. Although they are on the other side on the earth, they never stopped caring about me and kept encouraging me whenever I feel discouraged or lonely. Without their love, I will not be able to survive the life in a foreign country not to mention go this far as a PhD candidate.

TABLE OF CONTENTS

LIST OF TABLES

LIST OF FIGURES

KEY TO ABBREVIATIONS

A.D.M.E.	absorption distribution metabolism and excretion
ADRs	adverse drug reactions
ALP	alkaline phosphatase
ALT	alanine aminotransferase
AMD	amiodarone
AnnV	annexin V
APC	allophycocyanin
APCs	antigen-presenting cells
ASC	ascorbic acid
AST	aspartate aminotransferase
BID	BH3-interacting domain death agonist
BODIPY	C11-BODIPY581/591
BrdU	bromodeoxyuridine
CAMs	cellular adhesion molecules
CM-H_2DCFDA	5-(and-6-chloromethyl-2',7'-dichlorodihydrofluorescein diacetate acetyl ester
CPZ	chlorpromazine
CS	control serum
CYPs	cytochromes P450
DAA	deaminated amiodarone
DCF	2',7'-dichlorofluorescein
DCLF	diclofenac
DDEA	di-N-desethylamiodarone
DEA	desethylamiodarone
DOX	doxorubicin
ELISA	enzyme-linked immunosorbent assay
Etan	etanercept
ETC	electron transport chain
EU	endotoxin units
FADD	recruiting fas-associated protein with death domain
FDA	Food and Drug Administration
FSC	forward scatter
GGT	gamma-glutamyltransferase
GSH	glutathione
H&E	hematoxylin and eosin
HAL	halothane
HBSS	Hanks' Balanced Salt Solution
hERG	the human ether-a-go-go-related gene

HOCl	hypochlorous acid
HPLC	high performance liquid chromatography
IADRs	idiosyncratic adverse drug reactions
ICAM-1	intercellular adhesion molecule 1
IDILIs	idiosyncratic drug induced liver injuries
INH	isoniazid
IS	internal standard
LDH	lactate dehydrogenase
LPS	lipopolysaccharide
LTA	lipoteichoic acid
MHC	histocompatibility complex
MMP	mitochondrial membrane potential
MPT	mitochondrial permeability transition
MPTP	mitochondrial permeability transition pore
NAC	N-acetyl-L-cysteine
NAS	rabbit anti-rat PMN serum
NF-κB	nuclear factor-kappa B
NIH	National Institutes of Health
NONMEM	later nonlinear mixed-effects modeling
PAI-1	plasminogen activator inhibitor I
PAs	plasminogen activators
PBS	phosphate buffered saline
PGN	peptidoglycan
PI	propidium iodide
PIM	pimonidazole
PMNs	polymorphonuclear neutrophils
polyI:C	polyinosinic-polycytidylic acid
PPAR-	peroxisome proliferator-activated receptor
RAN	ranitidine
RIP1	receptor-interacting protein 1
ROS	reactive oxygen species
SLD	sulindac
SSC	side scatter
STS	staurosporine
TAT	thrombin-antithrombin complexes
TCR	T cell receptor
TdT	terminal deoxynucleotidyl transferase
TF	tissue factor
TLR4	toll-like receptor 4
TNF	tumor necrosis factor-alpha
TNF-R1	TNF receptor-1

TOCO	α-tocopherol
TRADD	TNF-R1-associated death domain protein
TRAF2	TNF receptor-associated factor 2
Trolox	6-hydroxy-2,5,7,8-tetramethylchromane-2-carboxylic acid
TUNEL	terminal deoxynucleotidyl transferase dUTP nick end labeling
TVX	trovafloxacin
ULN	upper limit of normal

CHAPTER 1

General introduction

1.1 Idiosyncratic adverse drug reactions (IADRs)

1.1.1 Overview of IADRs

Adverse drug reactions (ADRs) are one of the leading causes of death in the United States. Based on a meta-analysis of 39 prospective studiesin 1994, around 2,216,000 hospitalized patients developed serious ADRs (Lazarou *et al.* 1998). Among the reported cases, 76,000 to 137,000 were fatal, making ADRs the fourth to sixth leading cause of death in the United States, after heart disease (743,460), cancer (529,904), stroke (150,108), pulmonary disease (101,077), and accidents (90,523) (Lasser *et al.* 2002). During the clinical trial phases of newly developed drug candidates, only relatively small numbers of patients are tested for limited periods of time, and this paradigm doesn't always reveal ADRs that are seen in larger, more diverse populations.

ADRs can be classified into two categories: dose-dependent reactions (type A) and idiosyncratic reactions (type B). Type A reactions are dose-related. They occur in a consistent time frame during the drug therapy and are relatively predictable. A typical example is acetaminophen hepatotoxicity. On the contrary, idiosyncratic ADRs (IADRs) only occur in a small fraction (usually < 5%) of the patients who are treated with clinically "safe" doses. Because they occur at doses that do not cause toxicity in most patients, IADRs are currently unpredictable and hard to diagnose. Serious cases of IADRs are usually not discovered until a drug has been on the market for some time after its approval by the Food and Drug Administration (FDA) (Kaplowitz 2005; Roth *et al.* 2003; Uetrecht 2007). From 1975-1999, 10.2% of the newly approved drugs acquired a black box warning or were withdrawn from the market due to IADRs (Lasser *et al.* 2002).

The liver, which plays an important role in the metabolism of drugs, is a frequent target of IADRs. An example of drug induced hepatotoxicity is trovafloxacin (TVX), a broad-spectrum fluoroquinolone antibiotic, with extended half-life and significant activity against gram-positive pathogens (Melnik *et al.* 1998). From the drug's approval in 1998, severe hepatotoxicity, with the observations of hepatocellular necrosis and eosinophilic infiltration, was reported during TVX therapy. For more than 2 million prescriptions before June 1999, 140 cases of serious hepatic events were reported, including 14 acute liver failure, 6 deaths and 4 liver transplantations. The incidence of TVX-induced severe hepatotoxicity is 1 in 18,000, with no age or gender preference (Andrade and Tulkens 2011; Shaw *et al.* 2010). The liver toxicity was not associated with other fluoroquinolone antibiotics, such as levofloxacin, indicating that it is not a fluoroquinolone class effect. The low incidence and pharmacological action-unrelated toxicity support that TVX-induced hepatotoxicity is a typical IADR.

Some IADRs resulted in permanent disability or death. For example, troglitazone, a peroxisome proliferator-activated receptor (PPAR)-γ agonist, was used to treat type 2 diabetes. Although it was effective in improving insulin resistance, troglitazone was associated with severe idiosyncratic hepatotoxicity: among 1.92 million patients who took troglitazone between 1998 and 2001, 94 cases of liver failure were reported, contributing 10% of the IADRs recorded in those years (Graham *et al.* 2003).

In an animal experiment in cynomolgus monkeys, large doses of troglitazone (50 to 200-fold of the recommended human dose) were administrated by oral gavage for 52 weeks. No cases of liver histology or even elevations of hepatic enzyme activities in serum were observed (Rothwell *et al.* 2002). This observation underscores one of the

problems associated with IADRs: the adverse effects that are seen in people with most drugs that cause IADRs are not seen in experimental animals. Because of the lack of appropriate animal models, mechanisms of IADRs are not well understood, and the prediction of IADRs is especially difficult.

IADRs also lead to great financial loss for pharmaceutical companies. If the therapeutic area for which the drug was developed lacks effective drugs, an IADR-causing drug might be accepted because it is better to treat the majority of patients with no risk rather than to apprehend the drug based on IADRs that occurred in a very small portion of the patient population. This also depends on the balance between the therapeutic value and the severity of IADRs. But in most cases, the IADR-causing drugs have competitors that do not cause IADRs. Even though these competitors are usually not as effective in the therapeutic area, the risk of severe adverse reactions will make the IADR-causing drugs lose their competitive edge in the market, or in many cases these drugs will be suspended by the FDA and withdrawn from the market. The investment to develop such drugs will not be recouped in profit from sales.

1.1.2 Conventional hypothesis for the etiology of idiosyncratic drug induced liver injuries (IDILIs)

The mechanisms of IDILIs are not fully understood. Several hypotheses have been proposed, and extensive studies have been performed to explore them. Hypotheses, supporting evidence and general limitations of these conventional ideas are discussed below.

Metabolic polymorphism hypothesis

A large proportion of drugs involved in idiosyncratic hepatotoxicity are capable of forming reactive metabolites. As reviewed by Jennie L. Walgren, 62% (13 out of 21 selected drugs in the article) of the IDILI-inducing drugs have evidence of reactive metabolite formation (Walgren *et al.* 2005). The cytochrome P450s (CYPs) are a superfamily of enzymes that are primarily responsible for the metabolism of many drugs as well as other xenobiotic substances. Expression of CYPs can be affected by a variety of endogenous and exogenous factors, such as genetic variation, hormone levels, diet, inflammatory episodes and drug exposures (Pilgrim *et al.* 2011). Variable expression or activities of CYPs can be one of the contributors to IDILIs, because the formation of reactive metabolites varies among patients.

A good example for this metabolic polymorphism hypothesis is the anti-tuberculosis drug, isoniazid (INH). Acetylhydrazine and hydrazine, the major metabolites of INH, are thought to be responsible for the INH-induced liver injury (Metushi *et al.* 2011). The formation of these two metabolites following administration of INH was dependent on the activity of N-acetyltransferase as well as the activities of CYP subfamilies. Epidemiological studies have shown that the risk of INH-induced hepatotoxicity was related to several factors that can affect INH metabolism: N-acetyltransferase activity, rifamicin (CYPs inducer) administration, alcohol (CYPs inducer) consumption, CYP2E1 allele genotype (Ohno *et al.* 2000).

However, there are examples of drugs that form reactive metabolites but do not cause any apparent hepatotoxicity (e.g., ethinylestradiol and raloxifene). Many events need to occur in an individual prior to the onset of an IDILI, of which the metabolism polymorphism may only act as one of the contributors.

Hapten hypothesis

It has been shown 77 years ago that small molecules do not induce immune response unless they are covalently bound to proteins (Landsteiner and Jacobs 1935). In the hapten hypothesis, drugs (or more likely their reactive metabolites) covalently bind to proteins, and these protein adducts can be recognized by the immune system and trigger an immune response, which ultimately leads to liver damage. This hypothesis could explain the apparent lack of relation to dose for IDILIs and agrees with the observations that some IDILIs were detected after a period of time which is long enough to develop antibodies. The existence of antibodies to drug-protein moieties is found in both human patients and experimental rodents, but none of these antibodies are proved to be pathogenic to the liver. Although there is evidence that the antibody for d-penicillamine induces autoimmunity in rats, mice and monkeys (Shenton *et al.* 2004), liver injury is not observed in these animal models. In the case of halothane, it is clear that halothane is metabolized to reactive metabolites that can covalently bind to liver proteins, and antibodies are generated against these modified proteins. But many of the patients with antibodies in their blood did not develop IDILI, arguing against the liver-pathogenicity of these antibodies (Njoku *et al.* 2002). Moreover, IDILIs are observed in patients shortly after the first exposure to drugs (Clay *et al.* 2006). In these cases, an adaptive immune response that requires secondary exposure cannot be responsible for the liver damage.

Danger hypothesis

Generally, drugs or their reactive metabolite-modified proteins do not induce a significant immune response in the absence of stimulated antigen-presenting cells

(APCs). In addition to the interaction of T cell receptor (TCR) and major histocompatibility complex (MHC), the activation of T cells requires a co-stimulation signal: the binding of B7 on APCs and CD28 on T cells (Greenfield *et al.* 1998). Without this co-stimulation, the response is immune tolerance. In the danger hypothesis of IDILI, drug-stressed cells will release danger signals to stimulate APCs, and activated APCs with up-regulated co-stimulatory molecules will activate T cells to induce a significant immune response. It is unknown what these danger signals are, but they are probably dependent on the types of drugs, types of stresses and types of affected cells. For example, compared to non-infected patients, patients with infectious mononucleosis have greater risk of ampicillin-induced rashes, and HIV positive patients are more vulnerable to sulfamethoxazole/trimethoprim-induced adverse events (Fischl *et al.* 1988; Pullen *et al.* 1967). However, there is a lack of evidence in these two studies that the adverse reactions are because of adaptive immune responses. Also, animal experiments support that mild activation of the innate immune system (e.g. inflammation) can enhance the sensitivity of livers to xenobiotics induced damage without causing adaptive immune responses (Roth *et al.* 2003).

1.1.3 Inflammatory stress hypothesis for IDILI

Inflammation is a complex biological response to a variety of harmful stimuli, such as infections, tissue damage and irritants. Inflammation can be considered as local or systemic stresses originated from a combination of inflammatory cells and the mediators they produce. Inflammation participates in the pathogenesis of many diseases, such as cancers (De Marzo *et al.* 2007), cardiovascular diseases (Willerson and Ridker 2004) and diabetes (Das and Mukhopadhyay 2011) to name a few. Mild

inflammatory episodes occur commonly in people and might be unnoticeable under many circumstances. In particular, endotoxin generated by bacteria in the GI tract can translocate across the intestinal mucosa into the portal vein and induce a mild inflammation in the liver. The rate and magnitude of translocation is affected by many factors, including GI disturbance, alcohol consumption, diet alteration, surgery, etc. (Gardiner *et al.* 1995; Lepper *et al.* 2002; Roth *et al.* 1997).

Evidence from experimental animals indicates that mild inflammation can increase the sensitivity of individuals to hepatotoxic agents. In a rat study of aflatoxin B1, a naturally occurring mycotoxin known to cause liver injury in human and animals, cotreatment with a nontoxic but inflammatory dose of lipopolysaccharide (LPS), a cell wall component of gram-negative bacteria, decreased the threshold hepatotoxic dose of aflatoxin B1 by more than 10 fold (Luyendyk *et al.* 2002). These observations led to a hypothesis that an episode of modest inflammation could decrease the threshold for toxicity and thereby render an individual susceptible to an adverse drug reaction that would not otherwise occur (Roth *et al.* 2003). Minor or local abnormality of the liver caused by some drugs can be exaggerated into more serious and expanded injuries by inflammatory mediators.

lipopolysaccharide (LPS) and IDILI

LPS, the principal biologically active component of endotoxin, is widely used as an inflammagen in animal studies. It binds to the toll-like receptor 4 (TLR4) complex, activates inflammatory cells and leads to the release of proinflammatory mediators such as cytokines, lipid metabolites, reactive oxygen species, toxic proteases, etc. These mediators, along with the activated inflammatory cells, can cause liver damage by

themselves during severe inflammation. In the case of modest inflammation, they can disturb tissue homeostasis and lead to increased susceptibility of individuals to toxicant-induced tissue damage. It has been proved that LPS can increase rodents' sensitivity to several drugs that are known to cause IADRs in humans: a non-hepatotoxic dose of LPS can interact with chlorpromazine (CPZ, an antipsychotic drug), ranitidine (RAN, a H_2-receptor antagonist), diclofenac (DCLF, an anti-inflammatory drug), trovafloxacin (TVX, an antibiotic), sulindac (SLD, an anti-inflammatory drug), halothane (HAL, an inhaled anesthetic) or doxorubicin (DOX, an anti-cancer drug) to induce liver damage, in which the drug doses alone are non-hepatotoxic (Buchweitz *et al.* 2002; Deng *et al.* 2006; Dugan *et al.* 2010; Hassan *et al.* 2008; Luyendyk *et al.* 2003; Waring *et al.* 2006; Zou *et al.* 2009b). The details of these models are summarized in Table 1.1. Levofloxacin and famotidine are in the the same pharmacological class with TVX and RAN, but do not induce IDILIs in human patients.Concurrent inflammation failed to interact with levofloxacin or famotidine to induce liver injury in rodents. Inflammation can participate in IDILIs by a variety of different mechanisms. In the following sections of this chapter, the importance of various factors in an inflammatory response, e.g. cytokines, innate immune cell types, hemostatic system, mitochondrial damage and reactive oxygen species, will be introduced.

Table 1-1 LPS/drug cotreatment induces idiosyncratic-like liver injury in rodents

Drug	Indication	Causes IADRs in humans	Hepatotoxic to rodents when given with LPS
Sulindac	anti-inflammatory	Yes	Yes, in rats
Diclofenac	anti-inflammatory	Yes	Yes, in rats
Trovafloxacin	antibiotic	Yes	Yes, in rats and mice
Levofloxacin	antibiotic	No	No
Ranitidine	H_2-receptor antagonist	Yes	Yes, in rats
Famotidine	H_2-receptor antagonist	No	No
Chlorpromazine	antipsychotic	Yes	Yes, in rats
Halothane	anaesthetic	Yes	Yes, in mice
Doxorubicin	anti-cancer	Yes	Yes, in mice

(For interpretation of the references to color in this and all other figures, the reader is referred to the electronic version of this dissertation.)

1.2 Inflammation, a contributor to tissue injury

Inflammation is traditionally considered as local reactions causing redness, swelling, pain and heat. The modern view of inflammation involves not only innate immune cells (e.g. macrophages, natural killer cells and neutrophils), the mediators they produce (cytokines/chemokines, eicosanoids, ROS and proteases), but also the hemostatic and complement systems, endothelial and parenchymal cells, and altered gene expression and cell signaling events in an organism (Ganey *et al.* 2004).

Inflammation evolved as a self defense mechanism against harmful stimuli, e.g. microbial infections, but it also has the potential to be a contributor to tissue damage. For example, the inflammatory response to large amounts of LPS, e.g. during a gram-negative bacteria-induced sepsis, can damage liver and other organs, leading to multiple organ failure or even death (Hewett and Roth 1993). Neutrophils and macrophages are major cell types responding to LPS in the innate immune system. Other cell types in the liver, such as sinusoidal endothelial cells, stellate cells and bile duct epithelial cells, can also recognize LPS and contribute to the inflammatory response (Mencin *et al.* 2009). TLR4, a pattern recognition receptor, is the sensor for LPS on the surface of these cells and initiates an intracellular signaling network. The TLR4 pathway is a well studied pathway, and details and summary of this pathway are reviewed elsewhere (Akira and Takeda 2004). The following sections discuss the roles of some inflammatory factors result from TLR4 activation in the pathogenesis of some liver diseases and LPS/drug-induced liver injury in animal models.

1.2.1 TNF, an important cytokine in LPS/drug-induced liver injury

Tumor necrosis factor-alpha (TNF) production is known to be one of the earliest events in hepatic inflammation, triggering the expression of other cytokines, infiltration and activation of inflammatory cells, impairment of the hemostatic system and apoptosis and necrosis of hepatocytes.

TNF exerts its biological effects by binding to two plasma membrane receptors, TNF-R1 and TNF-R2. The majority of the biological effects of soluble TNF are mediated by TNF-R1. Upon activation, TNF-R1 recruits TNF-R1-associated death domain protein (TRADD), TNF receptor-associated factor 2 (TRAF2) and receptor-interacting protein 1 (RIP)1 to form complex I, which leads to the activation of transcription factor nuclear factor-kappa B (NF-κB) as well as kinase cascades, including p38 and JNK. Once complex I is released from the receptor, complex II is formed by recruiting fas-associated protein with death domain (FADD) and procaspase 8, which activates the apoptotic cascades. In hepatocytes, activated caspase 8 can cleave BH3-interacting domain death agonist (BID) into its truncated and active form, tBID, which in turn leads to release of cytochrome *c* and other proapoptotic mediators from mitochondria. This eventually results in activation of effector caspases that mediate apoptosis. Mitochondrial permeability transition (MPT) and generation of reactive oxygen species (ROS) are also involved in TNF-induced hepatocyte apoptosis (Wullaert *et al.* 2007).

TNF signaling is involved in the pathogenesis of various inflammatory liver diseases, such as acute and chronic hepatitis B and C virus infection, alcoholic hepatitis and etc. (Wullaert *et al.* 2007). An increased and prolonged serum TNF peak is found in mice treated with LPS and TVX (Figure 1-1A), and neutralization of TNF signaling by

etanercept (Etan) leads to a significant attenuation in serum alanine aminotransferase (ALT) activity, indicating attenuated liver injury (Figure 1-1B). The prolongation of LPS-induced TNF by TVX is important because when Etan was injected at the peak time of serum TNF to eliminate the prolongation, same level of protection was achieved comparing to when the whole TNF peak was neutralized by earlier Etan administration (Shaw *et al.* 2007). TNF is also involved in the LPS/RAN (Tukov *et al.* 2007) and LPS/SLD (Zou *et al.* 2009a) models, which makes it possibly a common mechanism shared among the LPS/drug-induced liver injury models.

Figure 1-1 Role of TNF in TVX/LPS model

Male C57/BL6 mice were treated with 150 mg/kg TVX (p.o.) and 3h later with 2×10^6 EU/kg LPS (iv). A, TVX significantly potentiated LPS-induced TNF increase in plasma. B, inhibition of TNF signaling by etanercept (ETAN) significantly reduced TVX/LPS-induced ALT increase in plasma (Shaw *et al.* 2007).

Figure 1-1 (cont'd)

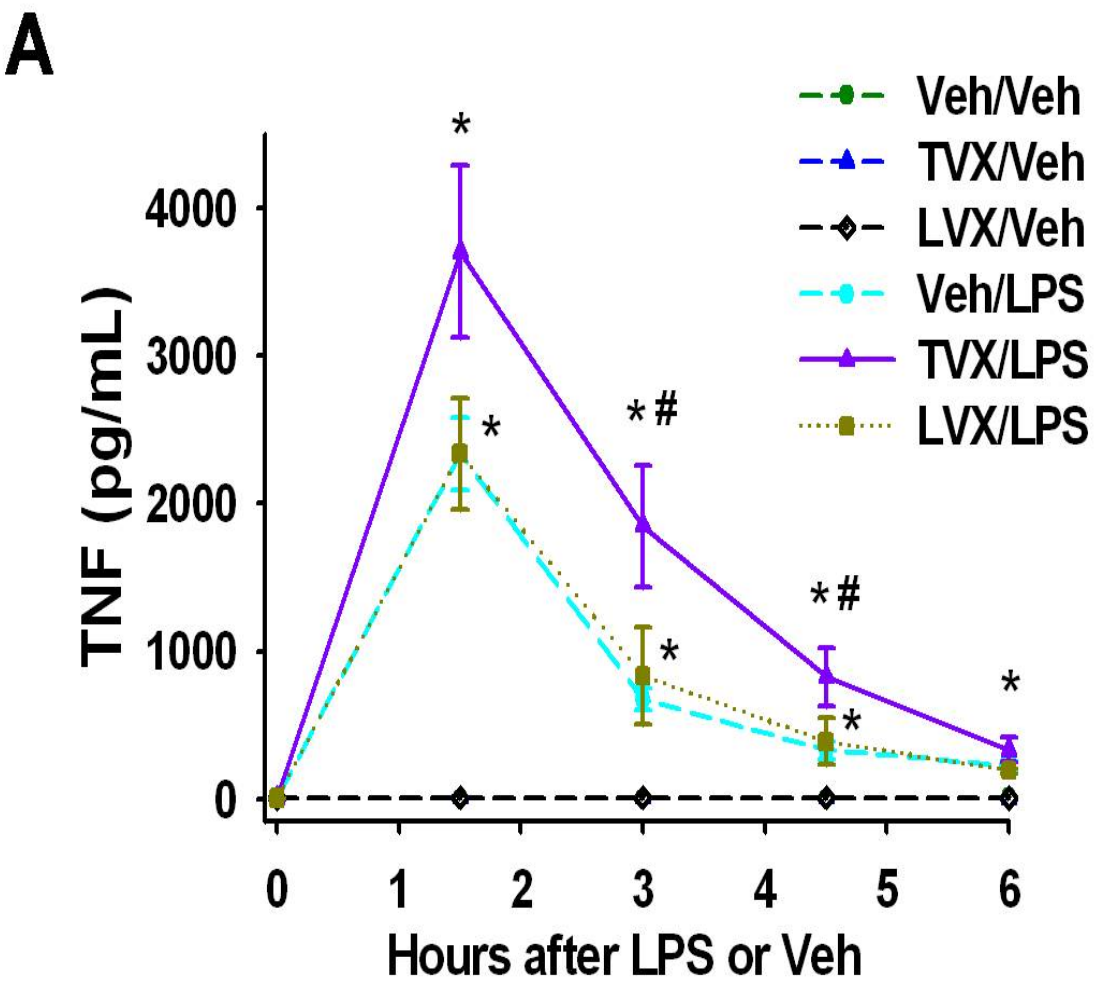

Figure 1-1 (cont'd)

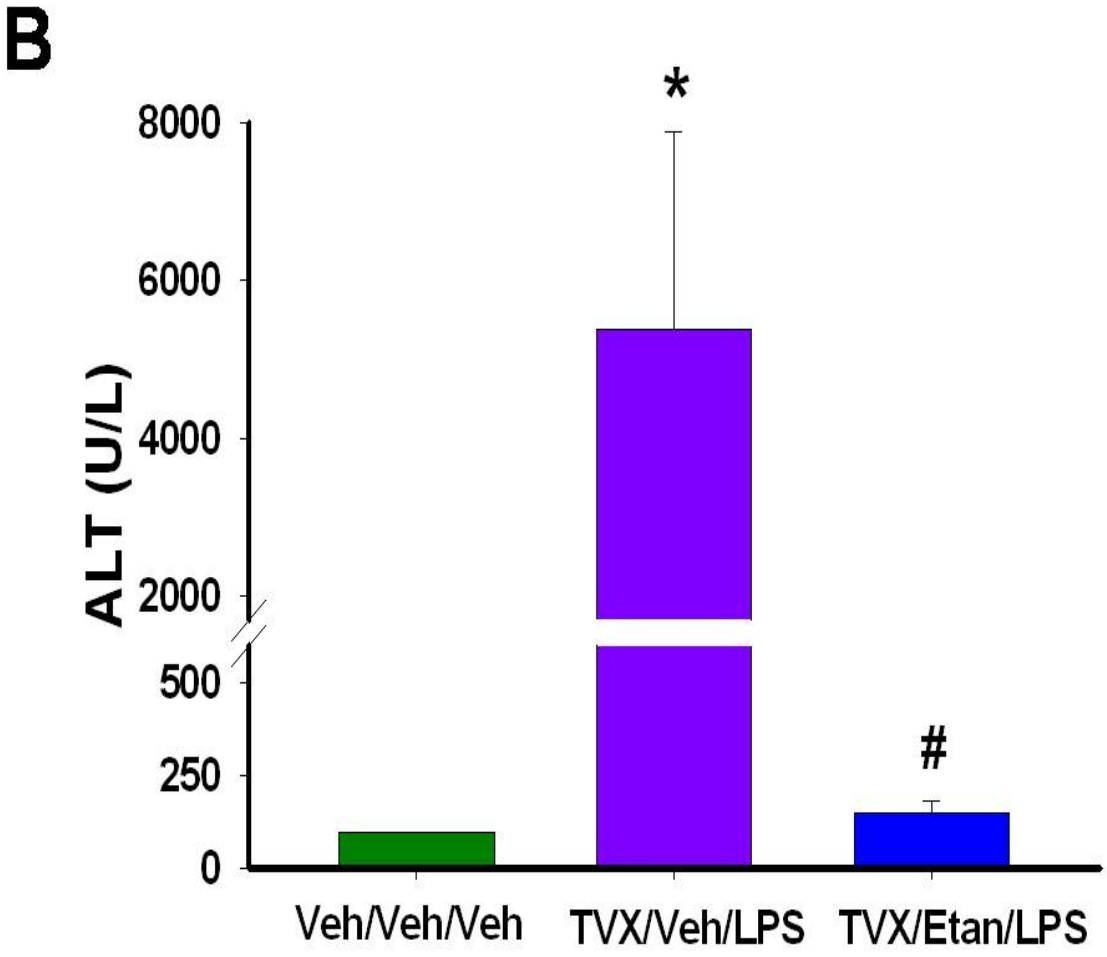

1.2.2 The hemostatic system and hypoxia

Vascular hemostasis is controlled by both coagulation and fibrinolytic systems. Coagulation can be activated through the extrinsic pathway or the intrinsic pathway. In the extrinsic pathway, tissue factor (TF) is activated and exposed to blood and activates factor VII. The activated TF-VII complex then leads to factor X activation, which cleaves prothrombin into thrombin. Thrombin converts fibrinogen into fibrin monomers, which then form fibrin clots in blood vessels when the fibrin becomes cross-linked. The activity of thrombin is controlled in part by antithrombin, which forms thrombin-antithrombin complexes (TAT) and inactivates thrombin. Fibrin clots are degraded by the fibrinolytic system, in which plasmin plays a pivotal role. The activation of plasmin is mediated by plasminogen activators (PAs). The activity of PAs is inhibited by plasminogen activator inhibitor I (PAI-1), an important negative regulator of the fibrinolytic system. An increase in active PAI-1 concentration dampens fibrinolysis and enhances fibrin deposition (Levi *et al.* 2003).

It is well known that inflammation can lead to activation of the hemostatic system. Cytokines produced by monocytes and vascular endothelial cells, such as TNF, can lead to tissue factor-mediated thrombin generation and PAI-1-induced impairment of fibrinolysis (Levi *et al.* 2003). Studies on LPS/RAN-induced liver injury in rats show that RAN coexposure significantly enhanced LPS-induced coagulation activation and fibrinolysis impairment, leading to higher degree of fibrin deposition in the liver. Inhibition of coagulation by heparin significantly reduced the activation of coagulation and led to attenuated liver damage (Luyendyk *et al.* 2004). Similar results were also

found in LPS/TVX and LPS/SLD models (Shaw *et al.* 2009b; Zou *et al.* 2009b), which raises the possibly that a common mechanism is shared among the LPS/drug models.

Intravascular fibrin deposition can impair blood flow and lead to tissue hypoxia. Hypoxia can lead to inhibition of aerobic metabolism, energy deficit (loss of ATP) and generation of ROS from mitochondria. As a consequence of these effects, physiological function of the liver is impaired, and damage occurs (Semenza 2004). Besides, hypoxia is also reported to cause generation of ROS in hep3b cells (Chandel *et al.* 1998). Hypoxia is involved in the progression of many liver diseases, such as hepatitis (Fuhrmann *et al.* 2010), cirrhosis (Corpechot *et al.* 2002) and chemical-induced liver injury (Sparkenbaugh *et al.* 2011), and also may be an important contributor in LPS/RAN- (Luyendyk *et al.* 2004), LPS/TVX- (Shaw *et al.* 2009b) and LPS/SLD-induced liver injury (Zou *et al.* 2009b).

1.2.3 Polymorphonuclear neutrophils (PMNs)

PMNs are the most abundant type of leukocytes in the human body and form an essential part of the innate immune system. The main function of PMNs is, once recruited to the site of inflammation, to eliminate invading microorganisms and remove dead or dying cells. In an extensive inflammatory response in the liver, the cytotoxic mediators released by activated PMNs can also lead to additional tissue damage, making PMNs a contributor to the pathogenesis of many acute inflammatory diseases in the liver, e.g. endotoxemia (Hewett *et al.* 1992), alchoholic hepatitis (Bautista 1997), concanavalin A-induced liver injury (Bonder *et al.* 2004) and ischemia-reperfusion injury (Jaeschke *et al.* 1990).

Three steps are required for PMN-mediated hepatotoxicity. First, in response to inflammatory mediators, such as TNF α, IL-1α/β, CXC chemokines, PAF or activated complement factors, PMNs accumulate in the liver microvasculature, specifically in sinusoids and postsinusoidal venules. These mediators lead to up-regulation of cellular adhesion molecules (CAMs) on the surface of PMNs and sinusoidal endothelial cells. PMNs accumulated in the liver vasculature do not cause tissue damage without transmigration into parenchymal tissue (Chosay *et al.* 1997). Accordingly, the second step is transmigration, which requires a chemotactic signal and the interaction of CAMs. The chemotactic signals can be released by necrotic hepatocytes, such as HMGB-1 and lipid peroxidation products (Curzio *et al.* 1986; Scaffidi *et al.* 2002), and they can also be released by PMNs already in the parenchyma. The firm adhesion and transmigration process involves interaction of β-integrins on PMNs and Intercellular adhesion molecule 1 (ICAM-1) or vascular cell adhesion molecule-1 (VCAM-1) on sinusoidal endothelial cells (Gujral *et al.* 2004). The third step necessary for PMN-mediated liver damage is activation of the PMNs after direct contact with target cells, in which degranulation of PMNs results in release of cytotoxic proteases and activation of NADPH oxidase to produce ROS.

PMNs are involved in animal models of LPS-potentiated hepatotoxicity, such as aflatoxin B1 (Barton *et al.* 2000), monocrotaline (Yee *et al.* 2003), TVX (Shaw *et al.* 2009d), RAN (Luyendyk *et al.* 2005) and SLD (Zou *et al.* 2011). Take the LPS/RAN model as an example. The facts that PMNs accumulated in the livers in response to LPS, and that LPS alone did not induce liver injury, suggest that the PMNs were not extravasated and activated after LPS exposure. On the other hand, markers for PMN

activation were detected in livers of rats cotreated with LPS and RAN (Luyendyk *et al.* 2005). Deng *et al* proved that RAN acted indirectly to effect PMN activation through the up-regulation of LPS-induced PMN chemokines, e.g. PAI-1 (Deng *et al.* 2007).

1.2.4 Mitochondrial damage and reactive oxygen species

ROS, such as superoxide, hydrogen peroxide and hydroxyl radical, are reactive molecules derived from partial reduction of diatomic oxygen. The electron transport chain (ETC) in the inner membrane of mitochondria, which is responsible for energy production from oxidative phosphorylation, is an important source of intracellular ROS. Complexes I and III are the major sites of electron leakage from the ETC. One by one reduction of molecular oxygen from escaped electrons can happen at a low rate under normal conditions and lead to generation of ROS. Cells have both enzymatic (SOD and catalase) and nonenzymatic (GSH, vitamin C and E, thioredoxin) antioxidant systems to eliminate ROS. Excessive accumulation of ROS can cause massive cellular damage, including lipid peroxidation, DNA damage and protein modification, which can lead to membrane disruption, mutagenesis and enzyme malfunction, respectively. ROS can also act as a regulator of cell signaling pathways. A number of signaling kinases such as JNK, p38, PI-3K, transcription factors including NF-κB, AP-1, HIF-1α, p53, and apoptotic effectors such as caspases, Bcl-2, and cytochrome *c* are under the regulation of ROS in certain conditions (Trachootham *et al.* 2008).

It is widely accepted that mitochondrial dysfunction significantly contributes to tissue damage and even organ failure. Ultrastructural changes of mitochodria, such as elongation, swelling, condensation and lack of cristae, were found in the livers of patients with septic shock (Vanhorebeek *et al.* 2005), nonalcoholic steatohepatitis

(Begriche *et al.* 2006), or viral hepatitis (Piccoli *et al.* 2009). Many studies have proved that cytokines/chemokines, lack of oxygen (hypoxia) and oxidative stress that occur during inflammatory responses can cause damage to mitochondrial lipids, proteins and DNA. For example, TNF is reported to affect complex I and III of the ETC, leading to increased ROS generation (Gudz *et al.* 1997; Higuchi *et al.* 1998). In hepatocytes, BID, which is truncated and activated in response to TNF signaling, can disrupt the integrity of the outer mitochondrial membrane and lead to MPT. As a result, the ETC on the inner membrane of mitochondria will be affected and generate excessive amounts of ROS (Wullaert *et al.* 2007). The ETC itself is also vulnerable to oxidative stress, so there is clearly a self-amplifying cycle of ROS generation and mitochondrial damage.

Mitochondrial damage and ROS generation were also involved in some models of drug-induced hepatotoxicity. Many drugs that are implicated in IDILIs can impair mitochondrial function and/or induce MPT in hepatocytes (Boelsterli and Lim 2007). For example, tolcapone, trogalitazone and the majority of non-steroidal anti-inflammatory drugs can induce uncoupling of oxidative phosphorylation (Haasio *et al.* 2002; Konrad *et al.* 2005); leflunomide and perhexiline inhibit complex I/III on the ETC (Deschamps *et al.* 1994; Khutornenko *et al.* 2010); nucleoside analog reverse transcriptase inhibitors can lead to inhibition of DNA polymerase-γ, resulting in depletion of mitochondrial DNA (Carr 2003; Feng *et al.* 2001).

1.3 Amiodarone, an antiarrhythmic drug known to cause IADRs

Amiodarone (AMD) [2-butyl-3-(3', 5'-diiodo-4'α-diethylaminoethoxybenzoyl)-benzofuran] (Figure 1-2), is a class III antiarrhythmic drug that blocks the human ether-a-go-go-related gene (hERG) channel, resulting in prolonged QT interval and refractory

period. AMD is highly effective in increasing the survival of patients after myocardial infarction or congestive heart failure (Doval *et al.* 1994; Singh 1996). In clinical practice, AMD reduces the atrial fibrillation in patients with impaired ventricular function and is a favored drug when the maintenance of sinus rhythm is needed (Gill *et al.* 1992).

Figure 1-2 Amiodarone

2-butyl-3-(3', 5'-diiodo-4'α-diethylaminoethoxybenzoyl)-benzofuran

Figure 1-2 (cont'd)

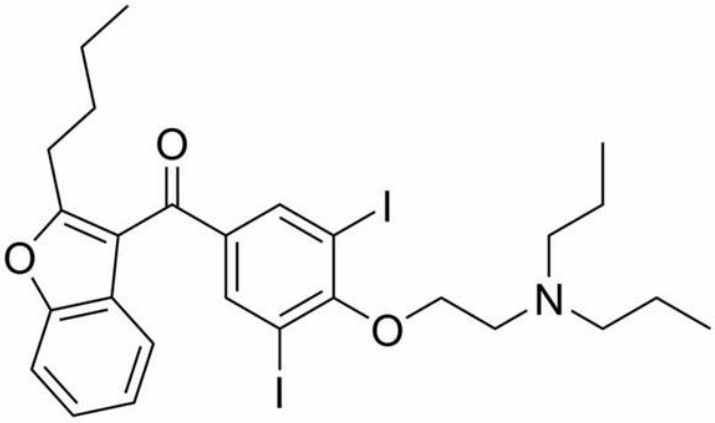

1.3.1 Absorption, distribution, metabolism, and excretion (A.D.M.E.) of amiodarone

AMD was developed in 1961 in Belgium and was approved by the FDA for the treatment of arrhythmias in 1985 in the US. It is composed of a highly lipophilic core (a benzofuran ring complexed to a diiodobenzene ring) and a hydrophilic side chain attached to the diiodobenzene ring (Figure 1-2). After oral administration, AMD is absorbed slowly with a highly variable bioavailability (65%±22%). Differential first-pass metabolism at the intestinal mucosa and liver might be responsible for this variability (Pourbaix *et al.* 1985). Maximum serum concentration was achieved 3h to 7h after a single oral administration (Pollak *et al.* 2000).

Distinct polarities of the two extremities in the chemical structure enable AMD to obtain amphiphilic characteristics and interact with both the lipid bilayers and the aqueous matrix of cells and their organelles. The strong lipophilic core makes AMD accumulate in tissues with high adipose content. In a two-year pharmacokinetic study of oral AMD therapy in 77 patients, the volume of distribution in the peripheral compartment (12,700 L) was much larger than that in the central compartment (882 L); and the elimination half life (55 day) was much longer than the intercompartmental distribution half life (17h). This means that AMD moves from serum to peripheral tissue 78 times faster than it is cleared from the body (Pollak *et al.* 2000). As a result, at the early stage of AMD therapy, in order to maintain effective concentrations in the blood, a large portion of the daily input was required to fill the pool of the peripheral tissue. After the dosing was stopped, the decrease of AMD concentration in the blood was compensated because AMD would return into the blood from peripheral tissue.

The metabolism of AMD is mainly performed in the liver, and N-deethylation is the most important pathway (Figure 1-3). Desethylamiodarone (DEA), the deethylation product, is the primary metabolite. DEA can reach a level comparable to AMD during the maintenance of oral AMD therapy, and it shares similar pharmacological properties with AMD: antiarrhythmic effects, high volume of distribution and long half life (Shayeganpour *et al.* 2008; Talajic *et al.* 1987). DEA may be further hydroxylated to 3'OH-DEA, dealkylated into di-N-desethylamiodarone (DDEA), or deaminated into deaminated amiodarone (DAA) (Ha *et al.* 2001). However, the serum concentrations of 3'OH-DEA, DDEA and DAA are much smaller than those of DEA or AMD (around 1/40-1/10) (Ha *et al.* 2005), and the biological significance of these minor metabolites is not clear. The deethylation of AMD in human liver is mainly catalyzed by CYP3A4 and CYP2C8; the importance of the two enzymes in this process is still under debate. CYP2C8 has a lower K_m towards AMD, while CYP3A4 is much more abundant in human liver (Ohyama *et al.* 2000; Trivier *et al.* 1993). AMD and its metabolites are eliminated though biliary excretion, with less than 1% being cleared by the kidney (Harris *et al.* 1983).

Figure 1-3 N-deethylation of AMD

Figure 1-3 (cont'd)

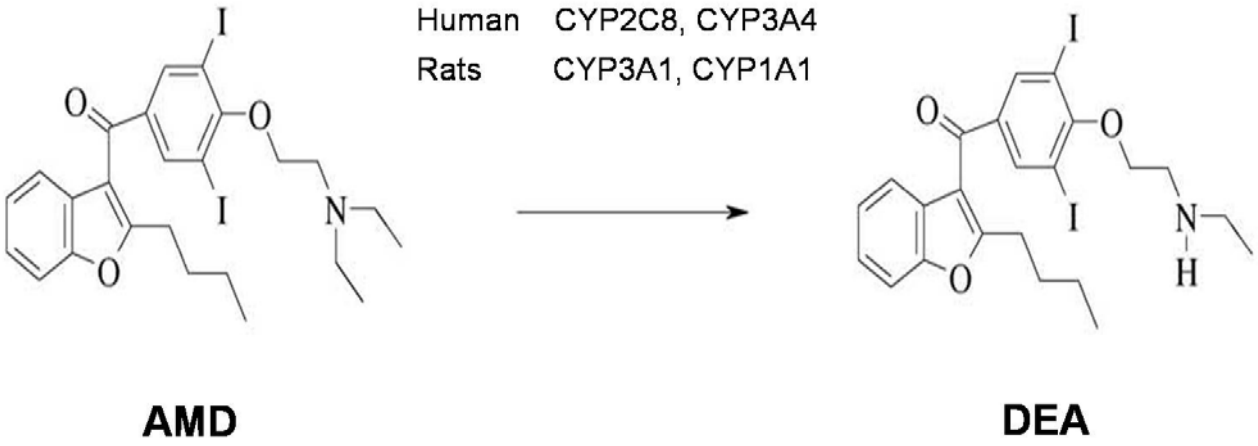

1.3.2 Idiosyncratic hepatotoxicity induced by amiodarone

The use of AMD has been associated with a variety of adverse effects, including liver dysfunction, pulmonary complications, thyroid dysfunctions and ocular disturbance (Rotmensch *et al.* 1984). Frequency of hepatic abnormalities in patients receiving long-term oral AMD ranges widely from 14% to 82%, mostly because the definitions of hepatic abnormalities are different in these studies. The FDA defines hepatic toxicity as serum transaminase activities greater than 3-fold of the upper limit of normal (ULN), whereas in many of the epidemiological studies, 2xULN was used as a criterion, resulting in a greater estimated risk (Babatin *et al.* 2008). It is clear that a spectrum of transaminase elevations was associated with AMD exposure.

Hepatic injuries have been reported as early as several days after initiating AMD oral administration (Benbassat and Shahar 1991). Some were reported with more than ten months latency, and some were reported even several months after the withdrawal of AMD therapy (Chang *et al.* 1999). In many of the cases, patients were asymptomatic except for mildly elevated hepatic enzymes in the serum, which went back to normal as the AMD therapy continued. Attempts to correlate duration of AMD therapy or the cumulative dose with the incidence of hepatotoxicity were unsuccessful (Lewis *et al.* 1989). But given the fact that AMD has wide variations in absorption, volume of distribution and elimination half-life, it may not be reasonable to draw a direct relationship between these parameters and toxicity. Later nonlinear mixed-effects modeling (NONMEM) by Pollak and Shafer showed that steady-state serum concentrations of AMD are better related to the risk of hepatotoxicity. The predicted serum ALT activities by the model showed an identical linear relationship with the ALT

activities measured in patients. The model predicted a 6% risk of having serum ALT over 3xULN with a 2.5 mg/L steady state serum concentration of AMD (Pollak and Shafer 2004). Clinically apparent symptomatic liver reactions, with serum transaminase more than 3-fold of ULN, are reported with a frequency of 1-3%.

Cases of liver reactions after intravenous administration of AMD are rare, but the damage can be acute and severe: serum activities of transaminases are elevated to 10-100 fold of ULN. In 68% of the reported cases of intravenous AMD-induced hepatotoxicity, liver injury occurred within 24 hours after the start of AMD loading. Centrilobular, bridging or panacinar necrosis was the major histological finding in these cases. In 20% of the cases, patients recovered from liver injury after stopping the intravenous loading of AMD, and later rechallenge with oral AMD did not cause any hepatotoxicity. Fatalities caused by fulminant hepatic failure are reported from both long-term oral and acute intravenous administration (Babatin *et al.* 2008; Lewis *et al.* 1989; Ratz Bravo *et al.* 2005).

The mechanism of AMD-induced idiosyncratic hepatotoxicity is still not clear. One hypothesis is that the intravenous AMD-induced toxicity is caused by the loading vehicle, polysorbate 80, because the intravenous AMD formulation is 50 mg/ml in 10% w/v (100 mg/ml) polysorbate 80, corresponding to 2 mg polysorbate 80 per 1 mg AMD. This hypothesis is supported by the E-Ferol syndrome in newborn infants (Balistreri *et al.* 1986), in which the intravenous loaded vitamin E is also solubilized in polysorbate 80. However, neither the case studies in the premature human infants (Lorch *et al.* 1985) nor the animal studies in new born rabbits (Rivera, Jr. *et al.* 1990) show conclusive evidence that polysorbate 80 is responsible for the toxicity. Also, the fact that AMD-

induced IDILI occurs after oral administration argues against the vehicle being the sole cause.

One effort to establish a model for AMD-induced liver injury in healthy rodents was unsuccessful. Neither short-term, large dose nor long-term, small dose of AMD led to observable changes in hepatic histology or serum enzyme chemistry (Young and Mehendale 1989). Indeed, young and healthy rodent is not a good animal model to mimic human patients who receive AMD therapy. Because arrhythmia happens more frequently in aged people, the mean age of AMD recipient is 62 for men and 69 for women (Pollak *et al.* 2000). Mild inflammation might be caused by co-existing rhythm disorders in a large portion of these patients and be a potential contributor to AMD-induced IDILI.

1.4 Hypothesis and specific aims

The purpose of this study was to **test the hypothesis that inflammatory stress induced by LPS potentiates amiodarone-induced hepatotoxicity in rats**. When the results demonstrated this interaction between inflammatory stress and amiodarone, the roles of possible contributors to AMD/LPS-induced liver injury, TNF signaling, coagulation system activation, PMN activation, caspase activation and lipid peroxidation, were explored.

Aim 1 Hypothesis

Cotreatment with nonhepatotoxic doses of AMD and LPS induces IDILI-like liver injury in rats. (CHAPTER 2)

Aim 2 Hypothesis

TNF is induced by AMD/LPS cotreatment and plays an important role in AMD/LPS-induced liver injury in rats. (CHAPTER 2)

Aim 3 Hypothesis

TNF potentiates the cytotoxicity of AMD through enhanced caspase activation and lipid peroxidation. (CHAPTER 3)

Aim 4 Hypothesis

Hemostatic system impairment and PMN activation are induced by AMD/LPS cotreatment and play important roles in AMD/LPS-induced liver injury in rats. (CHAPTER 4)

CHAPTER 2

Amiodarone exposure during modest inflammation induces idiosyncrasy-like liver injury in rats: role of tumor necrosis factor-alpha

Jingtao Lu, A. Daniel Jones, Jack R. Harkema, Robert A. Roth and Patricia E. Ganey

2.1 Abstract

Amiodarone (AMD), a class III antiarrhythmic drug, is known to cause idiosyncratic, hepatotoxic reactions in human patients. One hypothesis for the etiology of idiosyncratic adverse drug reactions (IADRs) is that a concurrent inflammatory stress results in decreased threshold for drug toxicity. To explore this hypothesis in an animal model, male, Sprague-Dawley rats were treated with nonhepatotoxic doses of AMD or its vehicle and with saline vehicle or lipopolysaccharide (LPS) to induce low-level inflammation. Elevated alanine aminotransferase (ALT), aspartate aminotransferase (AST), alkaline phosphatase (ALP), and gamma-glutamyltransferase (GGT) activities, as well as increased total bile acid concentrations in serum and midzonal hepatocellular necrosis were observed only in AMD/LPS-cotreated rats. The time interval between AMD and LPS administration was critical: AMD injected 16h before LPS led to liver injury, whereas AMD injected 2h to 12h before LPS failed to cause this response. The increase in ALT activity in AMD/LPS cotreatment showed a clear dose-response relationship with AMD as well as LPS. The metabolism and hepatic accumulation of AMD were not affected by LPS coexposure. Serum concentration of tumor necrosis factor-alpha (TNF) was significantly increased by LPS and was slightly prolonged by AMD. In Hepac1c7 cells, addition of TNF potentiated the cytotoxicity of both AMD and its primary metabolite, mono-N-desethylamiodarone (DEA). In vivo inhibition of TNF signaling by etanercept attenuated the AMD/LPS-induced liver injury in rats. In summary, AMD treatment during modest inflammation induced severe hepatotoxicity in rats, and TNF contributed to the induction of liver injury in this animal model of idiosyncratic AMD-induced liver injury. (Supported by NIH R01DK061315).

2.2 Introduction

Idiosyncratic adverse drug reactions (IADRs) typically occur only in a small fraction of patients who are treated with certain drugs at therapeutic doses. IADRs are usually unrelated to the pharmacological target of the drug. They present a serious human health problem and are usually not predicted by current preclinical safety evaluation during drug development. During the period 1975 to 2000, 10% of newly approved drugs were withdrawn from the US market or received black box warnings due to these adverse reactions (Roth *et al.* 2003; Uetrecht 2007).

The mechanisms by which IADRs occur are not clear. Evidence from experimental animals indicates that mild inflammation can decrease the threshold for toxicity and thereby render an individual susceptible to an adverse drug reaction that would not otherwise occur (Roth *et al.* 2003). Lipopolysaccharide (LPS), a cell wall component of gram-negative bacteria, is widely used as an inflammagen in these animal studies. A nonhepatotoxic dose of LPS can interact with nontoxic doses of several IADR-associated drugs from different pharmacologic classes to induce liver damage in rodents (Deng *et al.* 2006; Luyendyk *et al.* 2003; Waring *et al.* 2006; Zou *et al.* 2009b).

Amiodarone [2-butyl-3-(3',5'-diiodo-4'α-diethylaminoethoxybenzoyl)-benzofuran] (AMD), a class III antiarrhythmic drug, is effective in increasing the survival of patients after myocardial infarction or congestive heart failure (Singh 1996). Since the approval of AMD by the U.S. Food and Drug Administration in 1985, the use of this drug has been associated with a variety of adverse effects, including liver dysfunction, pulmonary complications, thyroid dysfunctions and ocular disturbance (Rotmensch *et al.* 1984).

The reported frequency of liver abnormalities in patients receiving AMD varies from 14% to 82% (Lewis *et al.* 1989). Most of these reactions are mild, with serum transaminase elevation within 3-fold of the upper limit of normal (ULN), but some are more severe (Babatin *et al.* 2008). Cases of liver reactions after intravenous administration of AMD are rare, but damage can be acute and marked (Ratz Bravo *et al.* 2005). Fulminant hepatic failure or death associated with AMD hepatotoxcity has also been reported (Babatin *et al.* 2008).

There is evidence that the interaction between LPS-induced cytokines and drugs or their metabolites play an important role in the LPS-drug interaction (Zou *et al.* 2009a). Tumor necrosis factor-alpha (TNF) is a proximal mediator of the inflammatory cascade induced by LPS (Beutler and Kruys 1995) and is critically involved in many models of liver injury, such as ischemia/reperfusion (Teoh *et al.* 2004), alcoholic liver disease (Yin *et al.* 1999) and some drug/LPS-induced liver injury models (Shaw *et al.* 2009c; Tukov *et al.* 2007; Zou *et al.* 2009a). As an example, TNF selectively augmented the cytotoxicity of sulindac sulfide, which is the major toxic metabolite of sulindac (Zou *et al.* 2009a). In the case of amiodarone, the major metabolite of AMD is mono-N-desethylamiodarone (DEA), which shares similar pharmacological (Talajic *et al.* 1987) and pharmacokinetic (Shayeganpour *et al.* 2008) characteristics with AMD. DEA has antiarrhythmic properties, a very long half-life and accumulates in the liver and many other tissues. In primary hepatocytes, HepG2 cells and other cell types, DEA is much more cytotoxic than AMD (Waldhauser *et al.* 2006). The plasma concentration of DEA is greater in cases of AMD-associated IADRs (O'Sullivan *et al.* 1995), suggesting a possible role for this metabolite in AMD toxicity.

The purpose of this study was to test the hypothesis that inflammatory stress induced by LPS potentiates amiodarone-induced hepatotoxicity in rats. When the results demonstrated a hepatotoxic interaction between inflammatory stress and amiodarone, the roles of metabolism and TNF were explored.

2.3 Materials and methods

Materials.

Unless otherwise noted, all chemicals were purchased from Sigma-Aldrich (St Louis, MO). The activity of LPS (Lot 075K4038, derived from *Escherichia coli* serotype O55:B5) was 3.3 $\times 10^6$ endotoxin units (EU)/mg, which was determined by a Limulus amebocyte lysate endpoint assay kit from Cambrex Corp. (Kit 50-650U; East Rutherford, NJ). The reagents for the measurement of alanine aminotransferase (ALT), aspartate aminotransferase (AST), alkaline phosphatase (ALP) and gamma-glutamyltransferase (GGT) activities were purchased from Thermo Electron Corp. (Waltham, MA). The kit for total bile acids measurement was purchased from Diazyme Laboratories (Poway, CA).

Animals.

Male, Sprague-Dawley rats (Crl:CD(SD)IGS BR; Charles River, Portage, MI) weighing 250–370 g were used for *in vivo* studies. They were fed standard chow (Rodent Chow/Tek 8640; Harlan Teklad, Madison, WI) and allowed access to water ad libitum. Animals were allowed to acclimate for 1 week in a 12-hour light/dark cycle prior to experiments. They received humane care according to the criteria in the Guide for the Care and Use of Laboratory Animals.

Experimental protocol.

In all of the experiments, rats were fasted for 12h before administration of LPS, and food was returned thereafter. A 20mg/kg solution of AMD was made in its vehicle (0.18% Tween 80), and 4.1 $\times 10^5$ EU/ml solution of LPS was made in sterile saline. To

determine the optimal time interval between AMD and LPS treatments, rats were treated with AMD (300 mg/kg, ip) 2h, 8h, 12h, 16h or 20h before LPS (1.6×10^6 EU/kg, iv). For the evaluation of the dose-response relationship for AMD, rats were treated with AMD (0-400 mg/kg, ip) and 16h later with LPS (1.6×10^6 EU/kg, iv) or saline. For the evaluation of the dose-response relationship for LPS, rats were treated with AMD (400 mg/kg, ip) or veh and 16h later with LPS (0-1.6×10^6 EU/kg, iv). In subsequent studies, rats were treated with AMD (400 mg/kg, ip) or veh and 16h later with LPS (1.6×10^6 EU/kg, iv) or saline. In the etanercept treatment study, rats were treated with etanercept (8 mg/kg) or sterile water by s.c. injection 1 h before LPS.

Rats were anesthetized with isoflurane, and blood and liver samples were taken. Serum was prepared from blood, and plasma was collected into a syringe containing 3.2% sodium citrate (BD Biosciences; San Diego, CA). The right medial lobe of the liver was rapidly frozen for immunohistochemistry, and the left lateral lobe of liver was fixed in 10% neutral-buffered formalin and stored in 70% ethanol for histopathology.

Evaluation of liver injury.

Liver injury was estimated from the serum activities of ALT, AST, ALP and GGT, and from the serum concentration of total bile acids.

Formalin-fixed liver samples were embedded in paraffin, sectioned and stained with hematoxylin and eosin (H&E staining). The stained liver sections were examined using light microscopy.

Drug and metabolite analysis.

Serum samples and liver homogenates were mixed with acetonitrile containing ethopropazine as internal standard (IS). After vortexing and centrifugation, protein was removed, and the supernatant was diluted and transferred to autosampler vials for LC/MS/MS analysis. LC/MS/MS analysis was performed by use of a Shimadzu LC-20 high performance liquid chromatography (HPLC) system coupled to a QTRAP 3200 tandem quadrupole mass spectrometer (AB/Sciex) operated under control of Analyst v. 1.4.2 software. The Ascentis® Express C18 HPLC Column (5 cm × 2.1 mm, 2.7 µm) was maintained at 50 °C. A volume of 2 µl was injected into the HPLC system and eluted with a gradient based upon 10 mM ammonium acetate in H_2O (solvent A) and methanol (solvent B): 0 min to 0.5 min, 10% solvent B; 0.5 min to 1min, 10% to 98% solvent B; 1 min to 4 min, 98% solvent B; 4 min to 6 min, 10% solvent B; flow rate, 0.3 ml/min. Positive mode electrospray ionization was used for all analyses. Mass spectrometry parameters, including declustering potential and collision energy, were optimized independently for each analyte and IS. Multiple reactions monitoring the m/z transitions were used for the quantitative analysis of AMD (*m/z* 646.1→201.1), DEA (*m/z* 618.1→547.0) and ethopropazine (*m/z* 313.1→114.1). The LC/MS/MS method achieved lower limits of quantification of ≤ 50 ng/ml for AMD and ≤ 5 ng/ml for DEA. Analytical reproducibility was judged to be ±10.2% in the middle of the calibrated range of concentrations. Pierce BCA protein assay kit (Thermo scientific, Rockford, IL) was used to determine protein concentration in the liver homogenates.

Serum TNF concentration.

The TNF concentration in serum was measured with an enzyme-linked immunosorbent assay (ELISA) kit (BD Biosciences; San Diego, CA).

Assessment of cytotoxicity *in vitro.*

The murine hepatoma cell line Hepa1c1c7 purchased from American Type Culture Collection (Manassas, VA) was used to assess cytotoxicity *in vitro*. Hepa1c1c7 cells were maintained in Dulbecco's modified Eagle's medium (Invitrogen, Carlsbad, CA) with 1% antibiotic–antimycotic (Invitrogen) and 10% heat-inactivated fetal bovine serum (SAFC Biosciences, Lenexa, KS) in 75-cm^2 tissue culture flasks at 37 °C in a humidified atmosphere of 95% air and 5% CO_2. Cells were plated in 96-well plates at 15,000 cells per well and allowed to attach for 8 h before medium was replaced. Various concentrations of AMD, DEA and/or TNF were added to designated wells, and cells were incubated under maintenance condition. Twenty-four hour later, lactate dehydrogenase (LDH) activity released into the culture medium was measured using the Cytotox-One Homogeneous Membrane Integrity Assay (Promega, Madison, WI). The percent LDH release was calculated as LDH in supernatant/(LDH in supernatant + LDH in cell lysate).

Statistical analysis.

The results are expressed as means ± S.E.M. One-way or two-way ANOVA was applied as appropriate; Tukey's method was employed as a post hoc test. Grubb's test was used to detect outliers. At least 3 biological repetitions were performed for each experiment. $P<0.05$ was set as the criterion for statistical significance.

2.4 Results

The time interval between AMD and LPS administration is important for the production of liver injury

Serum ALT activity did not increase from treatment with either LPS or AMD alone (Figure. 2-1). In the AMD/LPS group, administration of AMD at 16h or 20h before LPS resulted in significant serum ALT activity increase, whereas AMD injected 2 to 12h before LPS failed to cause this response. The 16h interval between AMD and LPS treatments was selected for future studies.

Dose-response relationships and time course of liver injury

Neither AMD alone nor LPS alone affected ALT activity at any of the doses tested. In rats cotreated with AMD and LPS, serum ALT activity was dependent on both AMD (Figure. 2-2 A) and LPS (Figure. 2-2 B) doses. Significant increases in ALT activity were observed with AMD doses ≥ 300 mg/kg ($p<0.05$) and with LPS doses ≥ 1.2×10^6 EU/kg ($p<0.05$). 400 mg/kg and 1.6×10^6 EU/kg were selected as AMD and LPS doses for subsequent studies, respectively.

In the time course study, the serum activities of both ALT and AST were measured as markers for hepatocellular injury (e. 2-3A,B). Neither AMD nor LPS alone affected serum ALT activities at any time examined. For the AST activity, LPS alone had no effect at any time examined, and AMD alone caused a slight increase at 2h, 4h and 10h. Significant elevation of serum ALT and AST activities were only observed in AMD/LPS-cotreatment, and the increases started between 4h and 6h after LPS administration and continued to increase through 10h.

At 10h after LPS administration, serum activities of ALP and GGT and concentration of bile acids were measured as indicators of cholestatic injury (Figure. 2-4 A~C). Only AMD/LPS cotreatment caused significant increases in these serum markers, whereas AMD or LPS treatment alone had no effect.

Hepatic histopathology

All of the saline-treated control rats were free of liver lesions (Figure. 2-5 A). No microscopic evidence of hepatic pathology was found in four of the six LPS-treated rats (Figure. 2-5 B). Liver sections from two of the LPS-treated rats had a few small foci of midzonal hepatocellular necrosis with an associated neutrophilic influx. In contrast, a widespread, mild–to-marked fibrinopurulent capsulitis was present in the liver sections from all of the AMD-treated rats (Figure. 2-5 C). This was characterized by a thickening of the hepatic capsule due to edema and a conspicuous inflammatory exudate comprising mainly neutrophils, lesser numbers of mononuculear cells, and various amounts of amorphorous, proteinacious material. This fibrinopurulent exudate was also often scattered along the outer peritoneal surface of the capsule. Focal areas of subcapular hepatocellular necrosis were occasionally associated with the capsulitis.

The most profound hepatic histopathology was found in animals treated with both AMD and LPS (Figure. 2-5 D). All of these rats had a mild-to–marked fibrinopurulent capsulitis with occasional subcapsular necrosis, similar to that found in the AMD-treated rats, but in addition, all of these animals had conspicuous areas of midzonal hepatocellular necrosis. The latter lesion ranged from widely scattered focal areas of necrosis in midzonal regions to widespread hepatocellular necrosis with coalescence of affected midzonal and occasionally centriacinar regions (bridging necrosis).

Accumulations of neutrophils were present in all of these necrotic regions. Periportal regions were spared of AMD/LPS treatment-related injury.

LPS did not affect the metabolism or hepatic accumulation of AMD

AMD and DEA concentrations in rat serum and liver homogenates were determined at various times after LPS administration (Figure. 2-6 A~D). From 2h to 10h after LPS or saline administration (i.e., 18h to 28h after AMD administration) the serum and tissue concentrations of AMD and DEA were unaffected by LPS cotreatment. The average serum concentrations of AMD and DEA were 1,100 ng/ml and 128 ng/ml, respectively; and the average liver concentrations of AMD and DEA were 157 ng/mg protein and 53 ng/mg protein, respectively.

AMD affected the concentration of TNF in serum

Serum TNF concentration was measured at 2h and 4h after LPS administration (Figure. 2-7). AMD by itself had no effect on serum TNF concentration. At 2h after LPS, the serum TNF concentrations in rats treated with AMD/LPS or with Veh/LPS were similar. However, by 4h after LPS, the concentration of TNF in serum of AMD/LPS-treated rats was significantly greater than that in Veh/LPS-treated rats.

TNF potentiated the cytotoxicity of AMD and DEA in Hepa1c1c7 cells

Hepa1c1c7 cells were exposed to AMD or DEA, and 24h later cytotoxicity was assessed by measuring LDH activity released into the culture medium (Figure. 2-8 A,B). Both AMD and DEA caused concentration-dependent LDH release. Significant cytotoxicity was observed with AMD concentrations greater than 20 ug/ml and DEA

concentrations greater than 7 ug/ml. Addition of TNF (3 ng/ml) did not cause cytotoxicity alone but significantly potentiated the cytotoxicity of AMD and DEA.

Neutralization of TNF *in vivo* attenuated AMD/LPS-induced liver injury

Etanercept is a soluble TNF receptor construct that inactivates TNF. Etanercept (8 mg/kg, s.c.) injected 1h before LPS inhibited the biological activity of TNF in rats and was not hepatotoxic by itself (Tukov *et al.* 2007; Zou *et al.* 2009a). The same treatment was used in this study. AMD/LPS cotreatment increased serum ALT activity, and etanercept significantly attenuated this increase (Figure. 2-9 A). Changes in serum ALT activity were supported by histological examination of H&E-stained liver sections: the severity and frequency of necrotic foci were markedly reduced in rats cotreated with etancercept (Figure. 2-9 B).

Figure 2-1 Effect of time interval between AMD and LPS on the induction of liver injury.

Rats were treated with AMD (300 mg/kg, ip) 2, 8, 12, 16 or 20h before LPS (1.6×10^6 EU/kg, iv). Serum ALT activity was measured 10h after LPS injection. #, * significantly different from AMD/Sal or Veh/LPS, respectively. $p < 0.05$, n=3-8.

Figure 2-1 (cont'd)

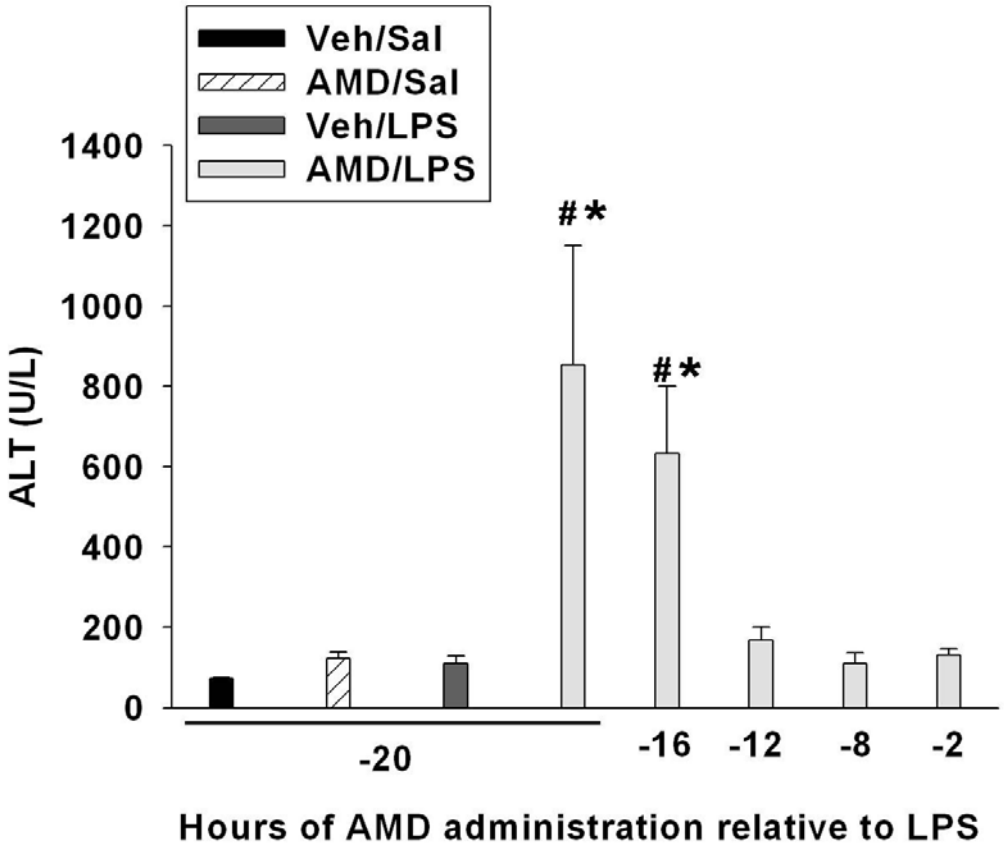

Figure 2-2 Dose-response relationships for AMD and LPS.

A, Rats were treated with AMD (0-400 mg/kg, ip) and 16h later with LPS (1.6 $\times 10^6$ EU/kg, iv). B, Rats were treated with AMD (400 mg/kg, ip) and 16h later with LPS (0-1.6 $\times 10^6$ EU/kg, iv). Serum ALT activity was measured at 10h after LPS administration for both data sets. #, significantly different from respective groups not given LPS; * significantly different from respective group not given AMD. $p < 0.05$, n=3-14.

Figure 2-2 (cont'd)

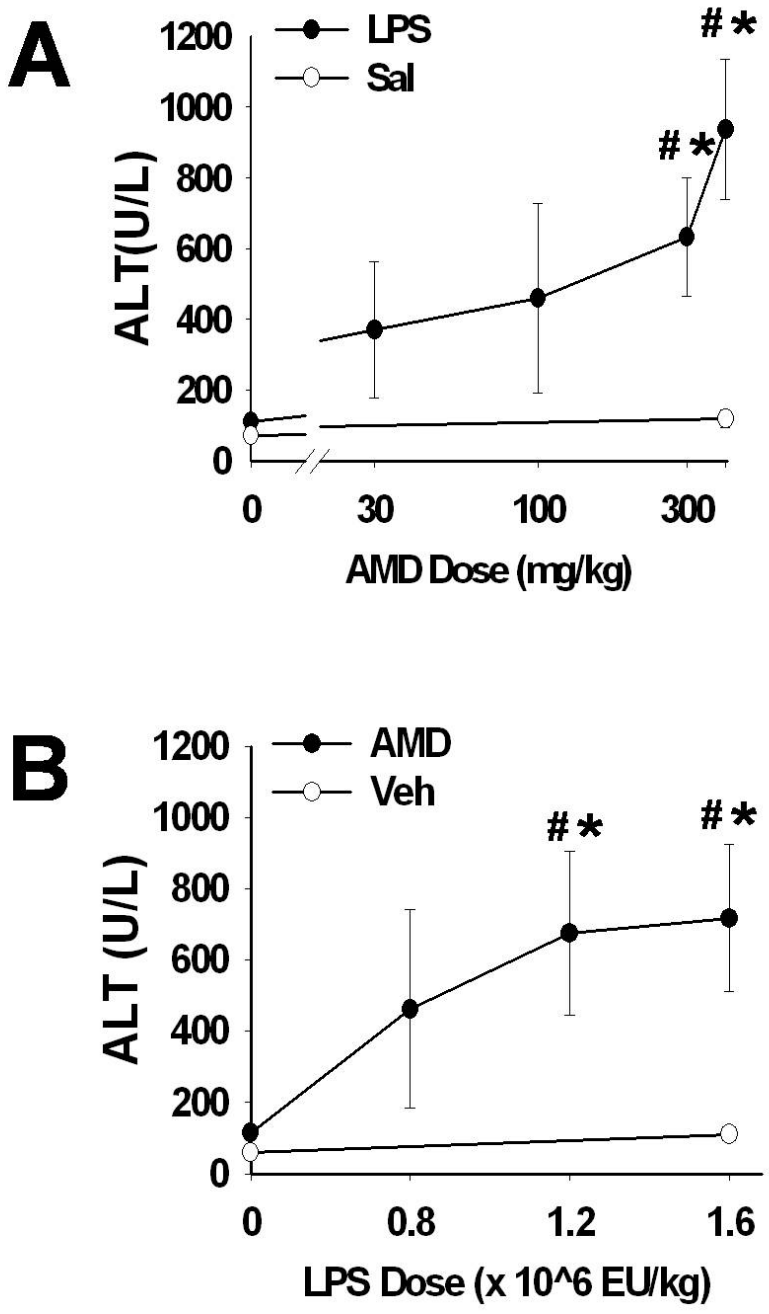

Figure 2-3 Development of liver injury.

Rats were treated with AMD (400 mg/kg, ip) or veh and 16h later with LPS (1.6×10^6 EU/kg, iv) or saline. They were examined 2, 4, 6 or 10h after LPS injection. Activities of ALT (A) and AST (B) in serum were measured. #, significantly different from respective groups not given LPS; * significantly different from respective group not given AMD. $p < 0.05$, n=4-9.

Figure 2-3 (cont'd)

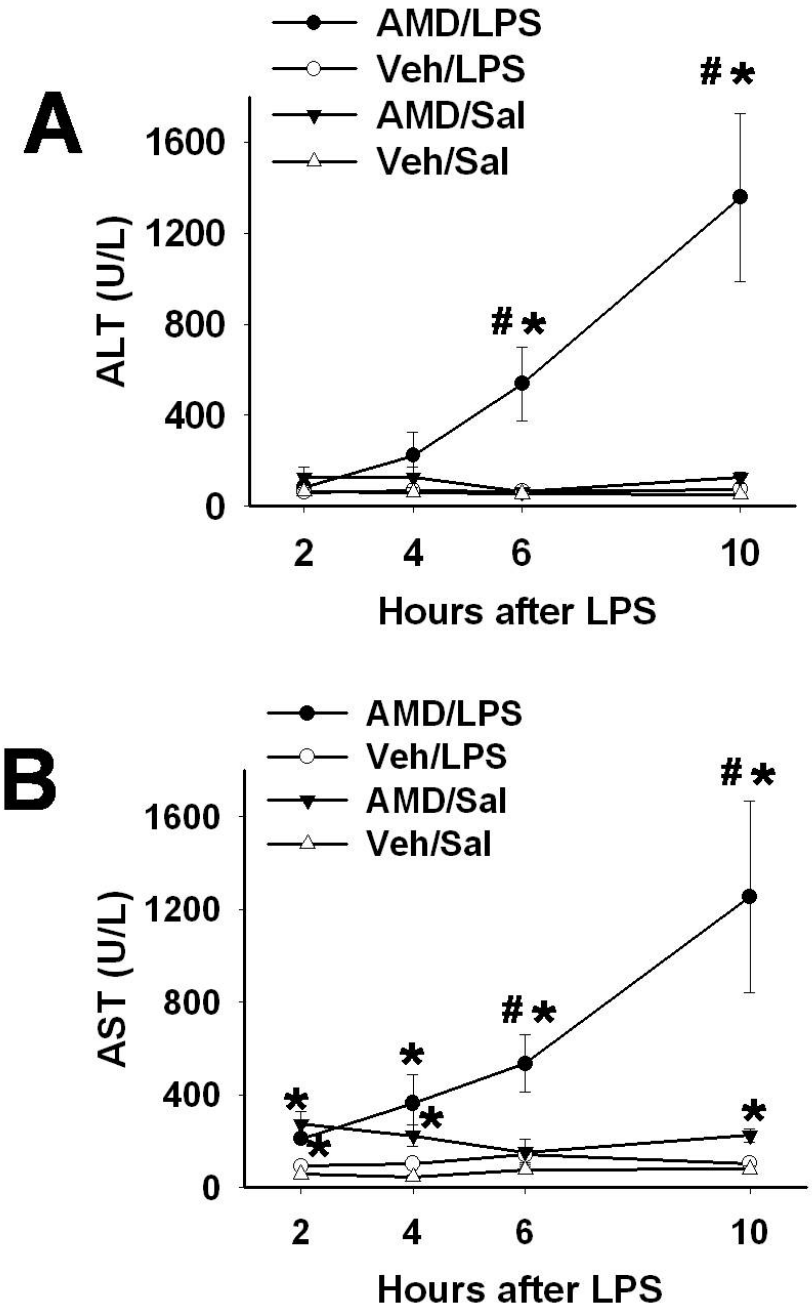

Figure 2-4 Markers of cholestasis after AMD/LPS cotreatment

Rats were treated with AMD (400 mg/kg, ip) or veh and 16h later with LPS (1.6×10^6 EU/kg, iv) or saline. Blood samples were collected at 10h after LPS administration. Serum markers for cholestatic liver injury were measured: A, alkaline phosphatase (ALP); B, gamma-glutamyltransferase (GGT); C, total bile acids #, significantly different from respective groups not given LPS; * significantly different from respective group not given AMD. $p < 0.05$, n=4-9.

Figure 2-4 (cont'd)

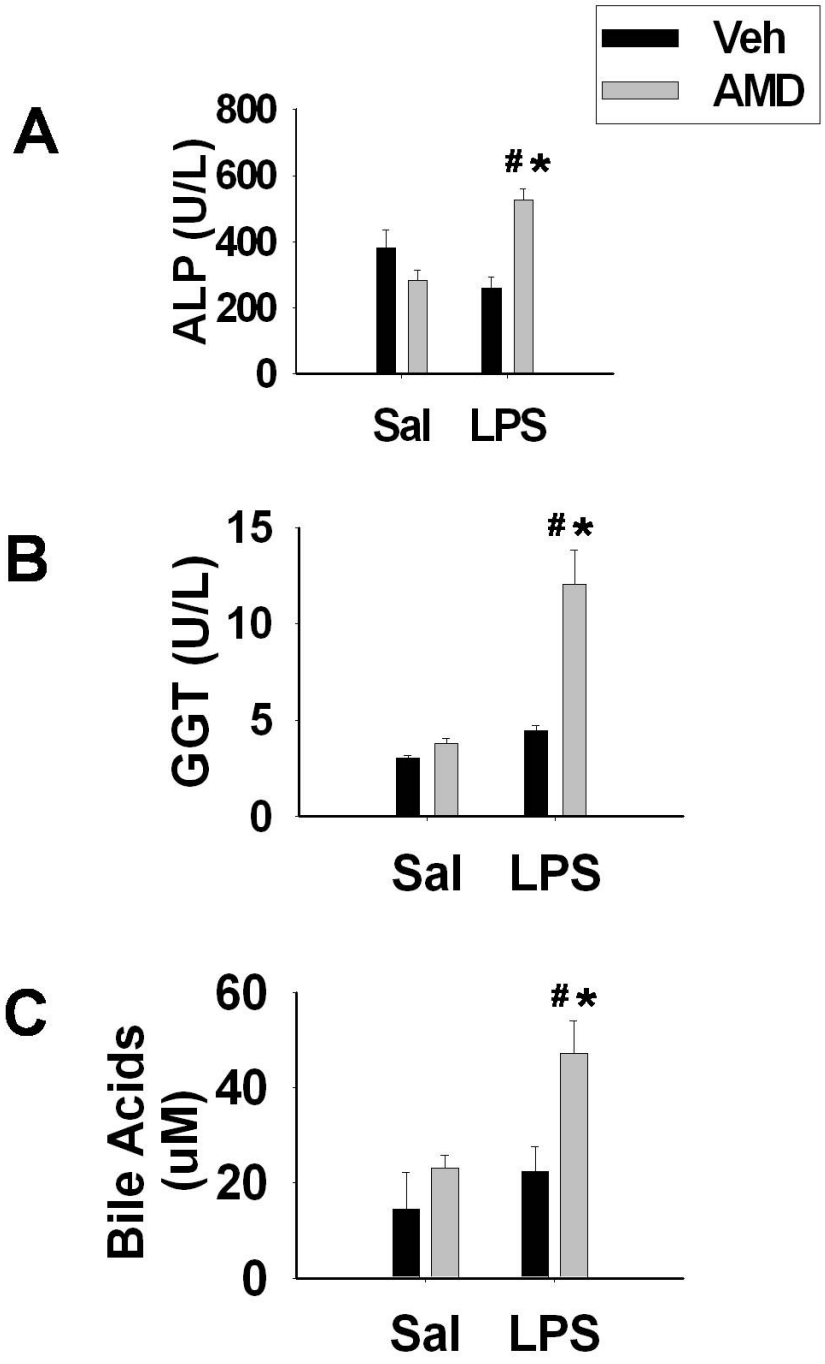

Figure 2-5 Hepatic histopathology

Rats were treated with AMD (400 mg/kg, ip) or veh and 16h later with LPS (1.6×10^6 EU/kg, iv) or saline. Liver tissue samples were collected at 10h after LPS administration. Formalin-fixed liver samples were embedded in paraffin, sectioned and stained with hematoxylin and eosin (H&E staining). Treatment groups: A, Veh/Sal; B, Veh/LPS; C, AMD/Sal; D, AMD/LPS. Legends: cv, central vein; p, portal vein; c, capsule; black arrow, fibrinopurulent capsulitis; white arrow, neutrophil infiltration; *, necrotic foci.

Figure 2-5 (cont'd)

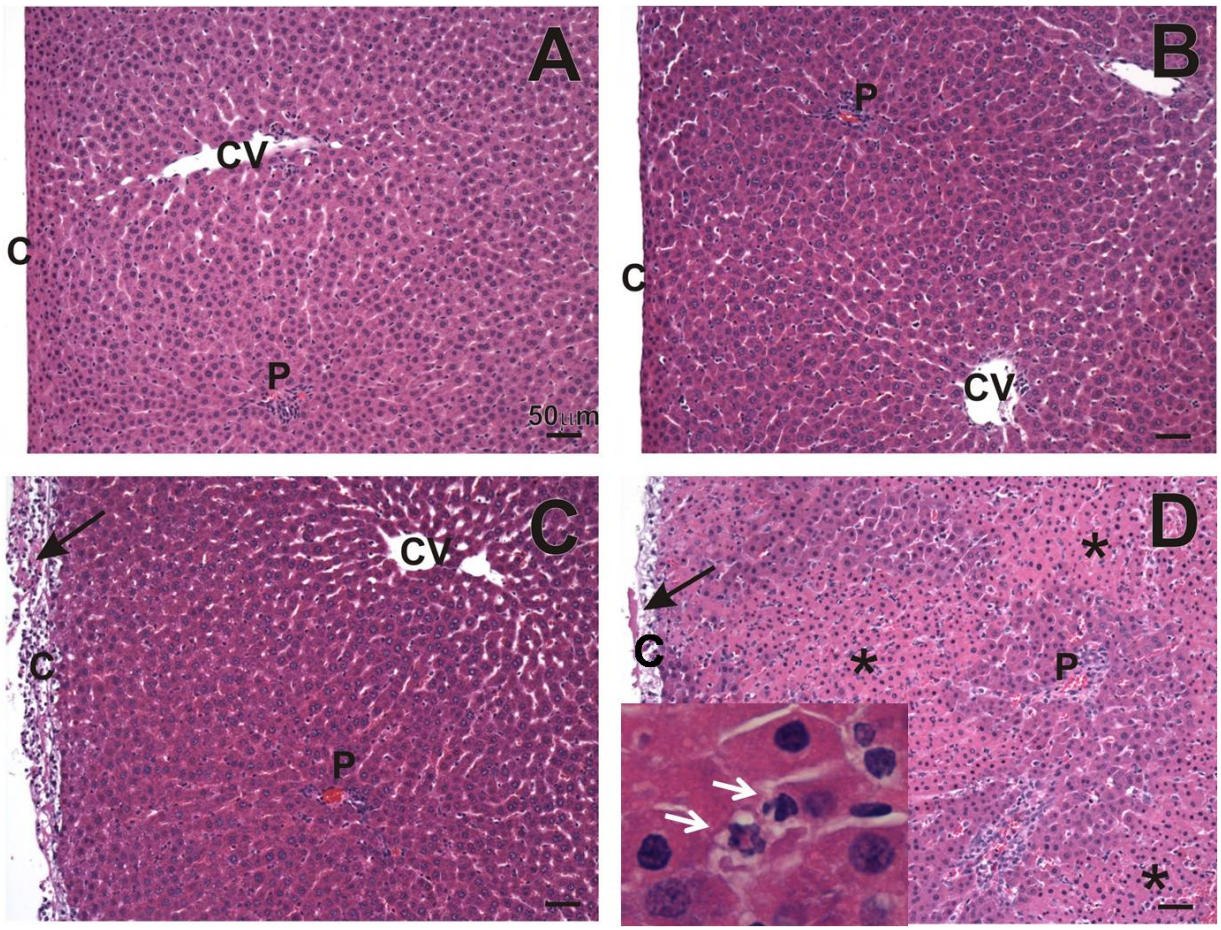

Figure 2-6 Serum and liver concentrations of AMD and DEA.

Rats were treated with AMD (400 mg/kg, ip) and 16h later with LPS (1.6×10^6 EU/kg, iv) or saline. Blood and tissue samples were collected at 2, 4, 6 or 10h after LPS injection. Serum concentrations of AMD (A) and DEA (B), and liver concentrations of AMD (C) and DEA (D) were measured with LC/MS/MS as described in Methods. n=4-9.

Figure 2-6 (cont'd)

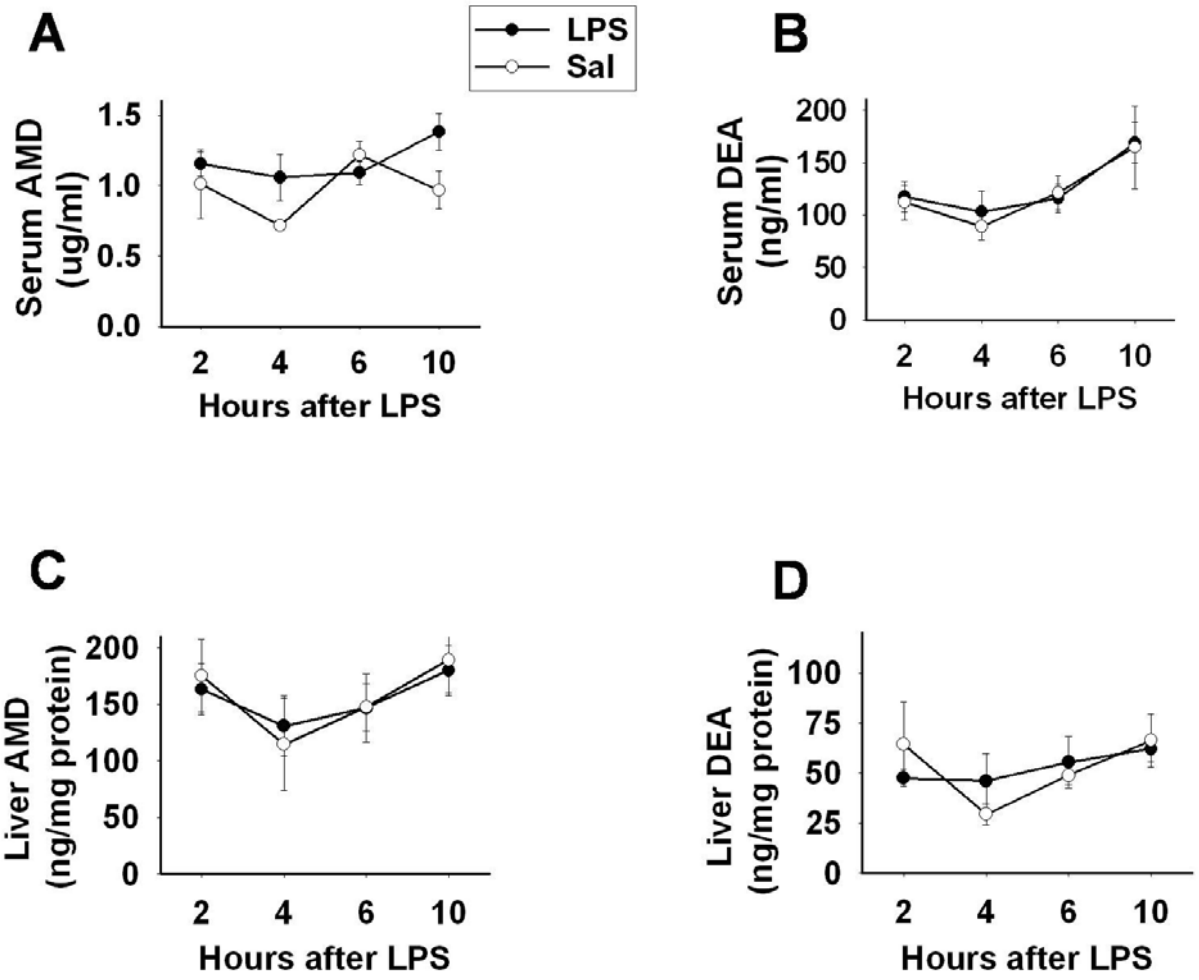

Figure 2-7 Serum concentration of TNF.

Rats were treated with AMD (400 mg/kg, ip) or veh and 16h later with LPS (1.6×10^6 EU/kg, iv) or saline. Blood samples were collected at 2 or 4h after LPS administration. Serum concentrations of TNF were measured with ELISA. #, significantly different from respective groups not given LPS; * significantly different from respective group not given AMD. $p < 0.05$, n=5-8.

Figure 2-7 (cont'd)

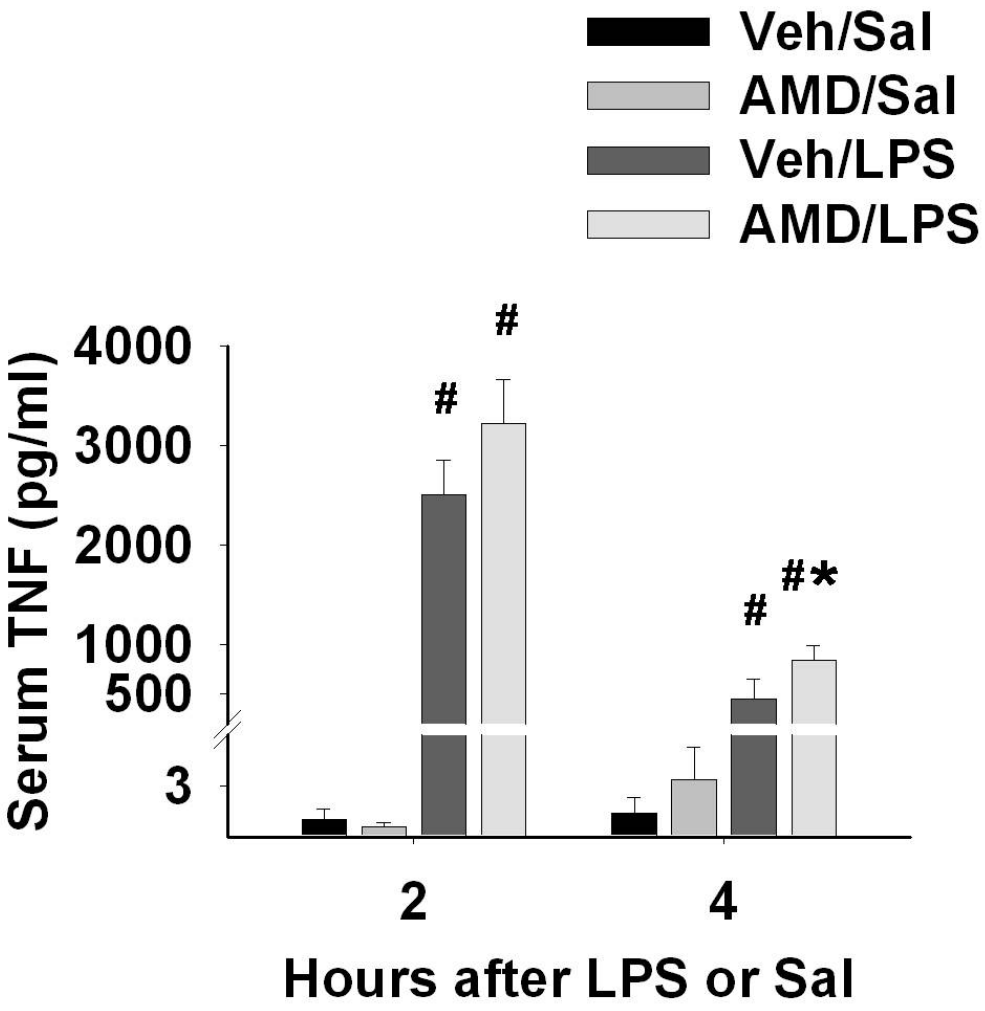

Figure 2-8 Effect of TNF on cytotoxicity of AMD and DEA *in vitro*.

Various concentrations of AMD (A) or DEA (B) were added to cultures of Hepa1c1c7 cells together with TNF (3ng/mL) or saline. Twenty-four h after treatment, LDH activity released into the culture medium was measured. The percent LDH release was calculated as described in Materials and methods. *, significantly different from respective groups not given TNF; #, significantly different from respective groups not given AMD. $p < 0.05$, n=3.

Figure 2-8 (cont'd)

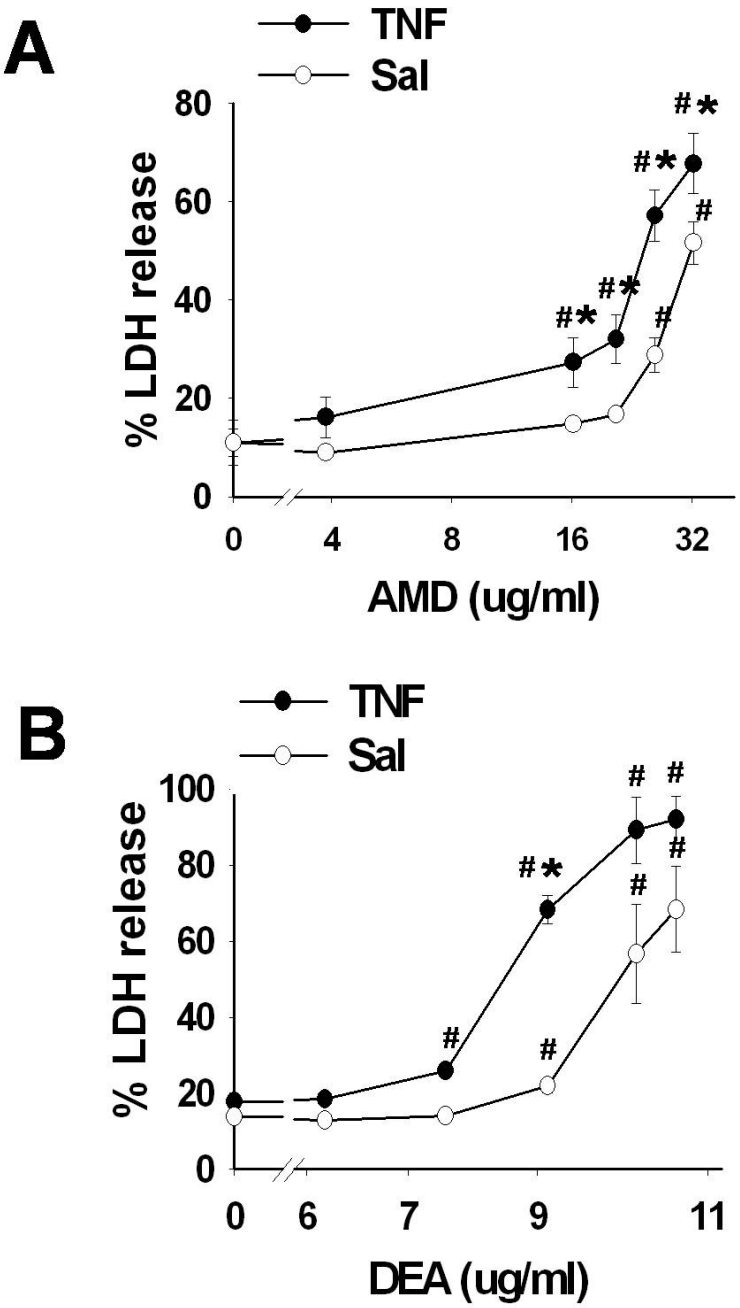

Figure 2-9 Effect of TNF inhibition on AMD/LPS-induced liver injury.

Rats were treated with AMD (400 mg/kg, ip) or vehicle and 16h later with LPS (1.6×10^6 EU/kg, iv) or saline. Etanercept (8mg/kg, s.c.) or its saline vehicle was given 1h before LPS. Rats were killed 10 h after LPS. A, Serum ALT activity #, significantly different from Veh/Sal/Sal. * significantly different from AMD/Sal/LPS . $P<0.05$, n=5-8. B, H&E stained liver slides. cv, central vein; *, necrotic foci.

Figure 2-9 (cont'd)

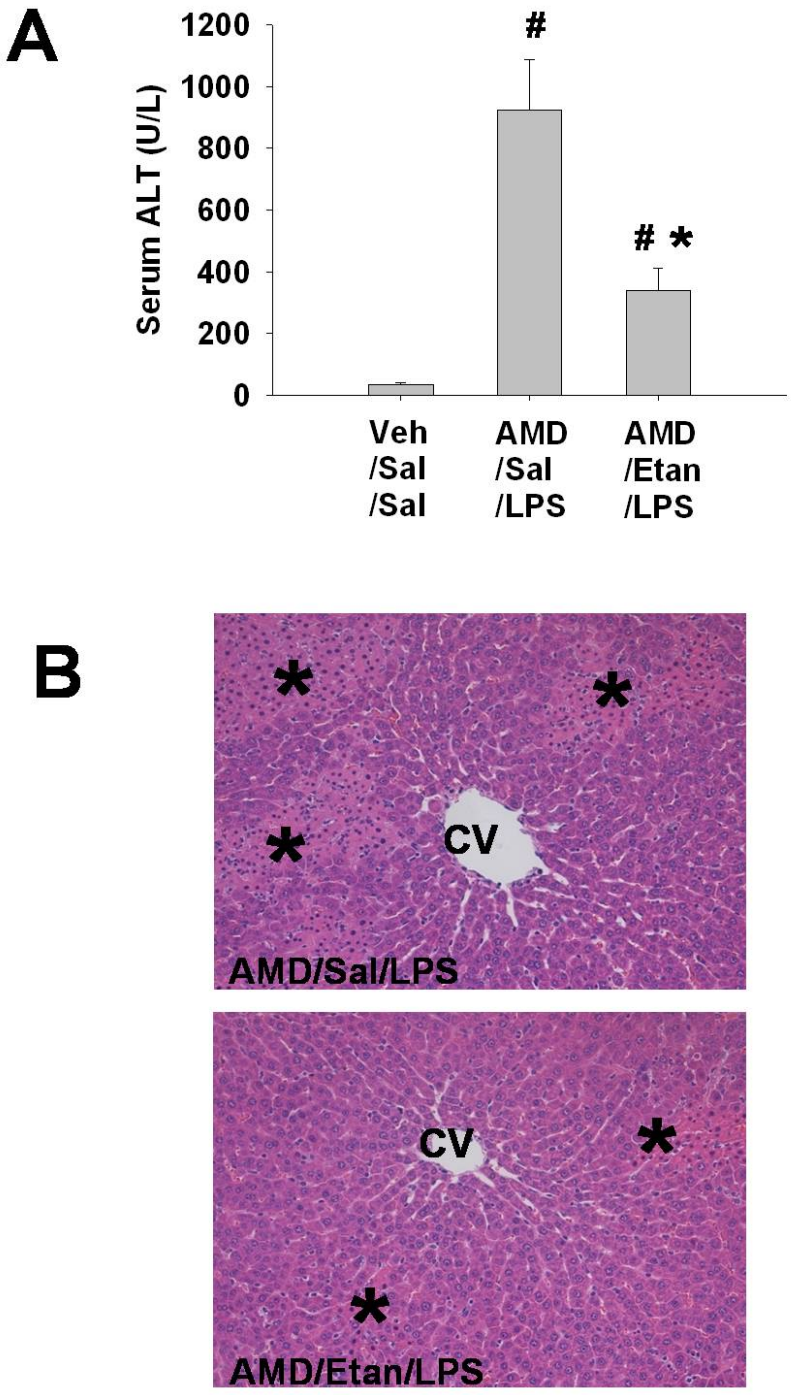

2.5 Discussion

Since its introduction to Europe in 1962, amiodarone has been associated with idiosyncratic hepatotoxicity (Lewis *et al.* 1989). A linear correlation between serum AMD concentration and serum ALT activities has been established (Pollak and You 2003); however, in that study the ALT values did not exceed 3×ULN and were not considered to be clinically significant. For the cases of severe liver injury caused by intravenous amiodarone loading, patients' serum ALT activities were up to 10-206×ULN. There was usually a 24h- to 72h-delay between the initial loading of AMD and the onset of elevation in ALT activities; and in many cases, the ALT activity returned to normal after a few days of continuation of maintenance dosing (Ratz Bravo *et al.* 2005). Accordingly, it is hard to draw a simple linear relationship between the magnitude or frequency of severe hepatotoxicity and serum AMD concentration. An effort to establish a model for AMD-induced liver injury in healthy rodents was unsuccessful. Neither short-term, large dose nor long-term, small dose administration of AMD led to observable liver damage (Young and Mehendale 1989). The cause of severe AMD hepatotoxicity is more likely to be a combination of AMD and other factors, for example, inflammatory episodes. In the present study, regardless of cotreatment with LPS, the serum concentration of AMD was about 1100 ng/ml, which is very close to the steady-state serum concentration of AMD in human patients (1500ng/ml) under long-term, oral amiodarone therapy (Pollak *et al.* 2000). Our findings support that at this clinically relevant concentration of AMD in serum, hepatotoxicity can be induced by a concurrent inflammatory episode related to entotoxin exposure.

Previous studies in rodents have suggested a possible association between inflammation and liver injury for several drugs associated with human IADRs, including chlorpromazine (Buchweitz *et al.* 2002), ranitidine (Luyendyk *et al.* 2003), diclofenac (Deng *et al.* 2006), trovafloxacin (Shaw *et al.* 2007), sulindac (Zou *et al.* 2009b) and halothane (Dugan *et al.* 2010). The results of the present study expand these findings and demonstrate that a nonhepatotoxic dose of AMD is rendered hepatotoxic when acute inflammation is triggered by LPS administration. Acute increases in serum markers for hepatocellular and cholestatic injury were found in rats cotreated with AMD/LPS. These resemble the clinical hepatic chemistry changes in human idiosyncrasy during AMD therapy (Ratz Bravo *et al.* 2005). The midzonal and bridging necrosis and infiltration of inflammatory cells in AMD/LPS are also consistent with some of the histological changes found in human patients (Babatin *et al.* 2008; Ratz Bravo *et al.* 2005). However, the histological characteristics in people with AMD-induced liver injury were variable. Different patterns of hepatocellular necrosis, such as midzonal, centrilobular, bridging and panlobular, have been reported (Lewis *et al.* 1989). Genetic differences, concurrent medications, and even different origins of inflammation might account for these varied responses; nevertheless, the AMD/LPS interaction model in rats mimics important aspects of AMD-induced IADRs in human patients.

The timing of AMD and LPS dosing in this model was important for the development of severe liver damage. A minimal interval of 16h was required for AMD and LPS to interact to induce liver injury. When LPS was injected within 16h after AMD, no liver injury was observed. Absorption, distribution, metabolism and clearance as well as toxicological actions could contribute to this timing requirement. The elimination of

AMD is primarily through hepatic metabolism and biliary excretion, and its half-life in plasma is very long (55 days in humans) (Pollak *et al.* 2000). Accordingly, the loss of AMD due to elimination within 16h is minimal. AMD has a dose-dependent effect on the respiratory chain and β-oxidation in the mitochondria (Fromenty *et al.* 1990b; Fromenty *et al.* 1990a), and it can also affect the function of lysosomes and other acidic organelles (Stadler *et al.* 2008). The 16h interval may be required for AMD to distribute into the liver, accumulate in organelles and sensitize hepatocytes to interact with LPS or its downstream cytokines.

In other drug/LPS models, there is also a dependence on the temporal relationship between administrations of drug and LPS, and the time interval needed for a maximal hepatotoxic response is different for different drugs (Shaw *et al.* 2007; Zou *et al.* 2009b). This time interval requirement might help to explain the low frequency of IADRs in human patients: i.e., only when the inflammatory episode happens at a certain time during drug therapy would idiosyncratic hepatotoxicity occur.

In rats, AMD is deethylated by cytochromes P450 (CYPs) 3A4, 1A1, 2D1 and 2C11 in the liver (Elsherbiny *et al.* 2008). DEA, the major metabolite, is 3- to 5-fold more toxic than AMD to cultured HepG2 cells (Waldhauser *et al.* 2006) and to primary rat hepatocytes (Gross *et al.* 1989). In our treatment of Hepa1c1c7 cells, a similar trend was observed (Figure. 2-8). The administration of LPS affects the expression and activities of CYPs in rats (Sewer *et al.* 1997). This raised the possibility that LPS might potentiate the toxicity of AMD by increasing its metabolism to DEA. To evaluate this, serum and liver concentrations of AMD and DEA were measured with LC/MS/MS. The average serum concentration of DEA in AMD-treated rats was 128 ng/ml, which is about

1/10 of the serum AMD concentration. This ratio is commonly seen in the serum after an intravenous loading dose of AMD, both in people (Ha *et al.* 2005) and rats (Shayeganpour *et al.* 2008). Neither the serum nor the liver concentration of AMD or DEA was affected by LPS cotreatment, suggesting that neither AMD accumulation nor DEA generation was affected by LPS.

Intratracheal instillation of AMD *in vivo* or exposure of alveolar macrophages to AMD *in vitro* led to TNF production (Futamura 1996; Reinhart and Gairola 1997). AMD treatment also increased TNF production by alveolar macrophages upon LPS stimulation (Punithavathi *et al.* 2003). In the present study, treatment of rats with AMD alone did not cause serum TNF elevation, but it did increase the concentration of TNF in serum of LPS-treated rats. These results suggest that the increased appearance of TNF in AMD/LPS-cotreated rats was probably not an additive effect; rather, AMD appeared to potentiate the production or diminish the clearance of TNF caused by LPS. The concentration of TNF in serum increases rapidly in LPS-treated rats, peaks at around 1.5-2h, and then returns to basal levels at around 6h (Tukov *et al.* 2007). In the present study, the concentration of TNF around the peak time (i.e. 2h) in LPS-cotreated rats was not affected by AMD, but the TNF concentration was greater in AMD-cotreated rats at a later time (4h). These data suggest that AMD prolonged the elevation in TNF caused by LPS administration. This seemingly small difference in TNF concentration was shown to be critical to liver pathogenesis in another drug/LPS model of liver injury involving trovafloxacin (Shaw *et al.* 2009c). Accordingly, it is possible that prolongation of the LPS-induced TNF response is a critical event across models of LPS-drug interaction.

The importance of TNF in the AMD model was explored by preventing its binding to cellular receptors with etanercept. Etanercept pretreatment reduced hepatotoxicity, indicating that TNF has an important role in AMD/LPS-induced liver injury. Since no liver injury was observed after treatment with LPS alone, the large TNF peak caused by LPS was not hepatotoxic by itself; however, this amount of TNF could be critical for the induction of hepatocellular injury by potentiating the toxic effect of AMD and/or DEA. Signaling from an activated TNF receptor can lead to lysosomal leakage, mitochondrial damage and caspase activation (Wullaert *et al.* 2007). All three of these events were also found in AMD and DEA cytotoxicity *in vitro* (Agoston *et al.* 2003; Spaniol *et al.* 2001). Further support for a critical role for TNF came from our *in vitro* study in Hepa1c1c7 cells, in which TNF increased the cytotoxicity of both AMD and DEA. As a proximal proinflammatory cytokine, TNF can also contribute to liver damage by inducing downstream inflammatory events, such as coagulation activation and neutrophil activation (Shaw *et al.* 2009c; Tukov *et al.* 2007). The etanercept treatment herein reduced the ALT activity to half of the level seen in the absence of this inhibitor, whereas the same dose of etancercept reduced the ALT activity almost to control level in trovafloxacin/LPS and sulindac/LPS models (Shaw *et al.* 2007; Zou *et al.* 2009a). This suggests that other factors induced by LPS might act in parallel with TNF in the AMD/LPS model. In other models of potentiation of toxicity xenobiotic toxicity by LPS, other factors such as neutrophils (Luyendyk *et al.* 2005), the coagulation system (Shaw *et al.* 2009b) and prostanoids (Ganey *et al.* 2001) play important roles.

In summary, AMD was rendered hepatotoxic in rats in the presence of a coexisting inflammatory stress induced by LPS. AMD/LPS-cotreated rats developed

liver pathology and blood chemistry changes that resemble AMD-induced idiosyncratic hepatotoxicity in human patients. LPS did not interact with AMD by changing the metabolism or distribution of AMD. AMD enhanced the increase in plasma TNF concentration caused by LPS, and neutralizing TNF reduced liver injury from AMD/LPS-coexposure. Moreover, TNF potentiated the cytotoxicity of both AMD and DEA *in vitro*. These findings add support to the idea that inflammatory stress can interact with IADR-associated drugs to cause liver injury by a mechanism involving TNF and suggest that a similar mode of action might apply to several drugs that cause idiosyncratic hepatotoxicity in humans.

CHAPTER 3

Tumor necrosis factor-alpha potentiates the cytotoxicity of amiodarone in Hepa1c1c7 cells: roles of caspase activation and oxidative stress

Jingtao Lu, Kazuhisa Miyakawa, Robert A. Roth and Patricia E. Ganey

3.1 Abstract

Amiodarone (AMD), a class III antiarrhythmic drug, causes idiosyncratic hepatotoxicity in human patients. We demonstrated previously that tumor necrosis factor-alpha (TNF) plays an important role in a rat model of AMD-induced hepatotoxicity under inflammatory stress. In this study, we developed an *in vitro* model to study the roles of caspase activation and oxidative stress in TNF potentiation of AMD cytotoxicity. AMD caused apoptotic cell death in Hepa1c1c7 cells, and TNF cotreatment potentiated its toxicity. Activation of caspases 9 and 3/7 was observed in AMD/TNF- cotreated cells, and caspase inhibitors provided minor protection from cytotoxicity. Intracellular reactive oxygen species generation and lipid peroxidation were observed after treatment with AMD and were further elevated by TNF cotreatment. Adding water-soluble antioxidants (trolox, N-acetylcysteine, glutathione or ascorbate) produced only minor attenuation of AMD/TNF-induced cytotoxicity and did not influence the effect of AMD alone. On the other hand, α-tocopherol, a lipid-soluble antioxidant, prevented AMD toxicity and caused pronounced reduction in cytotoxicity from AMD/TNF cotreatment. α-Tocopherol plus a pancaspase inhibitor completely abolished AMD/TNF-induced cytotoxicity. In summary, activation of caspases and oxidative stress were observed after AMD/TNF cotreatment, and caspase inhibitors and a lipid-soluble free radical scavenger attenuated AMD/TNF-induced cytotoxicity. (Supported by NIH R01DK061315.)

3.2 Introduction

Amiodarone [2-butyl-3-(3', 5'-diiodo-4'α-diethylaminoethoxybenzoyl)-benzofuran] (AMD), is an antiarrhythmic drug effective for the treatment of myocardial infarction or congestive heart failure (Singh 1996). The use of AMD has been associated with a variety of adverse effects, including liver dysfunction, pulmonary complications, thyroid dysfunctions and ocular disturbance (Rotmensch *et al.* 1984). The U.S. Food and Drug Administration issued a black box warning for AMD for its ability to induce idiosyncratic hepatotoxicity. The frequency of symptomatic liver abnormalities in patients receiving AMD is 1% to 3% (Lewis *et al.* 1989). Many of these reactions are mild, but some can be acute and severe, especially during intravenous administration (Ratz Bravo *et al.* 2005). Fulminant hepatic failure or even death related to AMD treatment were reported (Babatin *et al.* 2008).

The mechanisms of AMD-induced idiosyncratic hepatotoxcity are not clear. Neither the magnitude nor the frequency of severe hepatotoxicity is directly related to the dose and duration of AMD therapy (Pollak and Shafer 2004). Attempts to establish a model with healthy rodents were unsuccessful: neither large-dose, short-term exposure nor small-dose, long-term exposure resulted in observable liver damage (Young and Mehendale 1989). The induction of severe AMD hepatotoxicity is more likely to be due to a combination of AMD and other factors, for example, inflammatory episodes.

Lipopolysaccharide (LPS) is widely used to induce an inflammatory response in animal studies. Results from studies in rodents indicate that liver injury results from cotreatment with LPS and some drugs that are associated with idiosyncratic hepatotoxicity in people (Deng *et al.* 2006; Luyendyk *et al.* 2003; Waring *et al.* 2006;

Zou *et al.* 2009b). This occurs with nontoxic doses of several drugs from different pharmacologic classes. One of these drugs is AMD. We reported previously that modest inflammation caused by LPS can interact with AMD to induce liver damage in rats (Lu *et al.* 2012). Tumor necrosis factor-alpha (TNF), a cytokine released upon LPS administration, is critically involved in this AMD/LPS-induced liver injury model: inhibition of TNF signaling by etanercept significantly attenuated AMD/LPS-induced hepatotoxicity (Lu *et al.* 2012). Furthermore, TNF potentiated the cytotoxicity of AMD in Hepa1c1c7 cells, providing a simplified model with which to study the intracellular events involved in the interactions between AMD and TNF *in vitro*.

The appearance of TNF is one of the earliest events after LPS exposure. TNF triggers the expression of other cytokines, infiltration and activation of inflammatory cells, impairment of hemostatic system, etc. (Beutler and Kruys 1995), and is cytotoxic to a variety of primary cells or transformed cell lines (Fransen *et al.* 1986). The majority of the biological effects from soluble TNF are mediated by TNF receptor-1 (TNF-R1). Upon binding to TNF, TNF-R1 can lead to the activation of a variety of signaling pathways, one of which involves procaspase 8 cleavage, which initiates an apoptotic cascade. In hepatocytes, mitochondria are involved in bridging caspase 8 to caspase 9, and eventually to effector caspases, e.g. caspase 3/7 (Wullaert *et al.* 2007). Loss of mitochondrial membrane potential, generation of reactive oxygen species (ROS), formation of the mitochondrial permeability transition pore (MPTP) and release of cytochrome *c* are critical to TNF-induced hepatocyte apoptosis (Bradham *et al.* 1998; Colell *et al.* 2001; Hatano *et al.* 2000).

AMD induces apoptosis and/or necrosis in many different cells (Kaufmann *et al.* 2005), including primary hepatocytes (Kaufmann *et al.* 2005) and hepatoma cell lines (Shojiro I *et al.* 2004). AMD inhibits the β oxidation of fatty acids (Fromenty *et al.* 1990b), inhibits complex I, II and III in the respiratory chain (Spaniol *et al.* 2001), decreases mitochondrial membrane potential (Yano *et al.* 2008), uncouples oxidative phosphorylation (Fromenty *et al.* 1990a) and increases the mRNA level of the proapoptotic protein bax (Choi *et al.* 2002). All of these events can lead to mitochondrial dysfunction and consequent ROS generation and caspase activation, and eventually result in cell death. Indeed, activation of caspase cascades, disruption of mitochondrial function and generation of reactive oxygen species (ROS) are important in AMD-induced cytotoxicity *in vitro*.

As our previous findings demonstrated that TNF potentiates the cytotoxicity of AMD. The purpose of this study was to investigate the mechanism of this interaction. We explored the roles of caspase activation, ROS generation and lipid peroxidation in the potentiation of AMD cytotoxicity by TNF.

3.3 Materials and methods

Materials

Unless otherwise noted, all chemicals were purchased from Sigma-Aldrich (St Louis, MO). The murine hepatoma cell line Hepa1c1c7 was purchased from American Type Culture Collection (Manassas, VA). Recombinant truncated form of murine TNF was purchased from R&D Systems (Minneapolis, MN).

Cell culture and assessment of cytotoxicity

Hepa1c1c7 cells were maintained in Dulbecco's modified Eagle's medium (Invitrogen, Carlsbad, CA) with 1% antibiotic–antimycotic (Invitrogen, Carlsbad, CA) and 10% heat-inactivated fetal bovine serum (SAFC Biosciences, Lenexa, KS) in 75-cm^2 tissue culture flasks at 37 °C in a humidified atmosphere of 95% air and 5% CO_2. Cells were plated in 96-well plates at 15,000 cells per well and allowed to attach for 8h before medium was replaced. Various concentrations of AMD and/or TNF were added to designated wells, and cells were incubated under maintenance condition for the times indicated in figures and legends. To assess cytotoxicity, the activity of lactate dehydrogenase (LDH) released into the culture medium was measured using the Cytotox-One Homogeneous Membrane Integrity Assay (Promega, Madison, WI). Cell lysate was generated by adding cell lysing reagent provided in the assay kit. The percent LDH release was calculated as LDH activity in supernatant/(LDH activity in supernatant + LDH activity in cell lysate).

Assessment of cell death using annexin V/propidium iodide stain

Early apoptosis was assessed using Annexin V/propidium iodide (AnnV/PI) Apoptosis Detection Kit (BD Biosciences, Pharmingen, San Diego, CA) according to the manufacturer's protocol. Briefly, Hepa1c1c7 cells treated with AMD and/or TNF were removed from tissue culture plates by trypsin digestion. After the recommended washing steps, $1x10^5$ cells were suspended in 100 µl of buffer with 5 µl of annexin V-allophycocyanin (AnnV-APC) and 5 µl of propidium iodide (PI). After 15 min incubation in the dark, 400 µl of labeling buffer were added to each sample. Cells treated with 5 µM staurosporine (STS) were stained as a positive control. Stained cells were measured immediately with a BD FACS Canto II flow cytometer. All FACS data were analyzed with Kaluza software (Beckman Coulter, Brea, CA). Quadrant cut-offs were determined from Sal/Sal-treated cells (negative control) and STS-treated cells (positive control).

DNA strand break and total DNA content assessment

A terminal deoxynucleotidyl transferase dUTP nick end labeling (TUNEL) kit (Invitrogen, Carlsbad, CA.) was used to detect DNA strand breaks and to assess total DNA content. Briefly, Hepa1c1c7 cells treated with AMD and/or TNF for the designated time were harvested using trypsin and then fixed in 4% formaldehyde for 30 min at room temperature. The cells were then stored in 70% ethanol at -20 °C overnight for permeabilization. The TUNEL reaction was performed at 4 °C overnight by addition of reaction mixtures containing bromodeoxyuridine (BrdU) and terminal deoxynucleotidyl transferase (TdT) per the kit instruction. After washing with PBS, the cells were incubated with Alexa Fluor 647-labeled mouse monoclonal antibody to BrdU, then with PI. PI is used to determine the total DNA content in each cell. Stained cells were measured immediately with a BD FACS Canto II flow cytometer. All FACS data were

analyzed with Kaluza software. The threshold for TUNEL-positive staining was determined according to the positive and negative control cells provided in the kit. Gating for the hypodiploid cells was determined according to Sal/Sal-treated cells stained with or without PI.

Visualization of cell morphology with modified Wright's stain

Hepa1c1c7 cells were plated in 10 mm culture wells at 750,000 cells per well and allowed to attach for 8 h before medium was replaced with medium containing AMD and/or TNF. After 48h, cells were washed 3 times with phosphate-buffered saline (PBS), fixed with 4% formaldehyde, and stained with modified Wright's stain. The stained cells were examined using light microscopy.

Determination of caspase activity

The Caspase-Glo8, Caspase-Glo9 and Caspase-Glo3/7 assays (Promega, Madison, WI) were used to measure the activities of caspase 8, 9 and 3/7, respectively. The cells were treated in 96-well plates under conditions described in the figure legend, and addition of the assay reagent resulted in cell lysis, cleavage of the substrates and generation of luminescence. The luminescent signal was measured in a SpectraMax Gemini fluorescent plate reader (Molecular Devices, Sunnyvale, CA).

Caspase inhibitors study

Caspase inhibitors or their vehicles were added to AMD- and/or TNF-containing medium for Hepa1c1c7 cell treatment: 40 μM pan caspase inhibitor z-VAD-FMK (R&D System, Minneapolis, MN), 20 μM caspase 9 inhibitor z-LEHD-FMK (R&D System, Minneapolis, MN) or 40 μM caspase 3/7 inhibitor Ac-DEVD-CHO (Calbiochem, La Jolla,

CA). After 48h incubation, cytotoxicity was assessed by measuring LDH release as described above.

Evaluation of intracellular reactive oxygen species (ROS)

ROS generation was assessed using 5-(and-6)-chloromethyl-2',7'-dichlorodihydrofluorescein diacetate, acetyl ester (CM-H_2DCFDA) (Invitrogen, Carlsbad, CA). Hepa1c1c7 cells were plated in 4-well Lab-Tek II chambered coverglass (Nalge Nunc International, Rochester, NY) at 15,000 cells per well and allowed to attach for 8h before medium was replaced. After treating with AMD and/or TNF for the times indicated, the cells were washed in PBS and stained with 10 μM CM-H_2DCFDA for 20min in Hanks' Balanced Salt Solution (HBSS). After one wash with HBSS, cells were photographed on an Olympus IX71 inverted fluorescent microscope, using green fluorescence filter sets: excitation 480/30 nm, emission 535/40 nm. Quantification of fluoresence was performed using Image J software: the integrated intensity for positive 2',7'-dichlorofluorescein (DCF) fluorescence from at least 10 randomly chosen microscope fields per well was measured, and the average was calculated as one replicate.

Water-soluble antioxidants treatment

6-hydroxy-2,5,7,8-tetramethylchromane-2-carboxylic acid (Trolox) is a water-soluble analogue of α-tocopherol. Glutathione (GSH) is a major endogenous antioxidant produced by cells. N-acetyl-L-cysteine (NAC) is an excellent source of sulfhydryl groups and stimulates GSH regeneration. Ascorbic acid (ASC) is a naturally occurring compound with antioxidant properties. 400 uM Trolox, 1 mM GSH, 1 mM NAC or 2 mM

ASC was added to the medium at the same time as AMD and/or TNF. 48h later, percent LDH release was measured as described above.

Evaluation of lipid peroxidation

C11-BODIPY581/591 (BODIPY) (Invitrogen, Carlsbad, CA) is a fluorescent probe used to detect lipid peroxidation in living cells, with excellent spectral separation of the nonoxidized (595 nm) and oxidized (520 nm) forms. Hepa1c1c7 cells were plated in 4-well, Lab-Tek II chambered coverglass and treated with AMD and/or TNF as indicated in figure legends. After incubation, cells were washed with PBS and stained with 20 μM BODIPY in HBSS for 30min. For the assessment of lipid peroxidation, images of the BODIPY-labeled cells were captured using an Olympus IX71 inverted fluorescence microscope, with green fluorescence filter sets: excitation 480/30 nm, emission 535/40 nm. Quantification of fluorescence was performed according to the method described above for ROS.

Lipid-soluble antioxidant treatment

α-tocopherol (TOCO; vitamin E), is a lipid-soluble free radical scavenger. Because lipid peroxyl radicals react more rapidly with TOCO than with polyunsaturated fatty acids, TOCO can terminate the chain reactions of lipid peroxidation and thereby protect cellular membrane systems (Traber 2007). TOCO, at the concentrations indicated in each study, was included in the incubation medium together with AMD and/or TNF. ROS generation, lipid peroxidation, LDH release and caspase 3/7 activation were measured as described above.

Statistical analyses

The results are expressed as means ± S.E.M. One-way or two-way ANOVA was applied as appropriate; Tukey's method was employed as a post hoc test. At least 3 biological repetitions were performed for each experiment. $P<0.05$ was set as the criterion for statistical significance.

3.4 Results

Concentration-response and time course of TNF potentiation of AMD-induced apoptotic cell death

Hepa1c1c7 cells were treated with various concentrations of AMD and/or TNF for 48h. TNF alone at concentrations up to 3ng/ml did not cause any increase in LDH release. AMD induced cytotoxicity at both 30μM and 40μM. TNF cotreatment significantly increased the cytotoxicity caused by AMD at all concentrations of AMD and of TNF tested (Figure 3-1. A). Concentrations of 35μM AMD and 3ng/ml TNF were chosen for subsequent experiments. AMD-induced cytotoxicity was apparent by 12h and increased only slightly through 48h. TNF potentiation of AMD-induced cytotoxicity started by 24h and continued to increase through 48h (Figure 3-1. B).

AnnV/PI staining after AMD and/or TNF treatment

AnnV/PI stain, TUNEL stain and modified Wright's stain were employed to differentiate the cell death pathways in this model of AMD/TNF-mediated cytotoxicity. Annexin V is a protein with high affinity for phosphatidylserine, which is translocated from the inner to the outer leaflet of the plasma membrane during apoptotic cell death, as one of the earliest apoptotic morphological changes (Koopman *et al.* 1994). PI is a fluorescent DNA dye that is excluded by intact membrane of viable cells (Jones and Senft 1985). Accordingly, AnnV and PI are used in conjugation to determine the state of cell death: cells with AnnV-/PI- staining are considered healthy and viable; cells with AnnV+/PI- staining are in early apoptosis; and cells with AnnV+/PI+ staining are in late apoptosis or are already dead.

Representative dot plots from flow cytometric analysis of cells treated with AMD and/or TNF are shown in Figure 3-2 A. Cells treated with Sal/Sal distributed mainly in the AnnV-/PI- quadrant and remained unchanged from 24h to 48h. Similar findings were observed in Sal/TNF-treated cells. Cells treated with AMD/Sal or AMD/TNF distributed less in the AnnV-/PI- quadrant and more in the AnnV+/PI- and AnnV+/PI+ quadrants. A trend of cells moving from AnnV-/PI- to AnnV+/PI- and eventually to AnnV+/PI+ quadrant from 24h to 48h was observed after AMD/Sal and AMD/TNF treatments.

Percentages of cells distributed in AnnV+/PI- and AnnV+/PI+ quadrants were calculated and plotted in Figure 3-2 B. The percent of Sal/Sal-treated cells in these two quadrants was small (<7%) at both times. Treatment with Sal/TNF did not change the percentage of the AnnV+/PI- cells or the AnnV+/PI+ cells. At 24h, AMD/Sal treatment caused a slight increase in AnnV+/PI- cells but did not affect the percentage of AnnV+/PI+ cells. At 48h, AMD/Sal increased the percent of both AnnV+/PI- cells and AnnV+/PI+ cells. TNF enhanced the AMD-induced elevation of AnnV+/PI- cells and AnnV+/PI+ cells at both times.

DNA strand breaks and total DNA content assessment after AMD and/or TNF treatment

One of the later steps in apoptosis is endonuclease-mediated DNA degradation of higher order chromatin structure into fragments ~300 kb. This is followed by internucleosomal DNA laddering, resulting in fragments of ~180 bp or its multiples (e.g. 360, 540 bp) (Wyllie 1980). Loss of DNA fragments from the cell results in hypodiploid cells (cells with DNA content less than normal diploid cells in G1 phase of the cell cycle).

Measuring hypodiploid cells is an alternative way to assess apoptotic cell death (Nicoletti *et al.* 1991).

Dot plots for TUNEL staining vs total DNA content and corresponding histogram plots for total DNA content in Hepa1c1c7 cells treated with AMD and/or TNF are shown in Figure 3-3. Very few TUNEL-positive cells were observed in the Sal/Sal and Sal/TNF treatment groups (<2%) at either 24h or 48h. AMD alone increased the percentage of TUNEL-positive cells at 24h (~11%) and 48h (~33%), and TNF cotreatment significantly enhanced these values (17% at 24h and 75% at 48h). A similar trend was observed in the percent of hypodiploid cells. Sal/Sal- and Sal/TNF- treated groups had very small percentages of hypodiploid cells (<2%). TNF cotreatment enhanced the AMD-induced effect to increase the percentage of hypodiploid cells at both 24h (7% to 14%) and 48h (14% to 33%).

AMD/TNF-induced morphological changes in Hepa1c1c7 cells

Cell size and granularity changes of Hepa1c1c7 cells treated with AMD and/or TNF were assessed from dot plots of forward scatter (FSC) vs side scatter (SSC) from AnnV/PI staining. The majority of the Sal/Sal-treated cells were stellate-shaped with small nucleus-to-cytoplasm ratio and prominent nucleoli (Figure 3-4 A1). These cells were likely the population colored in green in Figure 3-4 B1, as they were relatively large. This population of cells did not stain with either AnnV or PI (AnnV-/PI-) (Figure 3-4 C1). A very small portion of the Sal/Sal-treated cells were smaller in size, which had relatively round-shape (less stellate), large nucleus-to-cytoplasm ratio with, darkly stained cytoplasm and indistinct nucleoli (Figure 3-4 A1). These cells were likely the

population colored in red in Figure 3-4 B1. Most of these cells were AnnV+/PI+ (Figure 3-4 C1). Similar observations were found in Sal/TNF treated-cells (Figure 3-4 A2~C2).

In the AMD/Sal-treated group, there was a significant decrease in the number of stellate-shaped cells, and an increase in the smaller, darker stained, round cells with larger nucleus-to-cytoplasm ratio (Figure 3-4 A3). The shift of cell population from bigger size (green gate) to smaller size (red gate) was seen in Figure 3-4 B3. In Figure 3-4 C3, the green population appeared AnnV-/PI-, which was similar to the green population after treatment with Sal/Sal or Sal/TNF. However, a large portion of the red population was also AnnV-/PI-, indicating that the smaller sized cells in this treatment had not the transited from healthy to apoptotic

In the AMD/TNF-treated group, most of the cells were small and round-shaped and had higher nucleus-to-cytoplasm ratio and smaller nuclear size (Figure 3-4 A4). The green population was almost absent (Figure 3-4 B4). Most of the red population were distributed in AnnV+/PI- and AnnV+/PI+ (Figure 3-4 C4), indicating that they were in the transition from early apoptosis to late apoptosis.

Caspases activation and effect of caspases inhibitors

Caspase 9 activity was unaffected by treatment of Hepa1c1c7 cells with AMD or TNF alone (Figure 3-5 A). Cotreatment with AMD/TNF caused a 2-fold increase in caspase 9 activity by 12h that was sustained through 48h. AMD alone caused a less than 2-fold increase in caspase 3/7 activity from 12h through 48h (Figure 3-5 B). TNF alone did not affect caspase 3/7 activity but greatly increased caspase 3/7 activation caused by AMD. The AMD/TNF-induced increase in caspase 3/7 activity remained

around 3 fold from 12h to 24h and reached 7 fold by 48h (Figure 3-5 B). Caspase 8 activity was unchanged by any of the treatments at any time (data not shown).

The effects of 3 different caspase inhibitors on AMD/TNF-induced cyotoxicity were evaluated (Figure 3-6). Without the caspase inhibitors, baseline LDH release from Sal/Sal groups was around 20%. AMD alone or TNF alone caused a mild increase in LDH release (~30%), and AMD/TNF cotreatment enhanced LDH release (~70%). Caspase inhibitors did not cause any cytotoxicity by themselves and did not affect the cytotoxicity caused by AMD alone. Z-VAD (pancaspase) or Ac-DEVD (caspase 3/7) slightly attenuated the cytotoxicity caused by TNF alone. Z-VAD, z-LEHD (caspase 9) or Ac-DEVD slightly decreased the AMD/TNF-induced LDH release by 5 to 10% (Figure 3-6 A~C).

ROS generation and effect of water-soluble antioxidants on AMD/TNF-induced cytotoxicity

TNF alone did not cause an increase in ROS generation compared to Sal/Sal treatment (Figure 3-7 A). Elevated ROS production in the AMD-treated group started between 1h and 6h, and remained at the same level through 24h. TNF potentiated AMD-induced ROS at all times from 6h through 24h. Representative pictures for each treatment group at 6h are shown in Figure 3-7 B: bright green fluorescence from DCF was evenly spread throughout entire cells in AMD- and AMD/TNF-treated groups.

TNF alone or AMD alone induced minor LDH release, whereas TNF/AMD cotreatment caused a significant increase (Figure 3-8). Water soluble antioxidants caused very minor changes in Sal/Sal-, Sal/TNF- or AMD/Sal-induced LDH release. Trolox slightly increased LDH release from Sal/Sal and Sal/TNF treatments; NAC

decreased LDH release from Sal/TNF treatment; and ASC decreased LDH release from Sal/TNF and AMD/Sal treatments. All 4 water soluble antioxidants decreased AMD/TNF-induced LDH release, but the decreases were minor (5 to 10%).

Lipid peroxidation and the effect of lipid soluble antioxidant on AMD/TNF-induced cytotoxicity

Lipid peroxidation was assessed by measuring the fold changes of BODIPY green fluorescence (Figure 3-9 A). TNF alone did not increase BODIPY green fluorescence compared to Sal/Sal treatment. AMD alone caused a 2-fold increase by 6h, which was sustained through 24h. TNF enhanced AMD-induced changes in BODIPY green fluorescence from 6h through 24h. Representative images at 6h are presented in Figure 9 B. Sal/Sal- and Sal/TNF- treated cells were dim and homogeneous. Intracellular bright spots with greater intensity were seen after treatment with AMD alone, and these were more pronounced in AMD/TNF-treated cells.

Lipid peroxidation and ROS generation were quantified after the addition of the lipid soluble antioxidant, TOCO. Lipid peroxidation was not observed in Sal/Sal- and Sal/TNF-treated cells, and addition of TOCO was without effect (data not shown). The lipid peroxidation caused by AMD alone and by AMD/TNF was completely prevented by addition of TOCO (Figure 3-10 A). There was no ROS generation in the absence of AMD and no change with TOCO (data not shown). TOCO attenuated the ROS generation in cells treated with AMD alone or AMD/TNF (Figure 3-10 B).

The effects of TOCO on AMD- and/or TNF-induced cytotoxicity were tested at 48h (Figure 3-10 C). TOCO, at concentrations of 100μM and 200μM, significantly

reduced the cytotoxicity caused by AMD alone. At concentrations of 50μM-200μM, TOCO diminished the cytotoxicity caused by AMD/TNF cotreatment.

The effect of TOCO on caspase 3/7 activation was measured at 48h (Figure 3-10. D). TOCO did not affect the minor activation of caspase 3/7 caused by TNF alone, but it slightly increased the activation of caspase 3/7 in cells treated with either AMD alone or AMD/TNF.

Effect of combined inhibition of caspase activation and lipid peroxidation on AMD/TNF-induced cytotoxicity

The effect of combined treatment with TOCO and z-VAD was explored at 48h in cells treated with AMD and/or TNF. As seen in Figure 3-11, z-VAD slightly attenuated the cytotoxicity caused by TNF alone or AMD alone. TOCO abolished the cytotoxity of AMD alone, but did not affect the cytotoxity of TNF. Combination of the two completely abolished the cytotoxicity caused by AMD/TNF, in which TOCO provided a major contribution and z-VAD played a minor role.

Figure 3-1 TNF potentiation of AMD cytotoxicity

A, Hepa1c1c7 cells were treated with AMD and TNF at the concentrations indicated. After 48h incubation, the release of LDH was determined as described in the Materials and Methods. B, Hepa1c1c7 cells were treated with 35μM AMD and/or 3ng/ml TNF, and the release of LDH was measured at the indicated times. *significantly different from respective groups not given TNF; #significantly different from respective groups not given AMD. $p < 0.05$, n=4-6.

Figure 3-1 (cont'd)

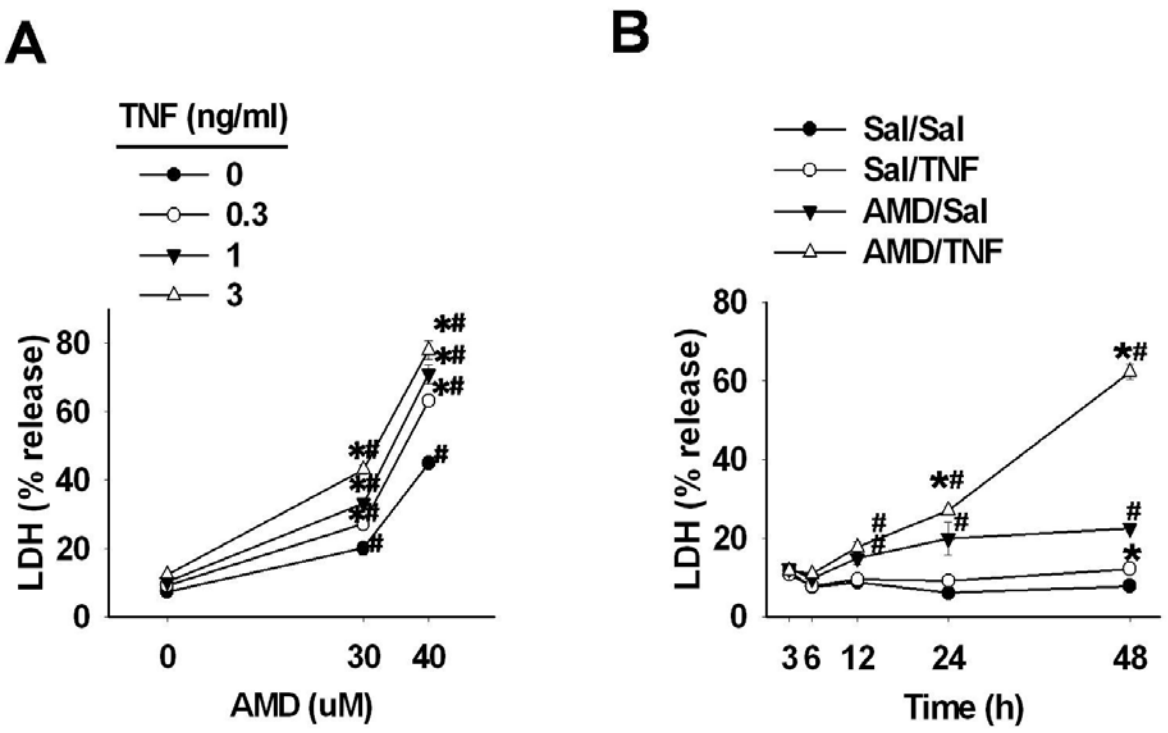

Figure 3-2 Annexin V/propidium iodide staining after AMD and/or TNF treatment

Hepa1c1c7 cells were exposed to 35μM AMD and/or 3ng/ml TNF for 24h or 48h and then stained with Annexin V (AnnV) and propidium iodide (PI) as described in the Materials and Methods. Quadrant cut-offs were determined from Sal/Sal-treated cells (negative control) and STS-treated cells (positive control). A, representative dot plots at 24h and 48h. B, percent of AnnV+/PI- cells. C, percent of AnnV+/PI+ cells. *significantly different from respective groups not given TNF; #significantly different from respective groups not given AMD. $p < 0.05$, n=4.

Figure 3-2 (cont'd)

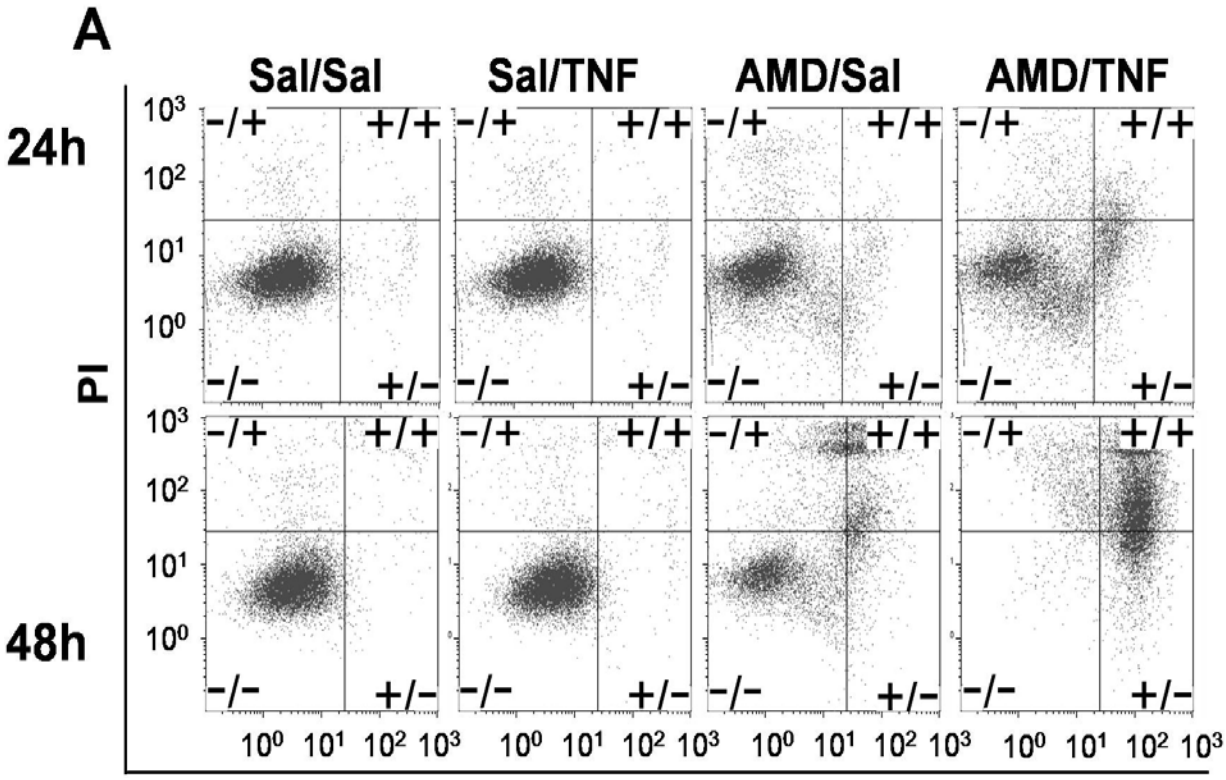

Figure 3-2 (cont'd)

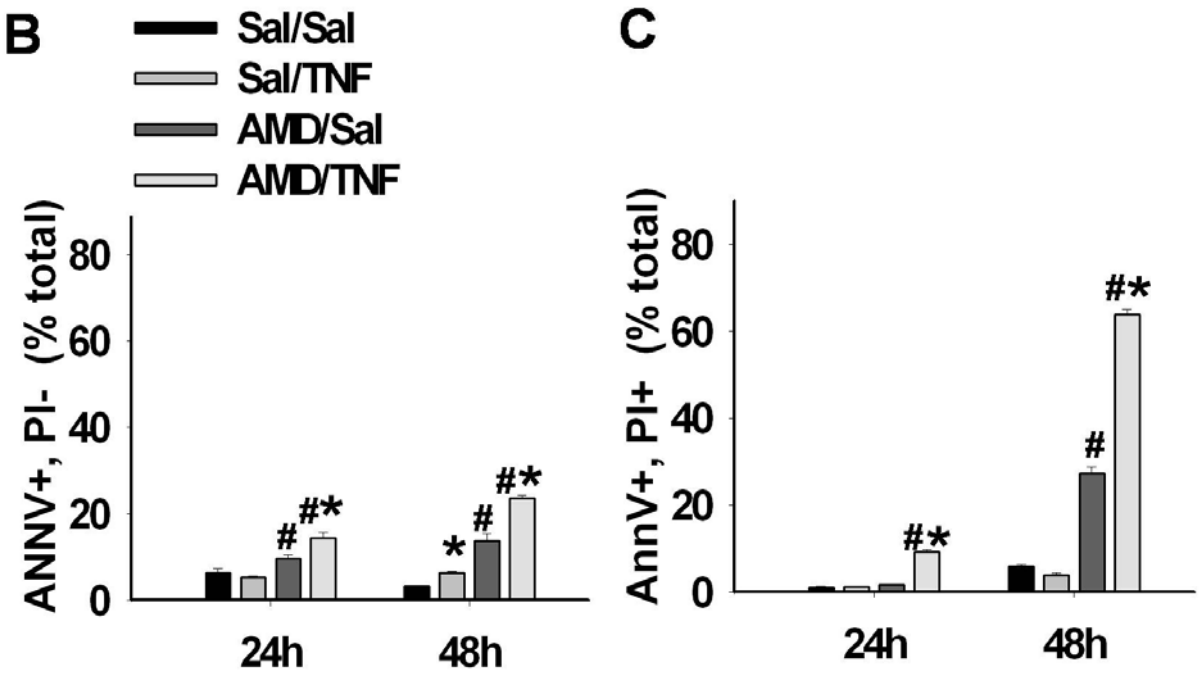

Figure 3-3 TUNEL staining after AMD and/or TNF treatment

Hepa1c1c7 cells were exposed to 35μM AMD and/or 3ng/ml TNF for 24h or 48h and then stained with TUNEL as described in the Materials and Methods. A, dot plots (TUNEL vs Total DNA) and corresponding histogram plots (cell count vs total DNA) at 24h. B, dot plots (TUNEL vs Total DNA) and corresponding histogram plots (Cell count vs Total DNA) at 48h.

Figure 3-3 (cont'd)

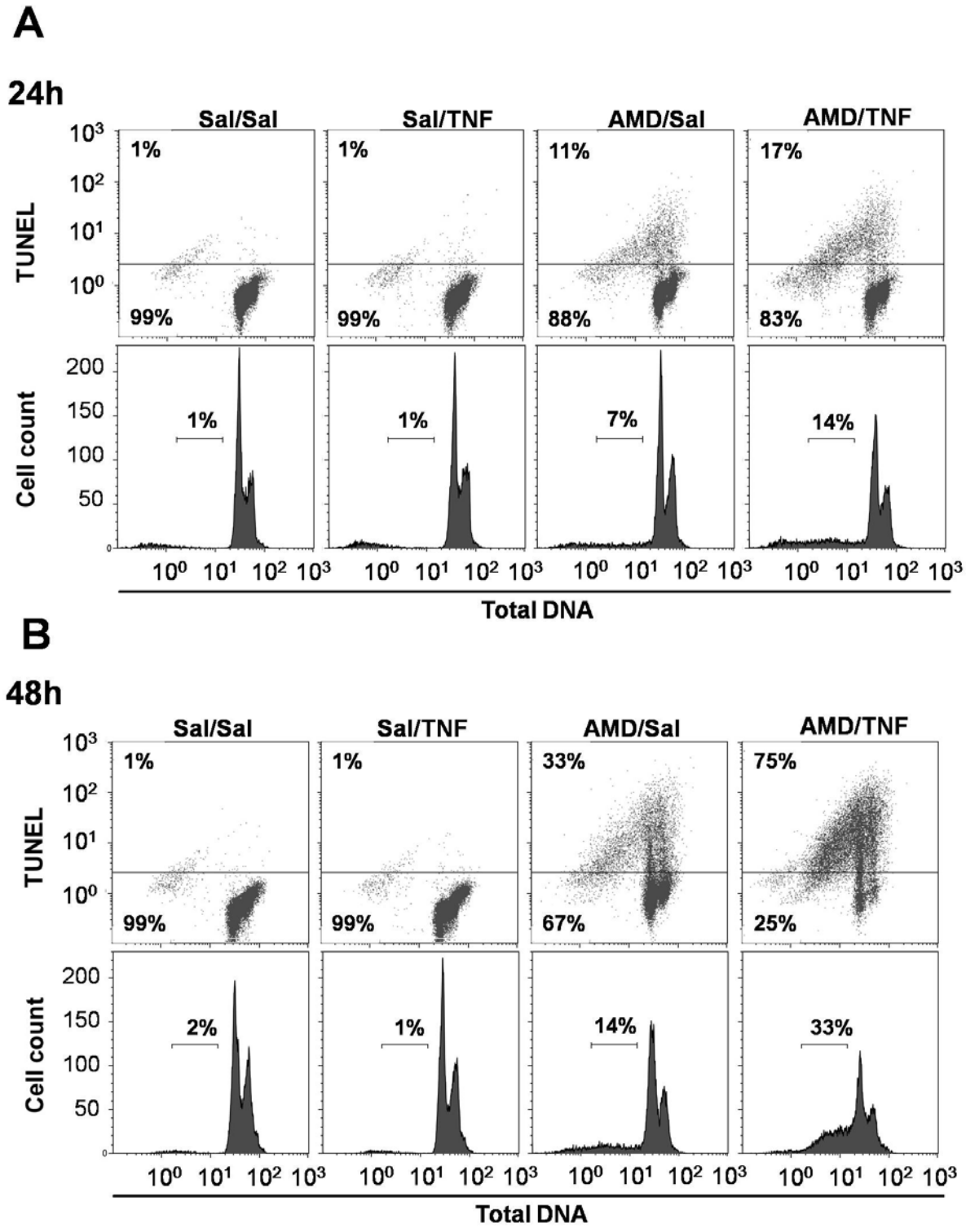

Figure 3-4 Morphological changes after AMD and/or TNF treatment.

Hepa1c1c7 cells were treated with 35μM AMD and/or 3ng/ml TNF for 48h. A, cells were stained with modified Wright's method as described in the Materials and Methods. Images from light microscopy were collected. B-C, cells were stained with AnnV/PI as described in the Materials and Methods. B, dot plots for forward scatter (FSC) vs side scatter (SSC). Gates distinguishing the small (RED) and large (GREEN) subgroups were drawn based on Sal/Sal treatment. C, dot plots for AnnV vs PI. Quadrant cut-offs were determined from Figure 3-2. GREEN and RED colors were derived from corresponding groups in plot B. (Row1, Sal/Sal; Row2, Sal/TNF; Row3, AMD/Sal; Row4, AMD/TNF)

Figure 3-4 (cont'd)

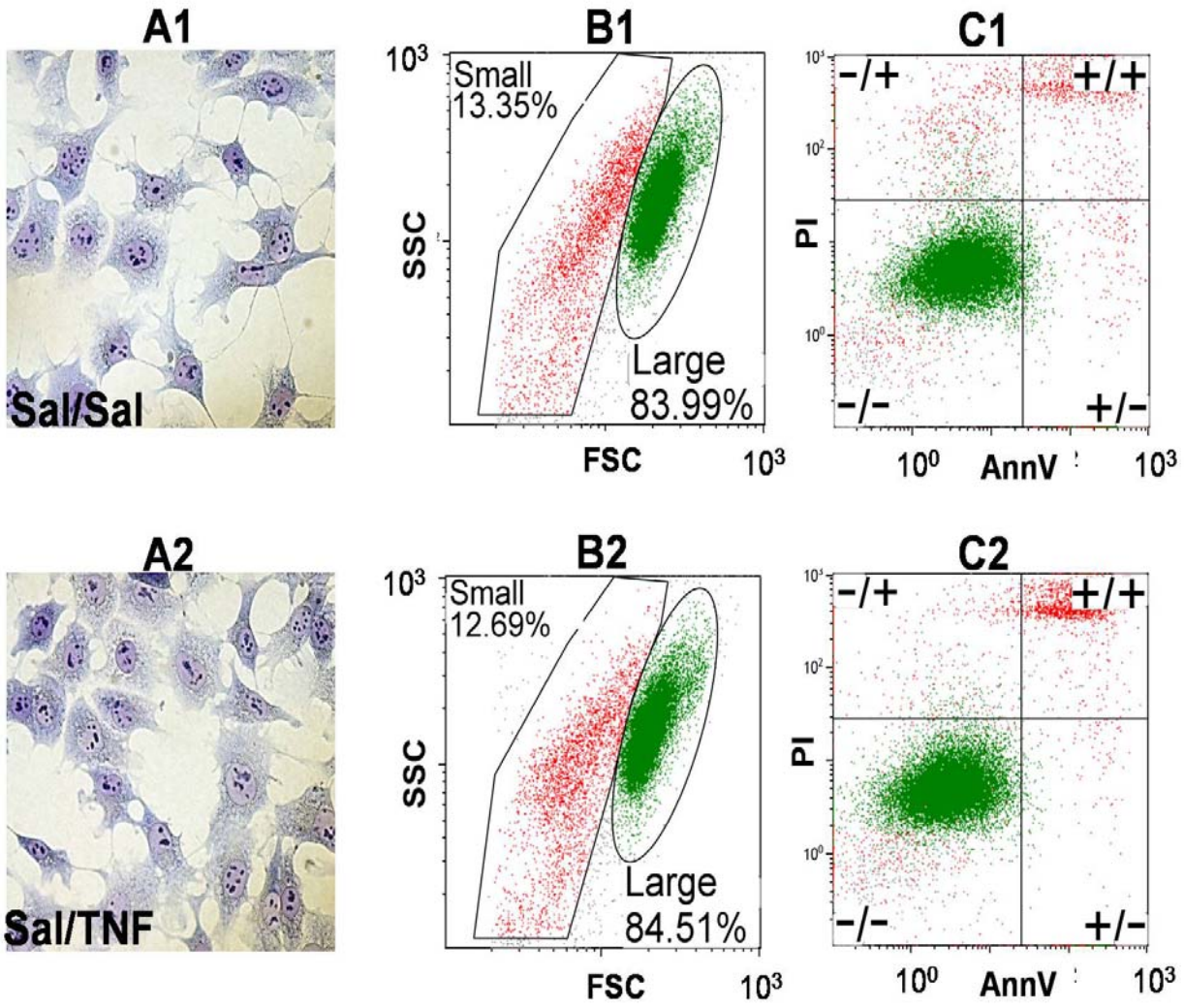

Figure 3-4 (cont'd)

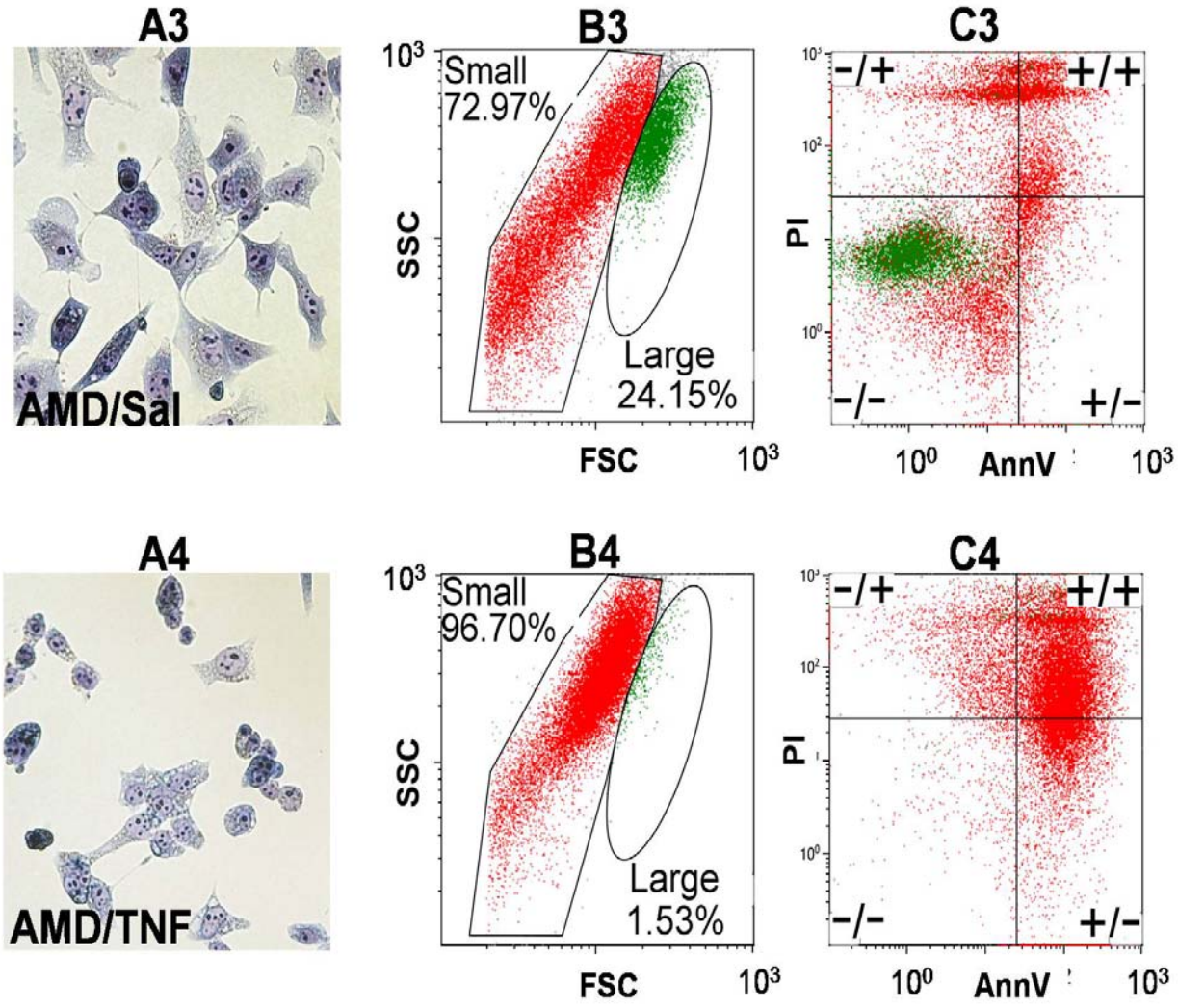

Figure 3-5 Activities of caspases after AMD and/or TNF treatment

Hepa1c1c7 cells were treated with 35μM AMD and/or 3ng/ml TNF for 1h, 12h, 24h or 48h, and activities of caspase 9 (A) and caspase 3/7 (B) were measured as described in the Materials and Methods. Results were presented as fold changes from Sal/Sal group. *significantly different from respective groups not given TNF; #significantly different from respective groups not given AMD. $p < 0.05$, n=3-5.

Figure 3-5 (cont'd)

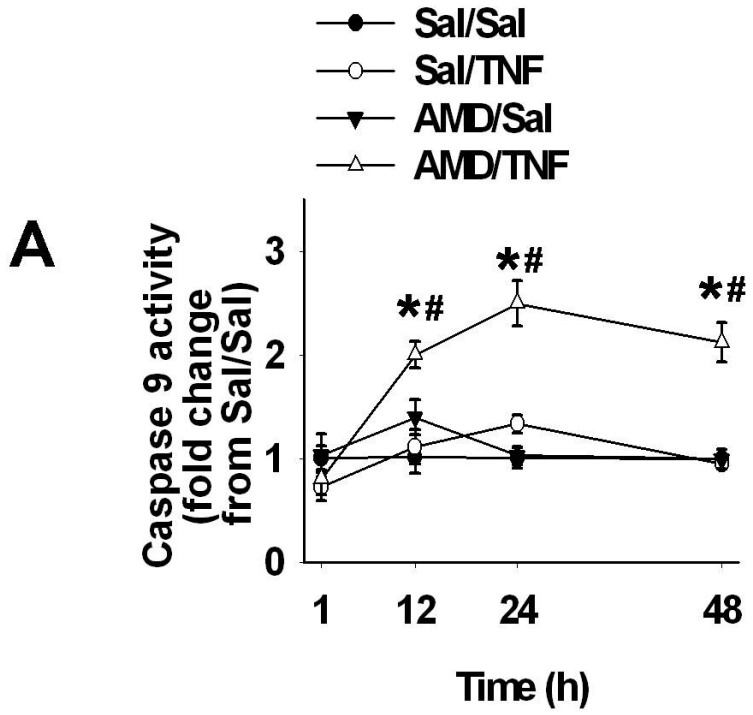

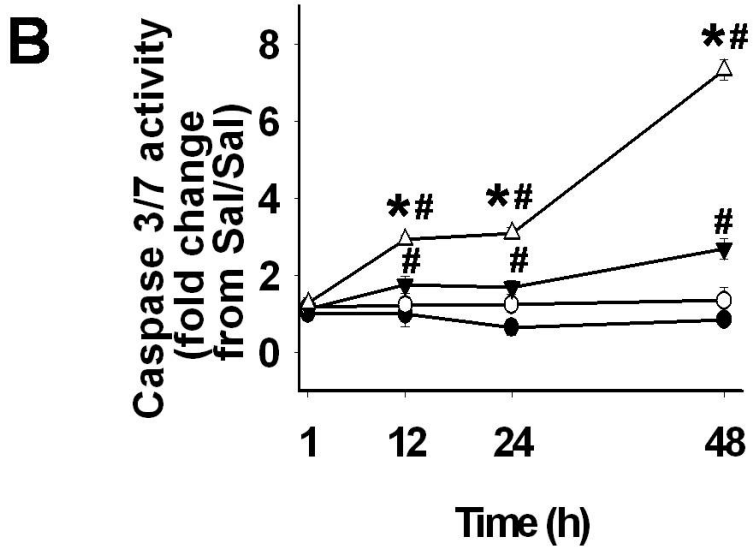

Figure 3-6 Protective effect of caspase inhibition on AMD/TNF-induced cytotoxicity

Hepa1c1c7 cells were treated with 35μM AMD and/or 3ng/ml TNF for 48h and with different caspase inhibitors or their vehicles: A, 40μM pancaspase inhibitor z-VAD-FMK; B, 20μM caspase 9 inhibitor z-LEHD-FMK; C, 40μM caspase 3/7 inhibitor Ac-DEVD-CHO; LDH release was measured as described in the Materials and Methods. *significantly different from respective groups not given TNF; #significantly different from respective groups not given AMD; @significantly different from respective groups not given caspase inhibitor. $p < 0.05$, n=3-6.

Figure 3-6 (cont'd)

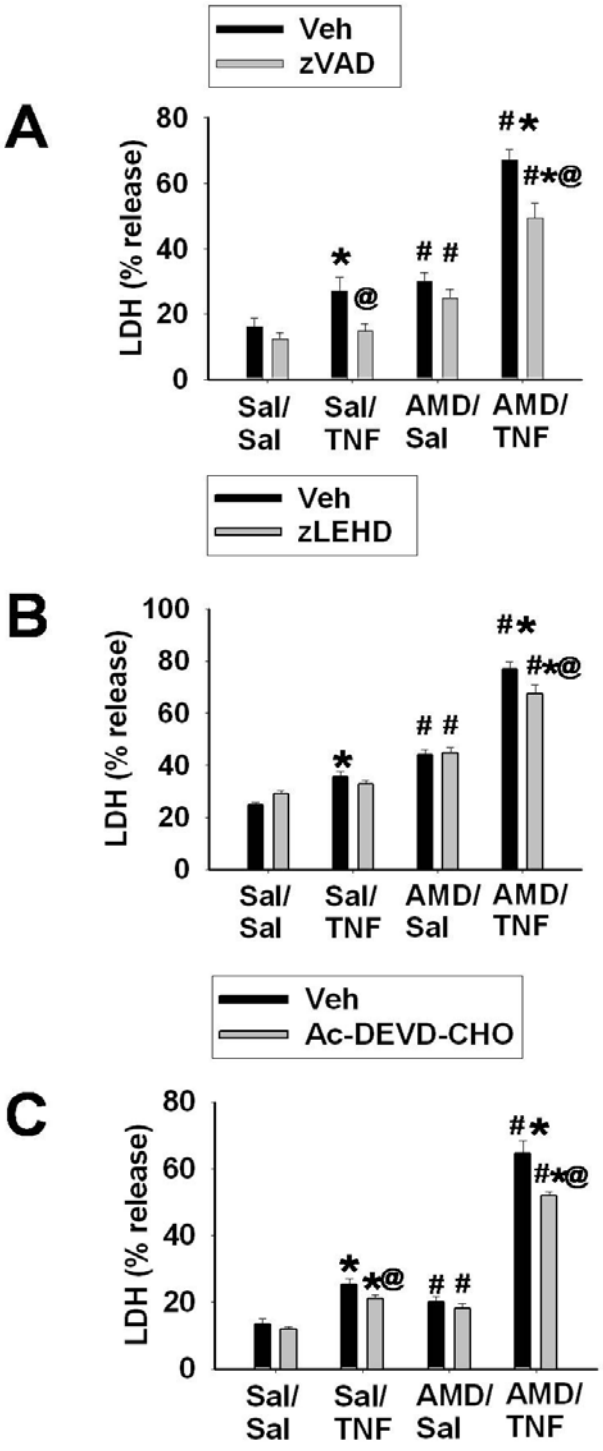

Figure 3-7 ROS generation in cells treated with AMD and/or TNF

Hepa1c1c7 cells were treated with 35μM AMD and/or 3ng/ml TNF for 1h, 6h, 12h or 24h and stained with CM-H_2DCFDA for intracellular ROS generation as described in the Materials and Methods. A, DCF fluorescence presented as fold change from Sal/Sal group; B, representative pictures for each treatment group at 6h. *significantly different from respective groups not given TNF; #significantly different from respective groups not given AMD. $p < 0.05$, n=3.

Figure 3-7 (cont'd)

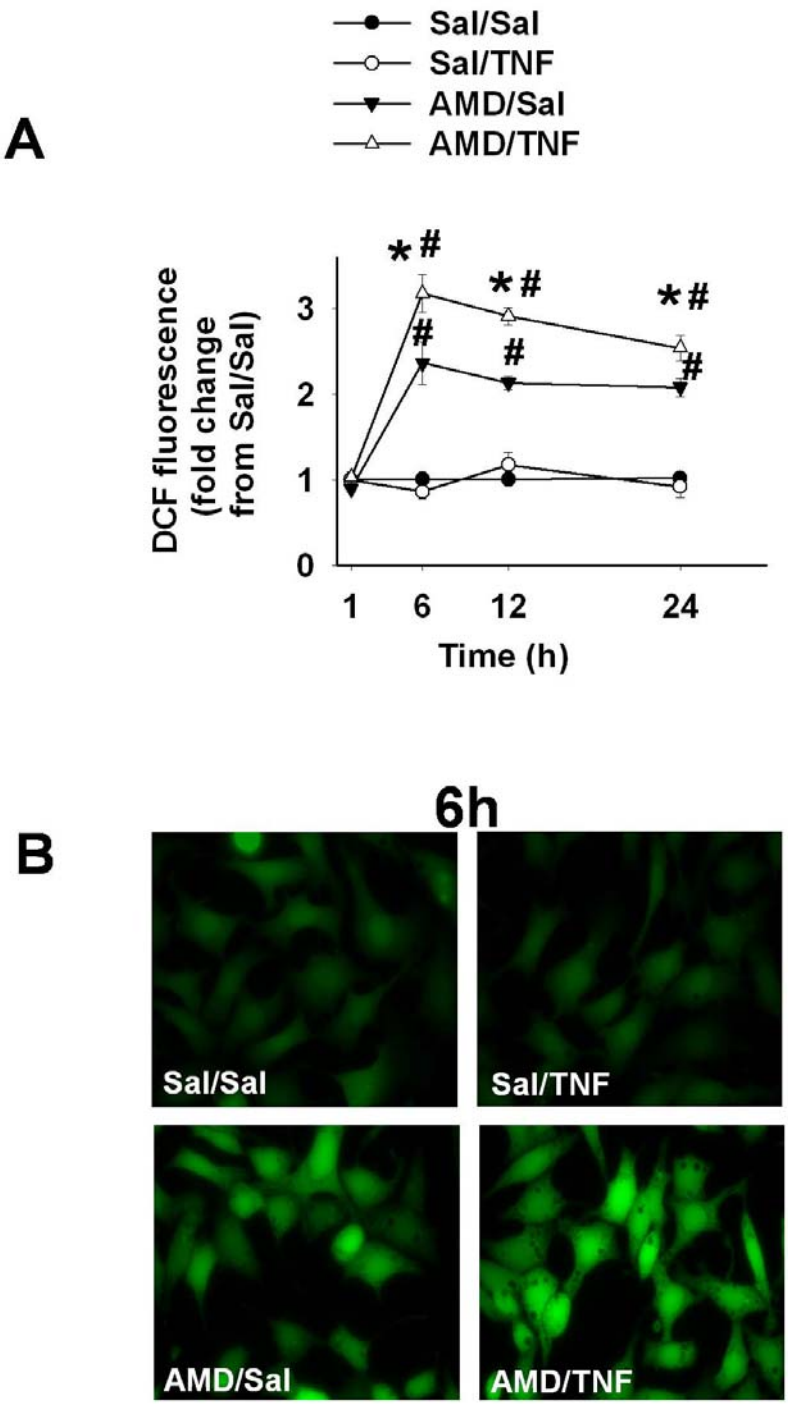

Figure 3-8 Protective effect of water-soluble antioxidants on AMD/TNF-induced cytotoxicity

Hepa1c1c7 cells were treated with 35μM AMD and/or 3ng/ml TNF for 48h, with different water-soluble antioxidants or saline: A, 400μM Trolox; B, 1mM glutathione (GSH); C, 1mM N-acetylcysteine (NAC); D, 2mM L-ascorbic acid (ASC). LDH release was measured as described in the Materials and Methods. *significantly different from respective groups not given TNF; #significantly different from respective groups not given AMD; @significantly different from respective groups not given antioxidant. $p < 0.05$, n=3-6.

Figure 3-8 (cont'd)

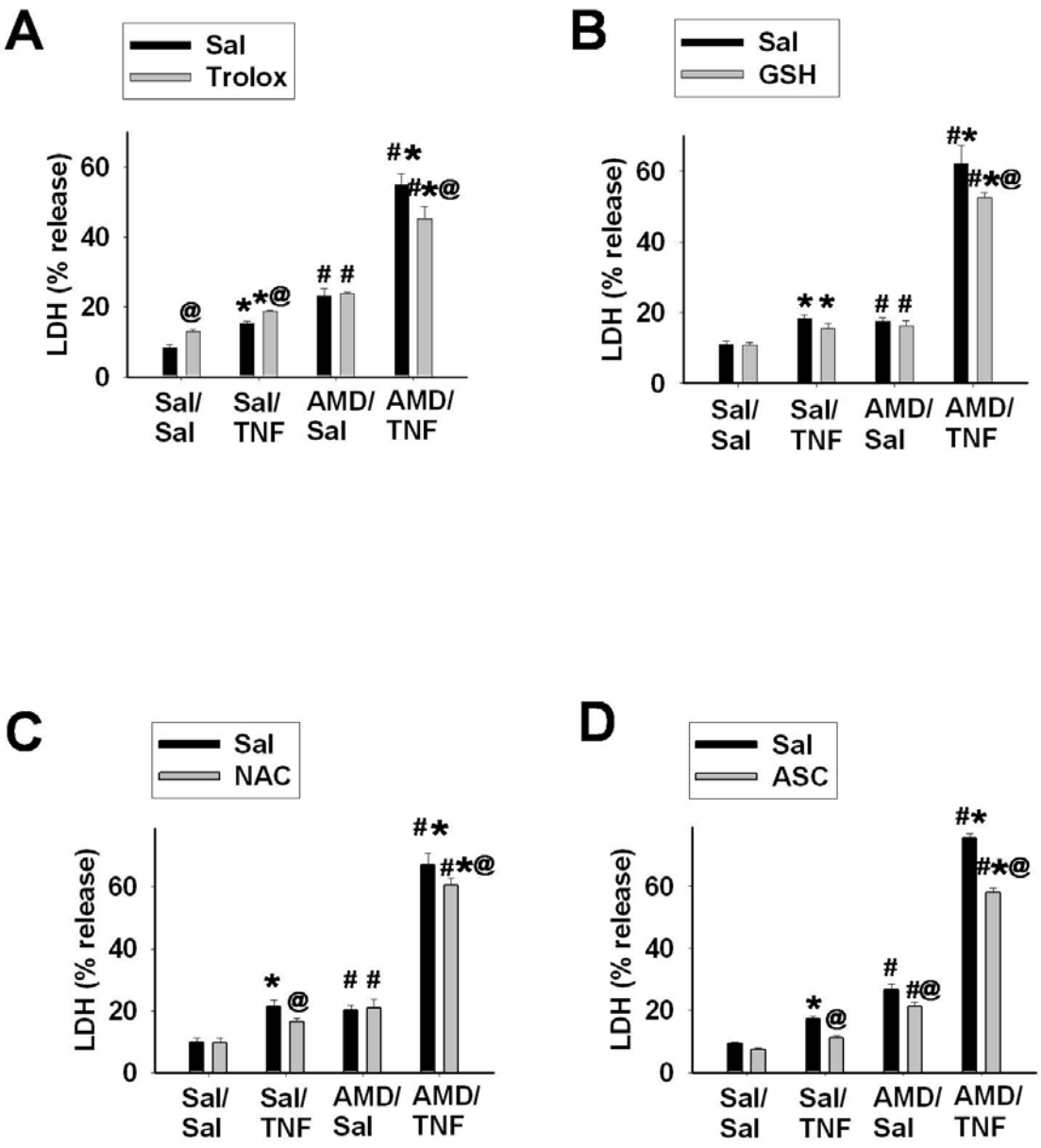

Figure 3-9 Lipid peroxidation in cells treated with AMD and/or TNF

Hepa1c1c7 cells were exposed to 35μM AMD and/or 3ng/ml TNF for 1h, 6h, 12h or 24h and stained with C11-BODIPY581/591 as described in the Materials and Methods. The green fluorescence from oxidized BODIPY was quantified as an indication of lipid peroxidation. A, fluorescence from oxidized BODIPY represented as fold changes from Sal/Sal group; B, representative pictures for each treatment group at 6h. *significantly different from respective groups not given TNF; #significantly different from respective groups not given AMD. $p < 0.05$, n=3.

Figure 3-9 (cont'd)

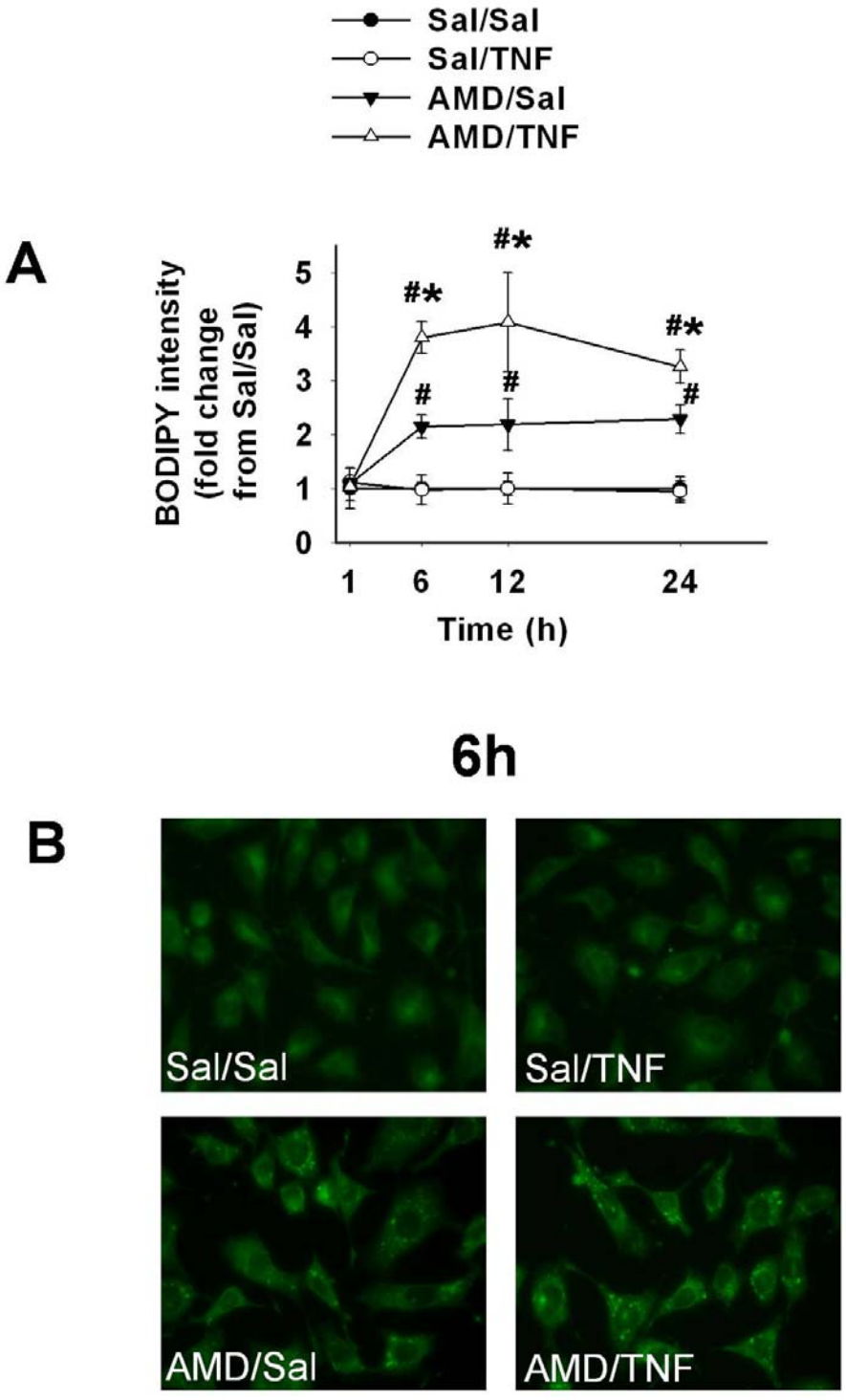

Figure 3-10 Protective effect of α-tocopherol on AMD/TNF-induced cytotoxicity

Hepa1c1c7 cells were treated with 35μM AMD and/or 3ng/ml TNF, together with α-tocopherol (TOCO, 100μM) or its vehicle. After incubation for indicated time, ROS generation (A) and lipid peroxidation (B) were measured as described in the Materials and Methods. C, TOCO was added to the medium at the concentrations indicated, and LDH release was measured after 48. D, 100μM TOCO or vehicle was added to the medium, and caspase 3/7 activity was measured after 48h. *significantly different from respective groups not given TNF; #significantly different from respective groups not given AMD; @significantly different from respective groups not given antioxidant. $p < 0.05$, n=3-5.

Figure 3-10 (cont'd)

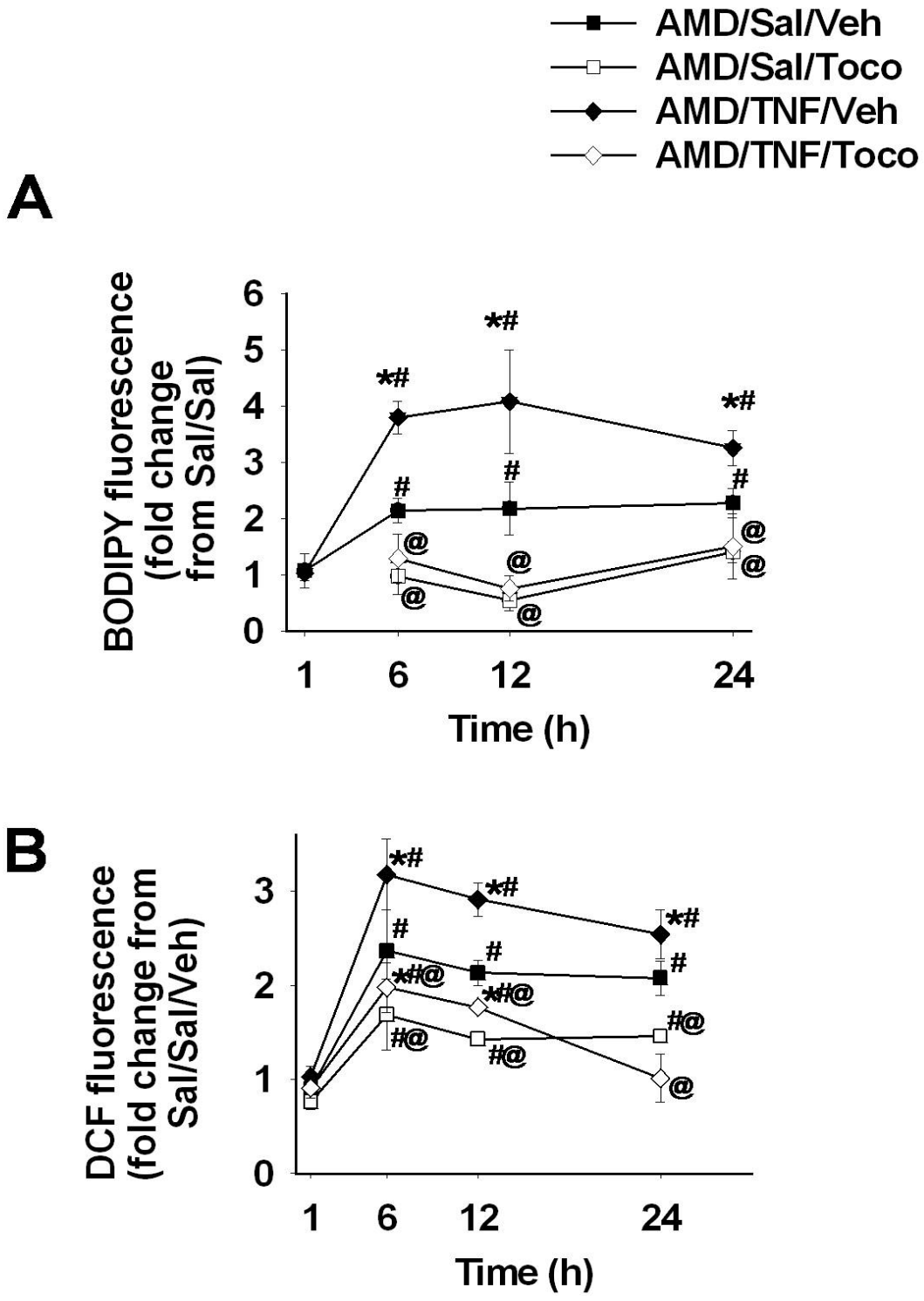

Figure 3-10 (cont'd)

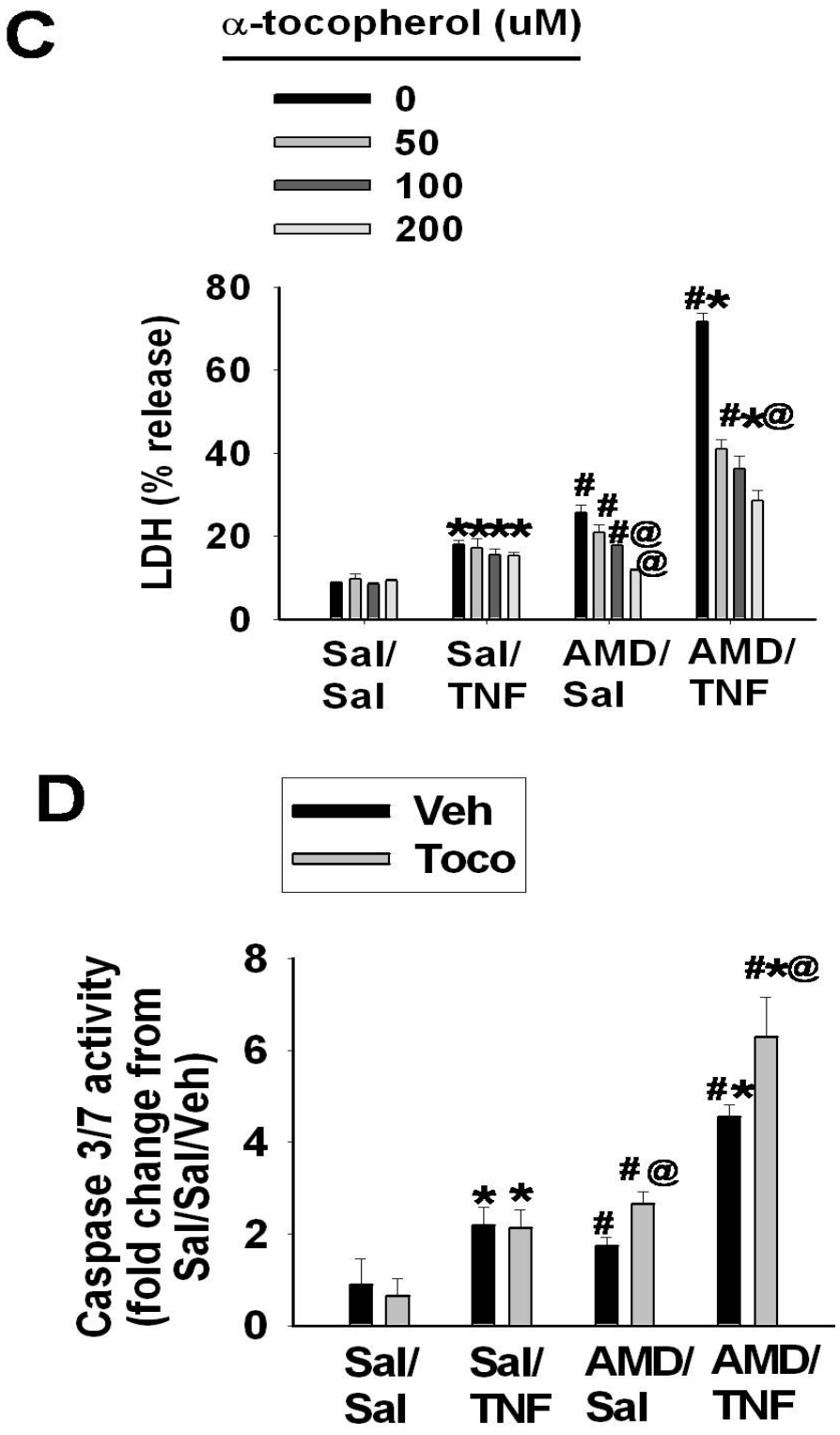

Figure 3-11 Effect of α-tocopherol and pancaspase inhibition on AMD/TNF-induced cytotoxicity

Cells were treated with 35μM AMD and/or 3ng/ml TNF, and TOCO (100μM) and/or zVAD (40μM) were added to the incubation medium. After 48h, LDH release was measured as described in the Materials and Methods. *significantly different from respective groups not given TNF; #significantly different from respective groups not given AMD; @significantly different from respective groups not given TOCO; b, significantly different from respective groups not given zVAD.

Figure 3-11 (cont'd)

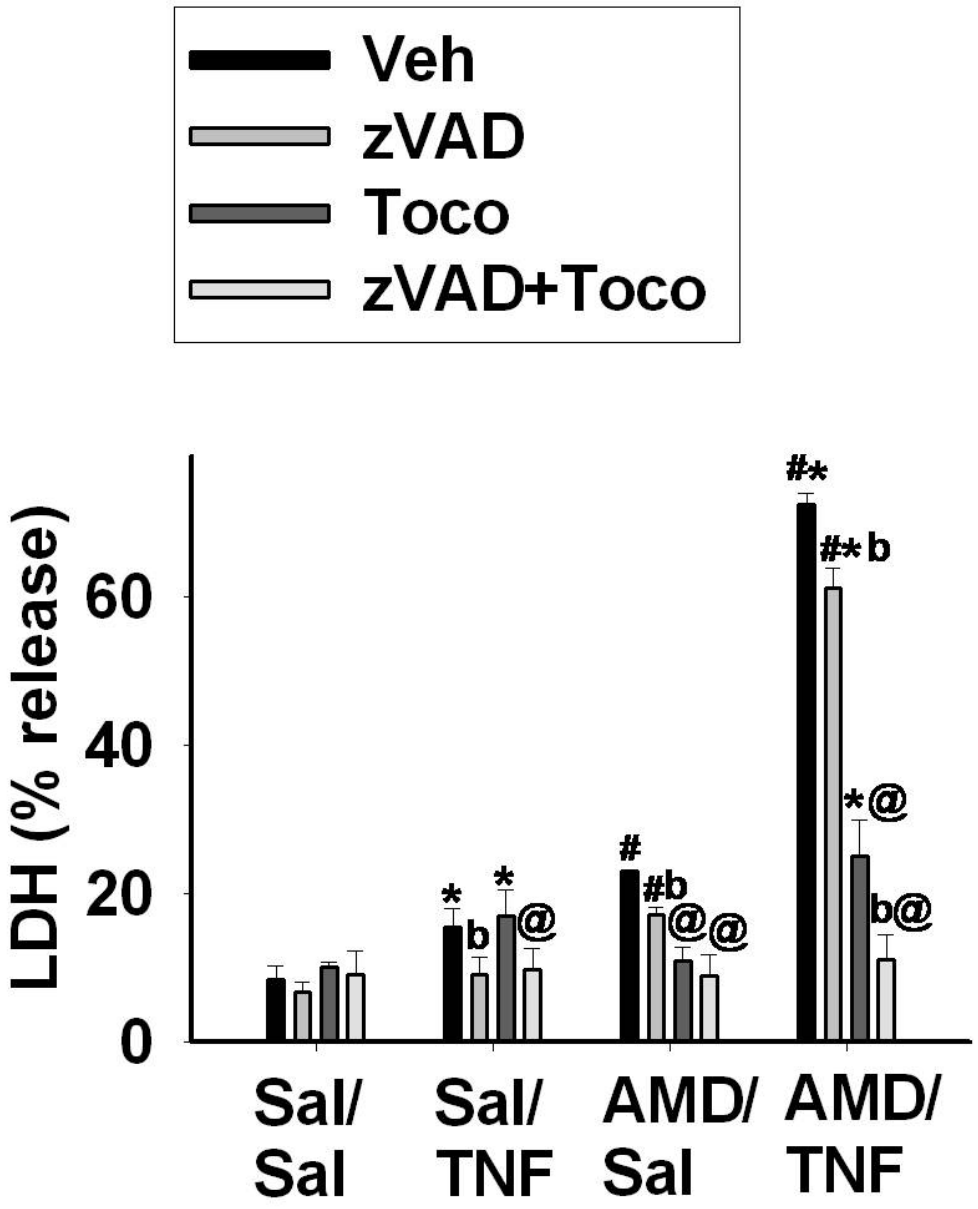

3.5 Discussion

As the pivotal cytokine induced by LPS administration, TNF is necessary for liver injury caused by AMD/LPS cotreatment in rats (Lu *et al.* 2012). One mechanism by which TNF might contribute to toxicity in this model is through the sensitization of hepatocytes to AMD-mediated toxicity. We previously reported that TNF potentiated AMD toxicity in Hepa1c1c7 cells during 24h incubation. We extended these findings in the present studies by using longer incubation duration and explored potential mechanisms of cell death. A greater difference between treatment with AMD alone and AMD/TNF was observed in the extent of cytotoxicity during this prolonged incubation (48h), possibly because the cytotoxic effects of AMD and TNF need longer time to accumulate and interact to precipitate cell death.

TNF administered together with certain other agents causes cell death in many cell types, including hepatocytes (Leist *et al.* 1994). TNF induces cell death mainly through an apoptotic pathway (Hentze *et al.* 2004; Jones *et al.* 2000). On the other hand, AMD induces cell death through pathways that vary among different cell types (Kaufmann *et al.* 2005; Mulder *et al.* 2011). The progression of cells from the AnnV-/PI- to AnnV+/PI- and then to AnnV+/PI+, detection of TUNEL-positive cells and observation of hypodiploid cells (Figure 3-2 and 3-3) all suggested that apoptosis occurred in cells treated with AMD alone or with AMD/TNF. Morphological changes, such as cytosolic shrinkage and nuclear fragmentation, supported this argument (Figure 3-4). That the percentage of AnnV+/PI+ and TUNEL-positive cells was similar to the percentage of LDH released into the medium suggested that apoptosis was the main cell death pathway. Similar findings were reported in AMD-treated (100uM, 8h) rat hepatocytes, in

which cytochrome *c* release, chromatin condensation, chromatin fragmentation and AnnV+/PI+ staining were all suggestive of an apoptotic cell death pathway (Kaufmann *et al.* 2005).

TNF-induced apoptosis in the presence of either an inhibitor of NF-κB or an inhibitor of transcription involved activation of caspases 8 and 3/7 (Jones *et al.* 1999b). AMD can also induce caspases 8 and 3/7 in a variety of cell types (Isomoto *et al.* 2006; Yano *et al.* 2008). In hepatocytes, activated caspase 8 cannot directly activate downstream caspase 9 or caspase 3/7. Instead, activated caspase 8 will cleave BH3-interacting domain death agonist (BID) into its truncated and active form, tBID, which in turn leads to release of cytochrome *c* and other proapoptotic mediators from mitochondria. These mitochondrial factors can then activate caspase 9 and eventually caspase 3/7. In this study, caspases 9 and 3/7 were activated after AMD/TNF cotreatment, whereas caspase 8 was not (Figure 3-5). Mitochondrial damage, which is the bridging step between caspase 8 and caspase 9 in TNF-induced apoptotic signaling cascades (Wullaert *et al.* 2007), is the most probable site where AMD and TNF had synergistic effect.

Inhibition of caspases activation can attenuate or abolish the cytotoxicity caused by TNF in the presence of an inhibitor of NF-κB (Jones *et al.* 1999a) or by AMD alone (Bargout *et al.* 2000). However, in this study, the same pancaspase inhibitor used in those studies did not affect the AMD-induced cytotoxicity and had only a very minor effect against the cytotoxicity caused by AMD/TNF. Similar results were found with inhibitors of caspase 9 and caspase 3/7 (Figure 3-6). These results suggest that caspase activation plays a minor role in AMD/TNF-induced cytotoxicity. As we

speculate enhanced mitochondrial alterations were the cause of downstream caspase activation, it is highly possible that other effectors from the mitochondrial damage, e.g. ROS generation, act as major contributors to AMD/TNF-induced cytotoxicity.

In hepatocytes, increased ROS production induced by TNF is important to its cytotoxic effect, and the respiratory chain on the inner membrane of mitochondria is the major source of TNF-induced ROS (Corda *et al.* 2001). The cytotoxicity of AMD is also linked to its ability to alter mitochondrial function and induce ROS generation. AMD inhibited both complex I and II mediated-respiration (Bolt *et al.* 2001), induced mitochondrial swelling and permeability transition (Varbiro *et al.* 2003), and decreased mitochondrial membrane potential (Yano *et al.* 2008). In this study, TNF alone did not induce ROS, but it significantly potentiated the ROS generation caused by AMD (Figure 3-7). There are a variety of pathways in mitochondria that can lead to degradation or disproportionation of normally generated ROS (Feissner *et al.* 2009). It is possible that TNF caused a small increase in ROS that was rapidly inactivated by the mitochondrial antioxidative enzymes.

The observation that water soluble antioxidants caused but a small reduction in AMD/TNF cytotoxicity (Figure 3-8) suggested that water-soluble oxidants played a minor role in cytotoxicity from AMD alone or from AMD/TNF cotreatment. TNF enhanced AMD-induced lipid peroxidation (Figure 3-9), and the major protective role of a lipid soluble radical scavenger (TOCO) (Figure 3-10) suggested that radicals generated from peroxidized lipids were major contributors to the cytotoxicity. AMD can inhibit the degradation of lipids, leading to lysosomal phopholipodosis (Bhandari *et al.*

2008), so it is possible that phospholipids that accumulate lysosomes are more vulnerable to oxidative stress and could be the initiating point of lipid peroxidation.

The fact that TOCO did not decrease caspase3/7 activation (Figure 3-10) indicated that the protective effect of TOCO is not mediated by inhibition of this enzyme. Treatment with TOCO and the pancaspase inhibitor together led to full protection against AMD/TNF-induced cytotoxicity (Figure 3-11), suggesting that lipid peroxidation and activation of caspases contribute to AMD/TNF-induced cytotoxicity, probably through different pathways.

In summary, TNF cotreatment potentiated the cytotoxicity induced by AMD in Hepa1c1c7 cells. Enhanced activation of caspases and lipid peroxidation were two separate contributors to AMD/TNF-induced cytotoxicity, and lipid peroxidation played the major role. These findings increase our understanding of the intracellular events that contribute to the potentiation of AMD cytotoxicity by TNF, a phenomenon that might underlie AMD-induced liver injury in humans.

Acknowledgments

The authors are grateful to Nicole Crisp for technical assistance in flow cytometry. This research is supported by grant R01DK061315 from the National Institutes of Health (NIH).

CHAPTER 4

Roles of the hemostatic system and neutrophils in liver injury from coexposure to amiodarone and lipopolysaccharide

Jingtao Lu, Robert A. Roth, Ernst Malle, Patricia E. Ganey

4.1 Abstract

Idiosyncrasy-like liver injury was induced by cotreating rats with amiodarone (AMD) and lipopolysaccharide (LPS). Rats were treated with AMD (400 mg/kg, ip) or veh and 16h later with LPS (1.6 $\times 10^6$ EU/kg, iv) or saline. The elevation in alanine aminotransferase (ALT) activity in the serum and the appearance of necrotic foci in the liver started between 4h and 6h after LPS and progressed through 10h (Lu *et al*. 2012). In this study, the roles of the hemostatic system and neutrophils in AMD/LPS-induced liver injury were explored. AMD did not affect the hemostatic system by itself but significantly potentiated LPS-induced activation of thrombin in the coagulation system and plasminogen activator inhibitor-1 (PAI-1) in the fibrinolysis system. Increased hepatic fibrin deposition and hypoxia were observed only in AMD/LPS-treated animals, starting before the onset of liver injury. Administration of anticoagulant heparin abolished AMD/LPS-induced hepatic fibrin deposition and reduced AMD/LPS-induced liver damage. LPS caused hepatic polymorphonuclear neutrophil (PMN) accumulation by itself, but PMN activation was observed only in AMD/LPS-treated rats. Rabbit anti-rat PMN serum (NAS), which reduced the AMD/LPS-induced PMN accumulation and prevented PMN activation, attenuated AMD/LPS-induced liver injury in rats. PMN depletion did not affect hepatic fibrin deposition. Anticoagulation prevented PMN activation without affecting PMN accumulation. In summary, both hemostatic system activation and PMN activation contributed to AMD/LPS-induced liver injury in rats, and coagulation activation was critical for the activation of PMNs.

4.2 Introduction

Amiodarone (AMD) [2-butyl-3-(3',5'-diiodo-4'α-diethylaminoethoxybenzoyl)-benzofuran], a class III antiarrhythmic used to treat myocardial infarction and congestive heart failure, is known to cause idiosyncratic liver dysfunction in human patients (Rotmensch *et al.* 1984). Cases of severe liver reactions, or even fatalities caused by fulminant hepatic failure are reported after both long-term oral and acute intravenous administration of AMD (Babatin *et al.* 2008; Lewis *et al.* 1989; Ratz Bravo *et al.* 2005). Like other drugs that can cause idiosyncratic liver injury, AMD is not hepatotoxic by itself in naive laboratory animals. However, AMD can interact with modest inflammation caused by lipopolysaccharide (LPS), leading to pronounced hepatotoxicity in rats (Lu *et al.* 2012).

Tumor necrosis factor-alpha (TNF), a cytokine released upon LPS administration, is critically involved in AMD/LPS-induced liver injury. The roles of other LPS-induced proinflammatory mediators, e.g., the hemostatic system and/or innate immune cells, have not been reported. Through the activation of Kupffer cells, hepatocytes, sinusoidal endothelial cells and other cell types, LPS can lead to alterations in the hemostatic system, such as tissue factor (TF)-mediated thrombin generation and plasminogen activator inhibitor-1 (PAI-1)-induced impairment of fibrinolysis (Levi *et al.* 2003). In LPS-treated rodents, coexposure to drugs that cause idiosyncratic hepatotoxicity in people, specifically ranitidine (RAN), trovafloxacin (TVX) or sulindac (SLD), enhanced LPS-induced coagulation activation and PAI-1 expression, leading to a much greater degree of fibrin deposition, hypoxia and more importantly parenchymal cell damage in the liver (Luyendyk *et al.* 2004; Shaw *et al.* 2009b; Zou *et al.* 2009b). Inhibition of aerobic

metabolism, loss of ATP production and generation of reactive oxygen species, all of which are induced by hypoxia, can contribute to liver injury. Inhibition of coagulation by heparin significantly reduced the activation of coagulation and led to attenuated hepatotoxicity in these models.

Polymorphonuclear neutrophils (PMNs) are the most abundant type of leukocytes in the human body and form an essential part of the innate immune system. The main function of PMNs is to eliminate invading microorganisms and remove dead or dying cells. However, the proteases and reactive oxygen species released by activated PMNs can lead to tissue damage, rendering PMNs a contributor to the pathogenesis of many acute inflammatory diseases in the liver, e.g. endotoxemia (Jaeschke *et al.* 1991), alchoholic hepatitis (Bautista 1997), concanavalin A-induced liver injury (Bonder *et al.* 2004) and ischemia-reperfusion injury (Jaeschke *et al.* 1990). PMNs are also involved in animal models in which LPS potentiated hepatotoxicity, such as aflatoxin B1(Barton *et al*. 2000), monocrotaline (Yee *et al*. 2003), allyl alcohol (Kinser *et al.* 2004), RAN (Luyendyk *et al*. 2005), TVX (Shaw *et al.* 2009d) and SLD (Zou *et al*. 2011).

The purpose of this study was to test the hypothesis that the hemostatic system and PMNs are critically involved in AMD/LPS-induced liver injury in rats. When the results demonstrated a significant importance of both coagulation activation and neuptrophil activation, the causal relationship between the two was explored.

4.3 Materials and methods

Materials

Unless otherwise noted, all chemicals were purchased from Sigma-Aldrich (St Louis, MO). The activity of LPS (Lot 075K4038, derived from *Eschericia coli* serotype O55:B5) was 3.3×10^6 endotoxin units (EU)/mg, which was determined by a Limulus amebocyte lysate endpoint assay kit from Cambrex Corp. (Kit 50-650U; East Rutherford, NJ).

Animals

Male, Sprague-Dawley rats (Crl:CD(SD)IGS BR; Charles River, Portage, MI) weighing 250–370 g were used for *in vivo* studies. They were fed standard chow (Rodent Chow/Tek 8640; Harlan Teklad, Madison, WI) and allowed access to water *ad libitum*. Animals were allowed to acclimate for 1 week in a 12-hour light/dark cycle prior to experiments. They received humane care according to the criteria in the Guide for the Care and Use of Laboratory Animals.

Experimental protocol

In the experiments, rats were fasted for 12h before administration of LPS, and food was returned thereafter. A 20mg/kg solution of AMD was made in its vehicle (0.18% Tween 80), and 4.1×10^5 EU/ml solution of LPS was made in sterile saline. Rats were treated with AMD (400 mg/kg, ip) or veh and 16h later with LPS (1.6×10^6 EU/kg, iv) or saline. Rats were anesthetized with isoflurane, and blood and liver samples were taken. Serum and plasma (0.32% sodium citrate, final concentration) was prepared from blood.

The right medial lobe of the liver was rapidly frozen in liquid nitrogen for immunohistochemistry, and the left lateral lobe of liver was fixed for 12h in 10% neutral-buffered formalin and then stored in 70% ethanol for histopathology.

Evaluation of liver injury

Hepatic parenchymal cell damage was estimated from the activity of alanine aminotransferase (ALT) in serum. ALT activity was measured using Infinity-ALT reagent from Thermo Electron Corp. (Waltham, MA). Formalin-fixed liver samples were embedded in paraffin, sectioned and stained with hematoxylin and eosin (H&E staining). The stained liver sections were examined using light microscopy.

Evaluation of hemostatic system impairment, hepatic fibrin deposition and liver hypoxia

The plasma concentration of thrombin-antithrombin (TAT) dimer was determined with an ELISA kit (Enzygnost TAT Micro, Siemens Healthcare Diagnostics, Newark, DE). The plasma concentration of active PAI-1 was measured with Rat PAI-1 assay kit from Molecular Innovations, Inc (Novi, MI).

Immunohistochemical staining for hepatic fibrin deposition was as described previously (Copple *et al*. 2002). Briefly, frozen liver sections were fixed in 10% buffered formalin containing 2% acetic acid for 30 min at room temperature. This fixation procedure solubilizes all fibrinogen and fibrin monomers, leaving only cross-linked fibrin in the liver sections. Sections were blocked with 10% horse serum in phosphate buffered saline (PBS), incubated with goat anti-rat fibrinogen antibody (1:1000, ICN Pharmaceuticals, Aurora, OH) at 4 °C overnight, and then with Alexa 594-labeled

donkey anti-goat secondary antibody (1:1000, Molecular Probes) for 3 h at room temperature.

Pimonidazole (PIM), a 2-nitroimidazole hypoxia marker, was used to identify hypoxic regions in liver (Arteel *et al*. 1995). PIM hydrochloride (Hypoxyprobe-1 from HPI, Inc. Burlington, MA) was given to rats at 120 mg/kg, i.v., 2 h before they were euthanized. Immunohistochemical staining of PIM-adduct was performed as described previously (Copple *et al.* 2004).

Quantification of images from immunohistochemical staining

Quantification of images was performed using Image J software: the fraction of the area that was positively stained was measured in at least 10 randomly chosen microscopic fields (magnification 100x). The fraction of positively stained area is defined as the size of positively stained area divided by the total size of image evaluated.

Anticoagulation

Inhibition of activation of coagulation was performed by administration of heparin. Rats were treated with AMD/LPS as described above, and heparin (3000units/kg, s.c.) or saline was administrated 0.5h after LPS. The animals were then euthanized 10h after LPS for sample collection. Hepatic fibrin deposition, serum ALT activity and histological changes on H&E-stained liver slides were assessed as described above. Hepatic PMN accumulation and activation were measured as described below.

Evaluation of hepatic PMNs accumulation and activation

Immunohistochemical staining for hepatic PMNs was performed as described previously (Copple *et al.* 2004). The number of PMNs in 10 to 20 randomly selected

high-power fields (400×) in liver sections was counted and an average calculated for each rat.

Hypochlorous acid (HOCl) is generated by activated PMNs and in tissues forms protein adducts, which are used as a marker of PMN activation. The monoclonal antibody (2D10G9, subtype IgG2bk) is specific for HOCl-modified epitopes (Malle *et al.* 1995). Immunohistochemical staining for HOCl-protein adducts in frozen liver sections was performed as described previously (Deng *et al.* 2007).

PMN depletion

A rabbit anti-rat PMN serum (NAS) (Intercell Techonologies, Jupiter, FL) was used to deplete circulating PMNs in rats. A previous study in rats demonstrated the efficacy of this NAS to deplete circulating PMNs (Snipes *et al.* 1995). Rats were given control serum (CS, normal rabbit serum) or NAS 2h before AMD. CS and NAS were diluted 1:1 in saline and injected intravenously at 0.5ml per rat. The rats were then treated with AMD/LPS as described above and euthanized 10h after LPS for sample collection. Total blood leukocytes were quantified with a Unopette White Blood Cell Determination kit (BD Biosciences, San Jose, CA). Differential counting for the percentage of PMNs and lymphocytes was performed with a Hema 3 Staining System (Fisher Diagnostics, Middletown, VA). Hepatic PMN accumulation and activation, serum ALT activity, histological changes on H&E stained liver slides, hepatic fibrin deposition were assessed as described above.

Statistical analysis

The results are expressed as means ± S.E.M. One-way or two-way ANOVA was applied as appropriate; Tukey's method was employed as a post hoc test. At least 3 biological repetitions were performed for each experiment. $P<0.05$ was set as the criterion for statistical significance.

4.4 Results

AMD enhanced alterations in the hemostatic system caused by LPS

The plasma concentration of TAT was measured as a marker of coagulation activation (Figure 4-1 A). LPS alone caused an increase in TAT concentration in the plasma, which peaked within 2h and returned to baseline by 10h after LPS. AMD alone did not affect TAT concentration. The concentration of TAT in plasma of AMD/LPS-treated rats tended to be greater than that in LPS-treated rats and was significantly so at 10h.

The plasma concentration of active PAI-1 was measured as a marker of fibrinolysis inhibition (Figure 4-1 B). LPS increased the concentration of active PAI-1 in plasma, an effect that started at or before 2h, peaked between 2h and 4h, and returned to baseline at 10h after LPS. AMD did not alter the concentration of active PAI-1 by itself but significantly enhanced the LPS-induced active PAI-1 peak from 4h through 10h.

AMD/LPS cotreatment induced fibrin deposition and hypoxia in the liver

Little fibrin was detected in the livers if rats treated with vehicle, AMD or LPS alone at either 4h or 10h after LPS (Figure 4-2 A). At both 4h and 10h, fibrin deposition was observed in rats cotreated with AMD/LPS, with the fraction of positively stained

area around 2 fold of those of all three other groups. Fibrin deposition was panlobular and sinusoidal in AMD/LPS-treated rats (Figure 4-2 B).

The time course of AMD/LPS-induced liver injury rats was determined previously: the elevation of serum ALT, AST activities and the development of hepatic necrosis started between 4h and 6h after LPS and progressed through 10h (Lu *et al.* 2012).

Liver hypoxia was evaluated by quantification of PIM-adducts staining at 4h after LPS (Figure 4-3 A), which is before the onset of hepatic parenchymal damage. Increased PIM-adduct staining was only observed in the liver sections from AMD/LPS-treated rats, whereas Veh/LPS or AMD/Sal did not cause increases compared to the Veh/Sal-treated group. Figure 4-3 B shows representative pictures of PIM-adducts staining at 4h after LPS. Minimal staining was observed in Veh/Sal, Veh/LPS or AMD/Sal treated groups (Figure 4-3 B). Positive staining in AMD/LPS-treated group localized mainly to the midzonal regions of the liver.

Anticoagulant heparin prevented hepatic fibrin deposition and attenuated AMD/LPS-induced liver injury

Treatment with heparin abolished the AMD/LPS-induced hepatic fibrin deposition at 10h after LPS (Figure 4-4 A). Heparin also diminished liver damage: ALT activity in serum was reduced by 60% (Figure 4-4B), and the area of hepatocellular necrosis was smaller after heparin treatment (Figure 4-4 C).

AMD affected LPS-induced hepatic PMN accumulation

Treatment with LPS alone caused an increase in the number of PMNs in the liver at 4h, and this effect was sustained through 10h. AMD alone did not cause PMNs to

accumulate in liver. At 4h, which is before the onset of liver injury (Lu *et al.* 2012), cotreatment with AMD led to fewer PMNs accumulated in the liver compared to Veh/LPS treatment. At 10h, which is near the peak of liver injury, AMD/LPS caused slightly greater hepatic PMN accumulation (Figure 4-5 A). PMN accumulation displayed a panlobular distribution in livers of rats treated with Veh/LPS or AMD/LPS before the onset of liver injury (4h) (data not shown). At 10h, PMNs in AMD/LPS-treated rats formed clusters around the necrotic regions (Figure 4-5 B), whereas PMNs in Veh/LPS-treated animals retained panlobular distribution.

AMD/LPS cotreatment induced PMNs activation

No positive staining for HOCL protein adducts was detected in any treatment group at 4h after LPS (Figure 4-6 A). At 10h after LPS, staining for HOCL protein adducts was observed only in the AMD/LPS-treated group. Staining in AMD/LPS-treated rats localized mainly to the midzonal regions of the livers (Figure 4-6 B).

PMN depletion attenuated AMD/LPS-induced liver injury

AMD/LPS-treated rats were pretreated with NAS or CS, and the numbers of circulating total leukocytes, lymphocytes and PMNs were quantified at 10h after LPS (Table 1). CS/AMD/LPS-treated rats had significant lymphocytopenia and neutrophilia compared to CS/Veh/Sal-treated rats. NAS dramatically decreased the number of circulating PMNs without affecting circulating lymphocytes after AMD/LPS treatment. The number of circulating PMNs in NAS/AMD/LPS-treated rats (275±40 /μl) was even smaller than the CS/Veh/Sal-treated rats (579±150 /μl).

CS/AMD/LPS-treated rats had similar hepatic PMN number (37±3 PMNs/400xHPF, Figure 4-7 A) compared to AMD/LPS-treated rats (40±2 PMNs/400x HPF, Figure 4-5 A), indicating AMD/LPS-induced hepatic PMN accumulation was not affect by CS. NAS attenuated the AMD/LPS-induced hepatic PMN accumulation by about 30%, but the number of hepatic PMNs in NAS/AMD/LPS-treated rats was still significantly higher than that of the CS/Veh/Sal-treated rats (Figure 4-7 A). PMNs in the NAS/AMD/LPS-treated rats were distributed panlobularly, and clustering of PMNs in the necrotic regions that was observed in the livers of CS/AMD/LPS-treated rats was not seen in rats treated with NAS/AMD/LPS (Figure 4-7 B). NAS completely abolished the AMD/LPS-induced positive staining of HOCL protein adducts (Figure 4-7 C), indicating that hepatic PMN activation was inhibited.

The effect of PMN depletion on AMD/LPS-induced liver injury was assessed at 10h after LPS. NAS reduced the AMD/LPS-induced increase in ALT activity by 40% (Figure 4-7 D). NAS also attenuated AMD/LPS-induced hepatic necrosis evaluated histologically (Figure 4-7 E).

Interaction of the hemostatic system and PMNs in AMD/LPS-induced liver injury

AMD/LPS-induced hepatic fibrin deposition was not affected by NAS (Figure 4-8). Heparin did not affect the AMD/LPS-induced accumulation of PMNs in the liver (Figure 9 A) or the clustering of PMNs in the necrotic area (Figure 4-9 B), however, it did reduce AMD/LPS-induced hepatic PMN activation (Figure 4-9 C).

Figure 4-1 Plasma markers of hemostatic system alteration after treatment with AMD and/or LPS

Rats were treated with AMD (400 mg/kg, ip) or veh and 16h later with LPS (1.6×10^6 EU/kg, iv) or saline. Plasma samples were collected at 2, 4, 6 or 10h after LPS injection. Concentrations of TAT (A) and active PAI-1 (B) in plasma were measured. #significantly different from respective groups not given LPS; *significantly different from respective group not given AMD. $p < 0.05$, n=4-9.

Figure 4-1 (cont'd)

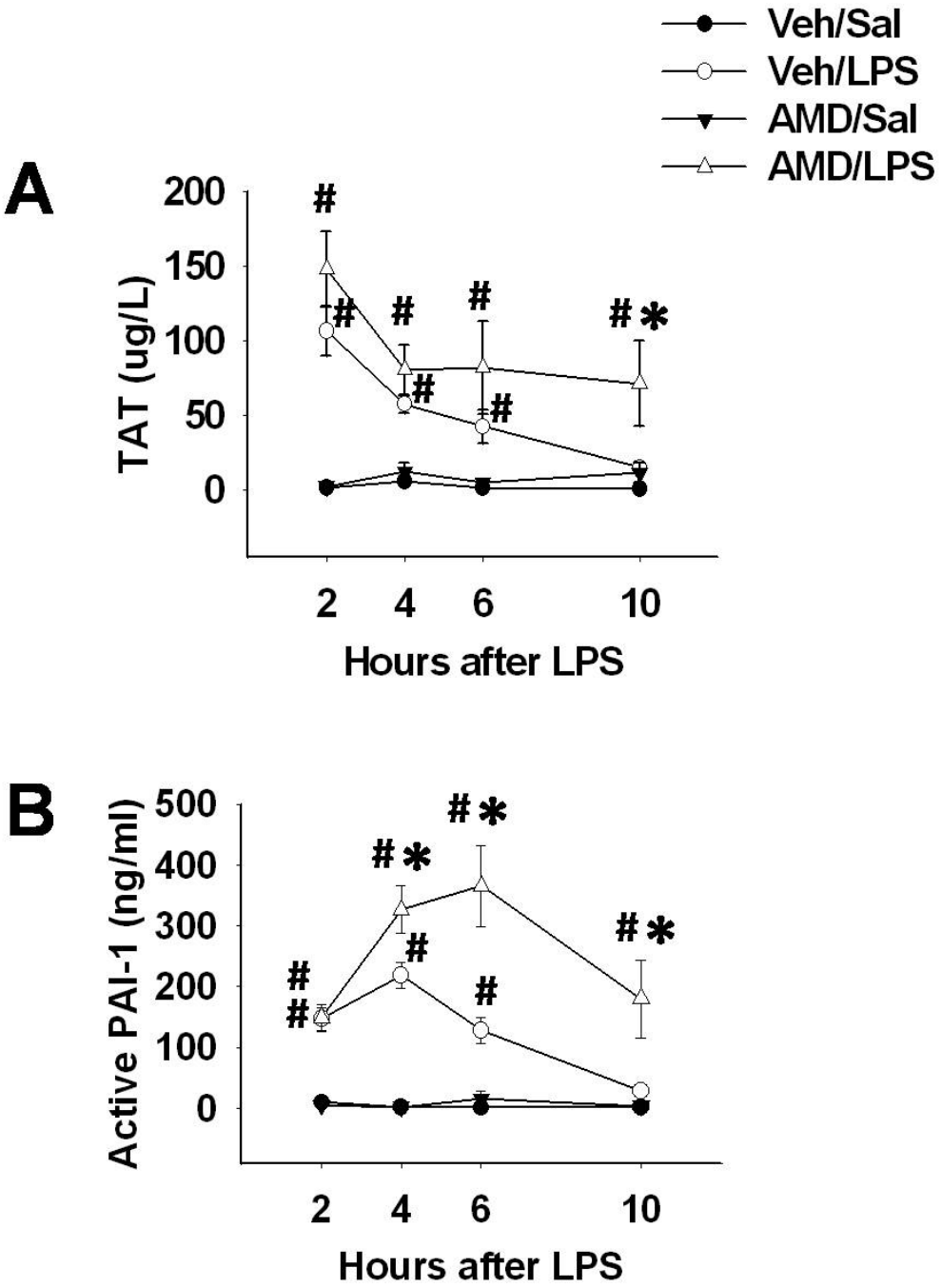

Figure 4-2 Hepatic fibrin deposition after treatment with AMD and/or LPS

Rats were treated with AMD (400 mg/kg, ip) or veh and 16h later with LPS (1.6×10^6 EU/kg, iv) or saline. Liver tissue samples were collected at 4h or 10h after LPS administration. A, fibrin deposited in the liver was immunochemically stained and quantified as described in Materials and Methods. #significantly different from respective group not given LPS; *significantly different from respective group not given AMD. $p < 0.05$, n=4-9. B, representative pictures of hepatic fibrin deposition at 4h after LPS.

Figure 4-2 (cont'd)

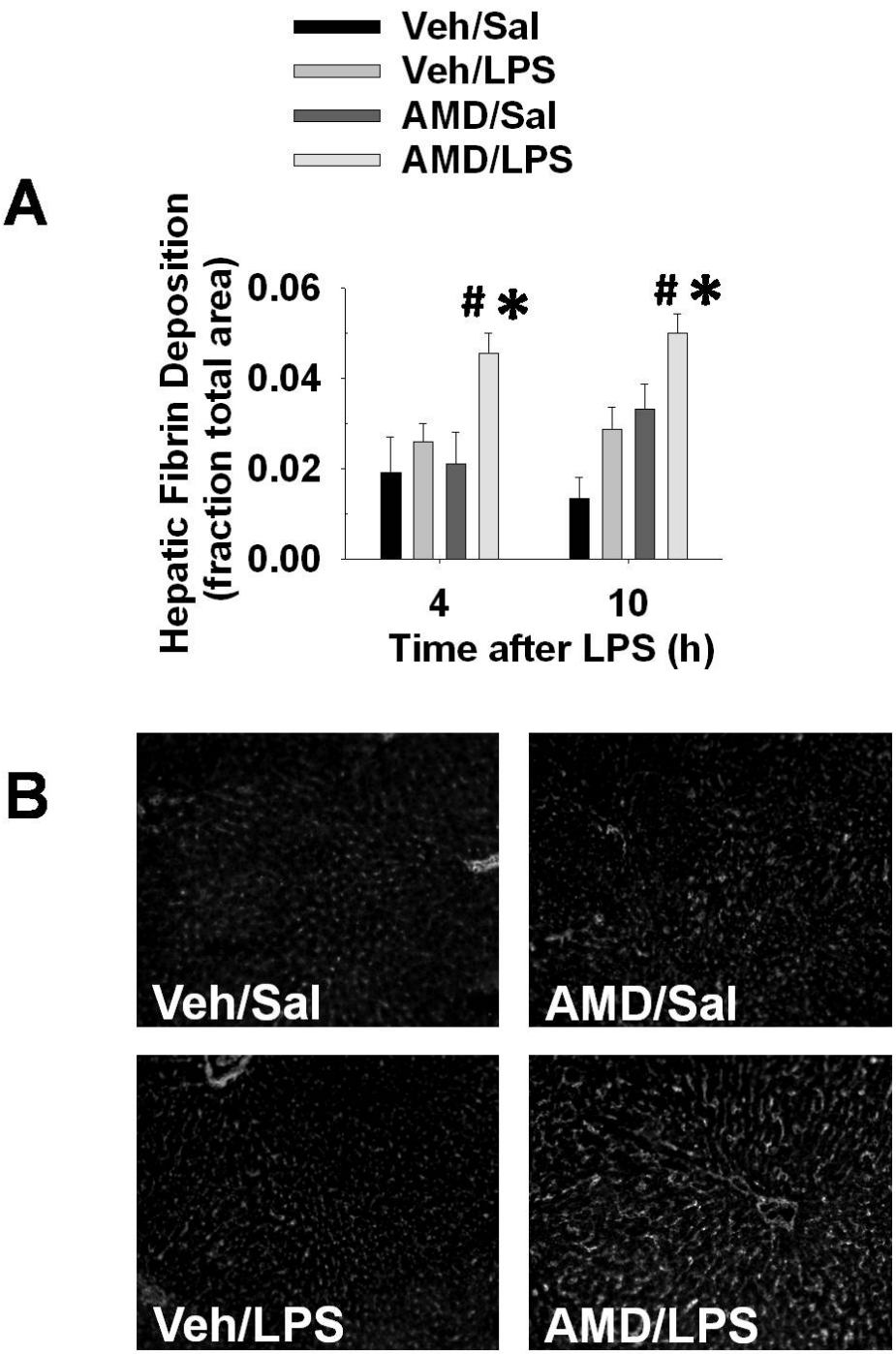

Figure 4-3 Hepatic hypoxia after treatment with AMD and/or LPS

Rats were treated with AMD (400 mg/kg, ip) or veh and 16h later with LPS (1.6×10^6 EU/kg, iv) or saline. PIM hydrochloride (120 mg/kg, i.v.) was given to rats at 2 h after LPS, and liver tissue samples were collected at 4h after LPS. A, PIM-adducted proteins were immunohistochemically stained and quantified as described in the Materials and Methods. #, significantly different from respective groups not given LPS; * significantly different from respective group not given AMD. $p < 0.05$, n=3-6. B, representative pictures of PIM-adduct staining at 4h after LPS.

Figure 4-3 (cont'd)

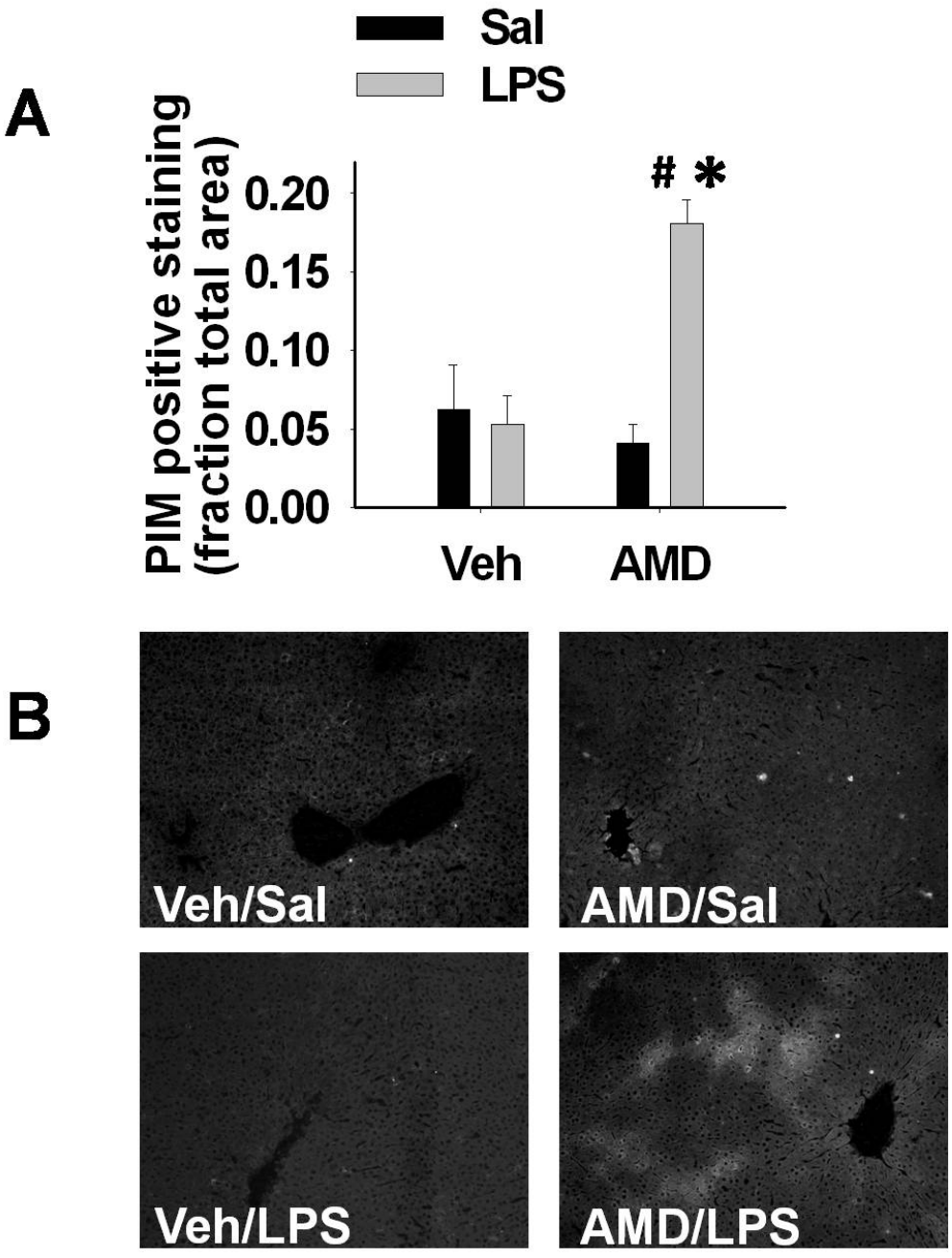

Figure 4-4 Effect of heparin on hepatic fibrin deposition and liver injury induced by AMD/LPS

Rats were treated with AMD (400 mg/kg, ip) or vehicle and 16h later with LPS (1.6×10^6 EU/kg, iv) or saline. Heparin (3000 units/kg, s.c.) or saline was administrated 0.5h after LPS. Animals were euthanized 10h after LPS for sample collection. Hepatic fibrin deposition (A) and ALT activity in serum (B) were quantified as described in the Materials and Methods. #significantly different from Veh/Sal/Sal. *significantly different from AMD/LPS/Sal. $p < 0.05$, n=3-7. C, representative pictures of H&E stained liver slides. Black arrow, necrotic foci.

Figure 4-4 (cont'd)

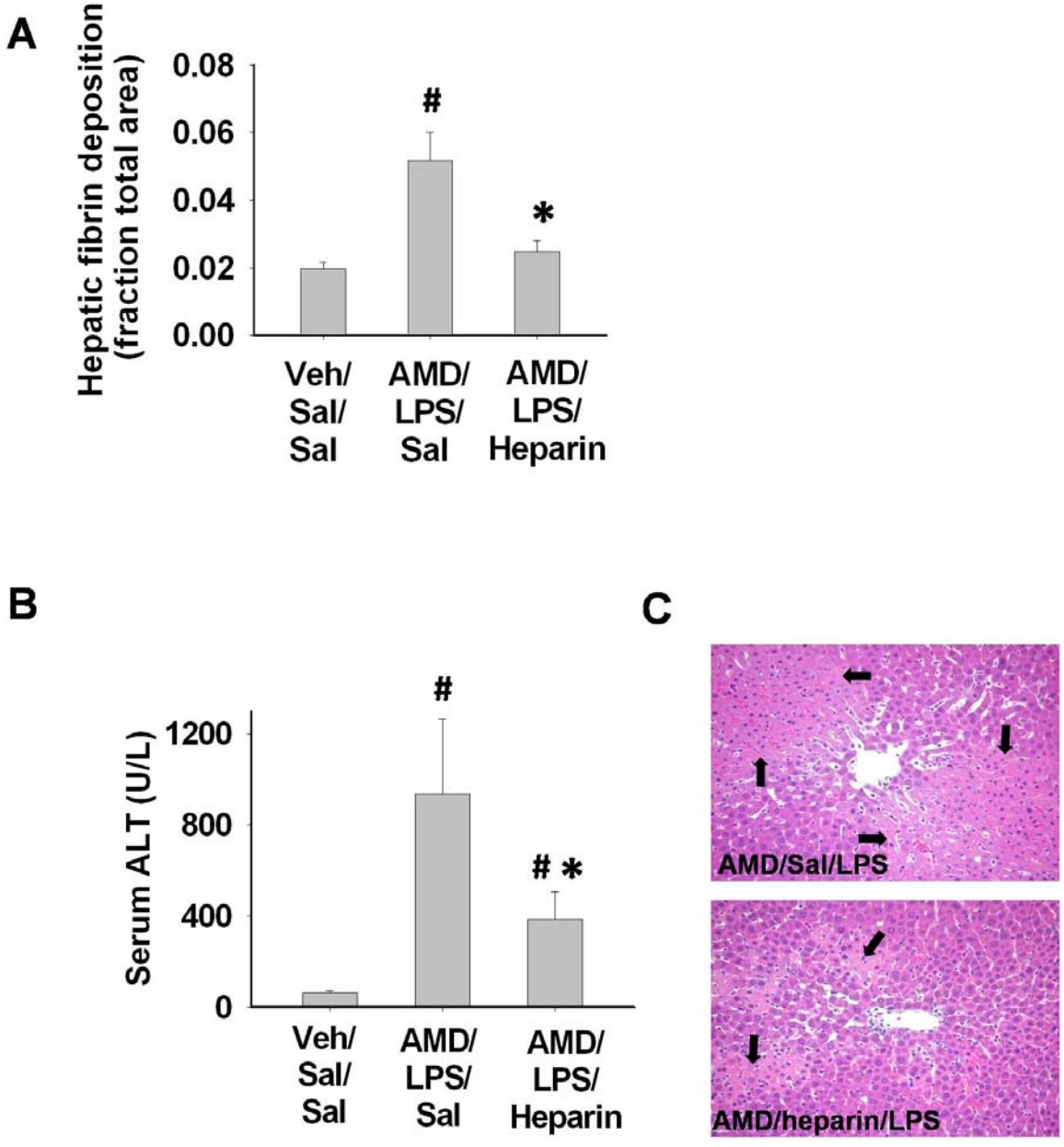

Figure 4-5 Hepatic PMN accumulation after treatment with AMD and/or LPS

Rats were treated with AMD (400 mg/kg, ip)) or vehicle and 16h later with LPS (1.6 $\times 10^6$ EU/kg, iv) or saline. Liver tissue samples were collected at 4h or 10h after LPS injection. PMNs accumulated in the liver were immunochemically stained, which appear red in the photo micrographs. A, the number of PMNs accumulated in the liver was quantified as described in the Materials and Methods. #significantly different from respective groups not given LPS; *significantly different from respective group not given AMD. $p < 0.05$, n=4-7. B, representative pictures of hepatic PMN accumulation at 10h after LPS.

Figure 4-5 (cont'd)

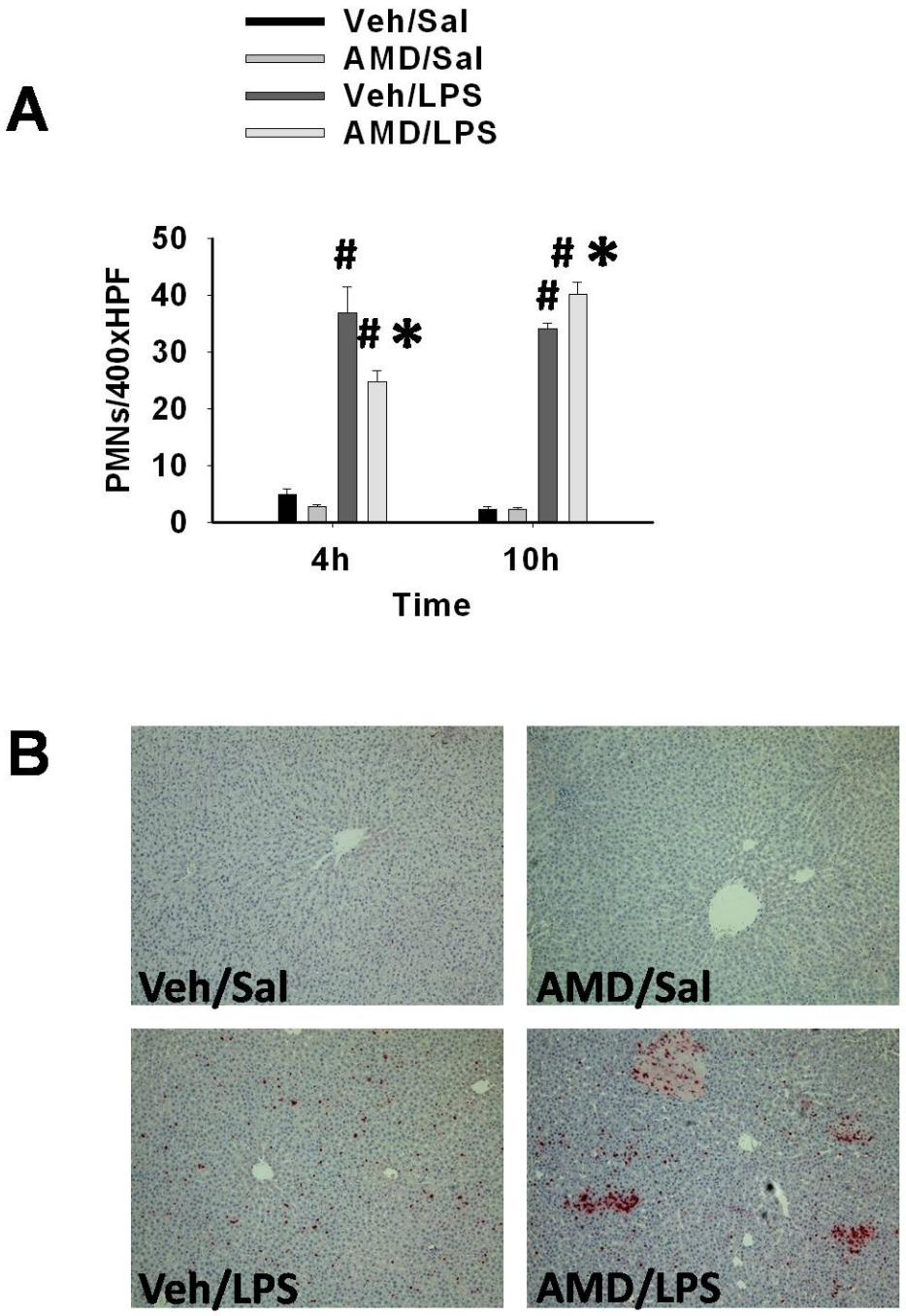

Figure 4-6 Hepatic PMNs activation after treatment with AMD and/or LPS

Rats were treated with AMD (400 mg/kg, ip)) or vehicle and 16h later with LPS (1.6 $\times 10^6$ EU/kg, iv) or saline. Liver tissue samples were collected at 4h or 10h after LPS injection. A, HOCL protein adducts in liver sections were immunochemically stained and quantified as described in the Materials and Methods. #significantly different from respective group not given LPS; *significantly different from respective group not given AMD. $p < 0.05$, n=4-9. B, representative pictures of HOCL-adducts staining at 10h after LPS.

Figure 4-6 (cont'd)

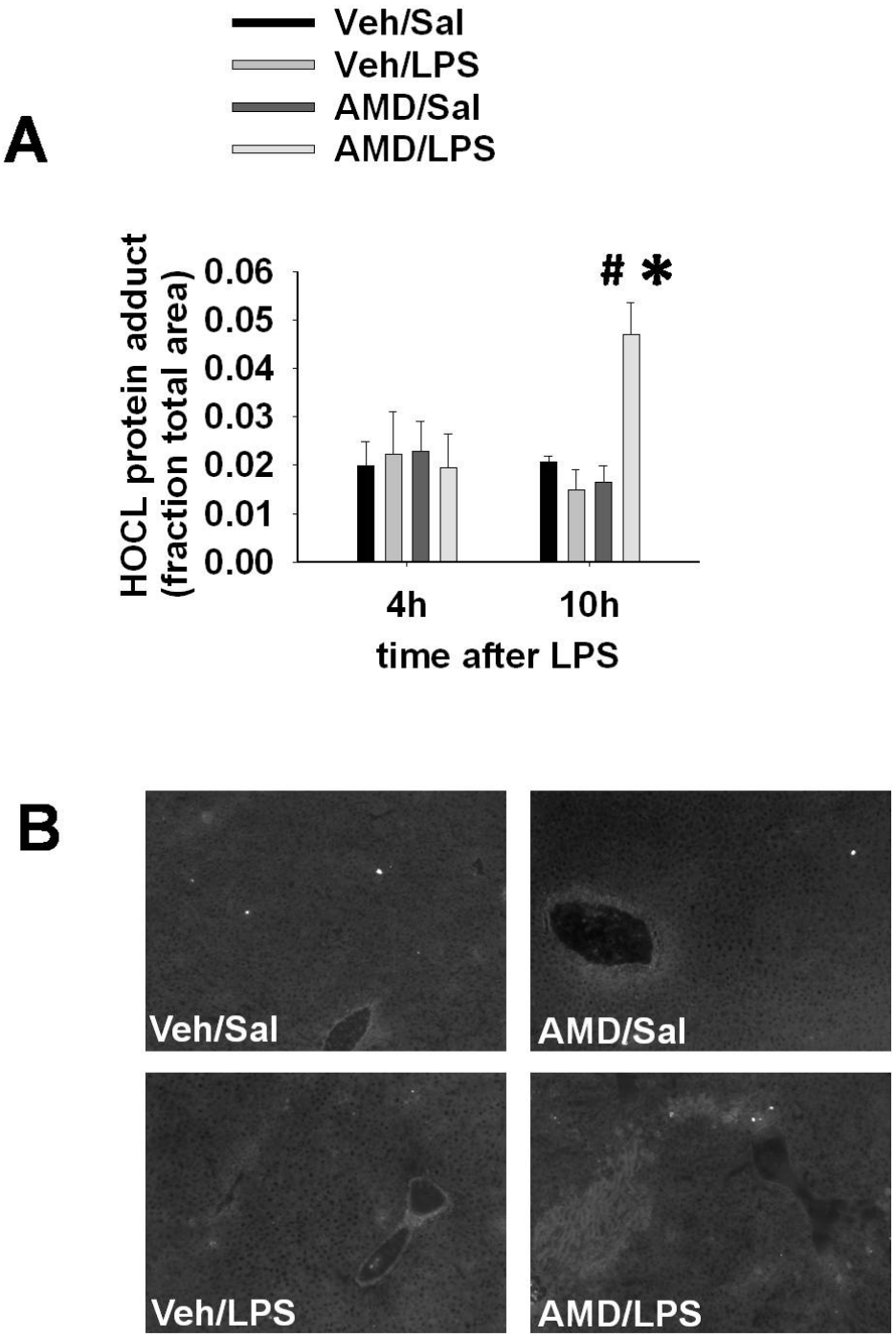

Table 4-1 Effect of PMN antiserum on circulating PMNs after treatment with AMD/LPS

Treatment	Leukocytes (no./ul)	Lymphocytes (no./ul)	PMNs (no./ul)
CS/Veh/Sal	5188±174	4609±198	579±150
CS/AMD/LPS	3745±257[a]	1523±173[a]	2222±199[a]
NAS/AMD/LPS	1407±123[ab]	1132±95[a]	275±40[ab]

Rats were treated with AMD (400 mg/kg, ip)) or vehicle and 16h later with LPS (1.6 $\times 10^6$ EU/kg, iv) or saline. NAS or CS (0.5 ml per rats, i.v.) was injected at 2h before AMD, and blood samples were collected at 10h after LPS. Total blood leukocytes, circulating PMNs and lymphocytes were quantified as described in the Materials and Methods. a, significantly different from Veh/Sal/CS. b, significantly different from AMD/LPS/CS. $p < 0.05$, n=5-12.

Figure 4-7 Effect of PMN antiserum on hepatic PMN accumulation and activation and liver injury induced by AMD/LPS

Rats were treated with AMD (400 mg/kg, ip) or vehicle and 16h later with LPS (1.6×10^6 EU/kg, iv) or saline. NAS or CS (0.5 ml per rats, i.v.) was injected 2h before AMD. Blood and liver tissue samples were collected at 10h after LPS. A, hepatic PMN accumulation; B, representative pictures of hepatic PMN accumulation; C, HOCl adduct staining; D, ALT activity in serum; E, representative pictures of H&E-stained liver sections were obtained as described in the Materials and Methods. #significantly different from Veh/Sal/CS. *significantly different from AMD/LPS/CS. $p < 0.05$, n=5-12. Black arrows, necrotic foci.

Figure 4-7 (cont'd)

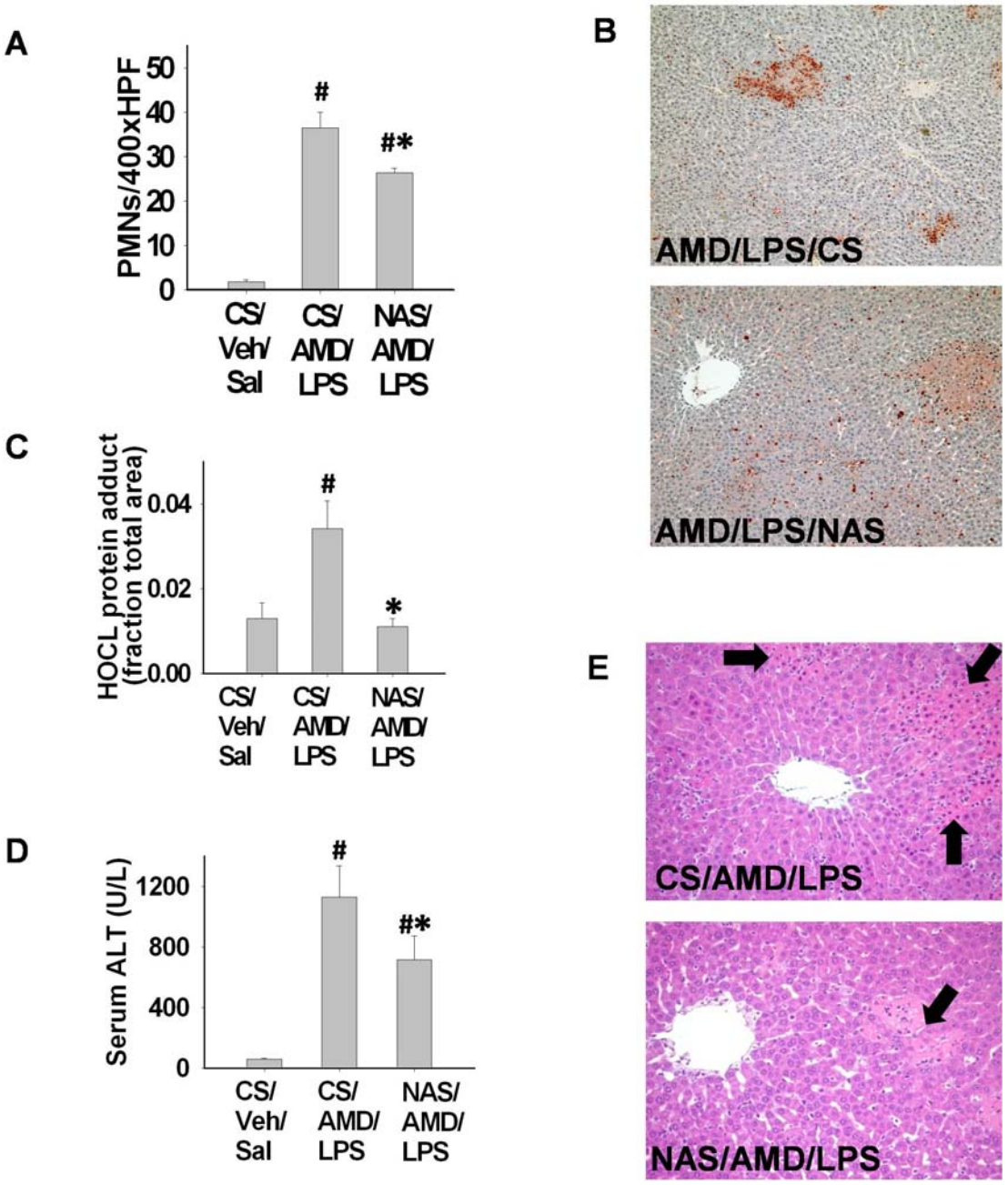

Figure 4-8 Effect of PMN antiserum on AMD/LPS-induced hepatic fibrin deposition

Rats were treated with AMD (400 mg/kg, ip) or vehicle and 16h later with LPS (1.6×10^6 EU/kg, iv) or saline. NAS or CS (0.5 ml per rats, i.v.) was injected 2h before AMD. Hepatic fibrin deposition was quantified in liver sections collected at 10h after LPS. #significantly different from Veh/Sal/CS $p < 0.05$, n=5-12.

Figure 4-8 (cont'd)

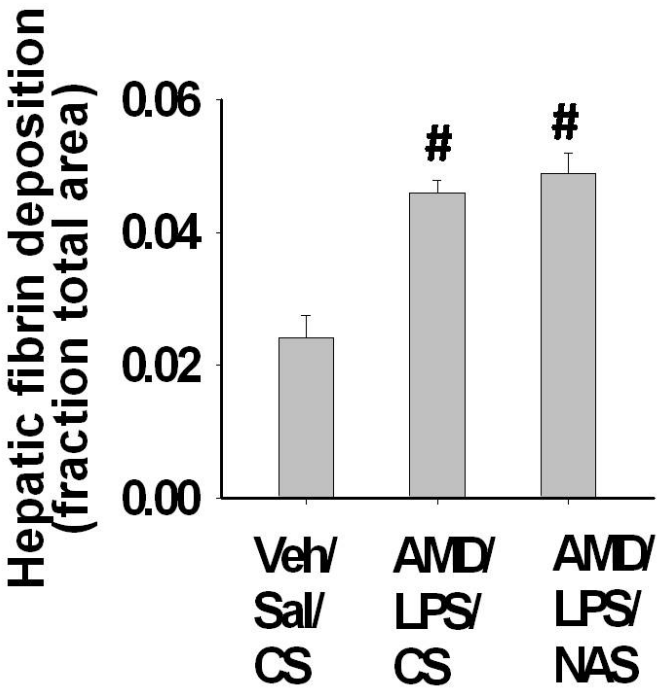

Figure 4-9 Effect of heparin on AMD/LPS-induced hepatic PMN accumulation and activation

Rats were treated with AMD (400 mg/kg, ip) or vehicle and 16h later with LPS (1.6×10^6 EU/kg, iv) or saline. Heparin (3000 units/kg, s.c.) or saline was administrated 0.5h after LPS. Animals were euthanized 10h after LPS for sample collection. A, hepatic PMN accumulation; B, representative pictures of hepatic PMN accumulation; C, HOCL adduct staining was obtained as described in the Materials and Methods. #significantly different from Veh/Sal/Sal. *significantly different from AMD/LPS/Sal. $p < 0.05$, n=3-7.

Figure 4-9 (cont'd)

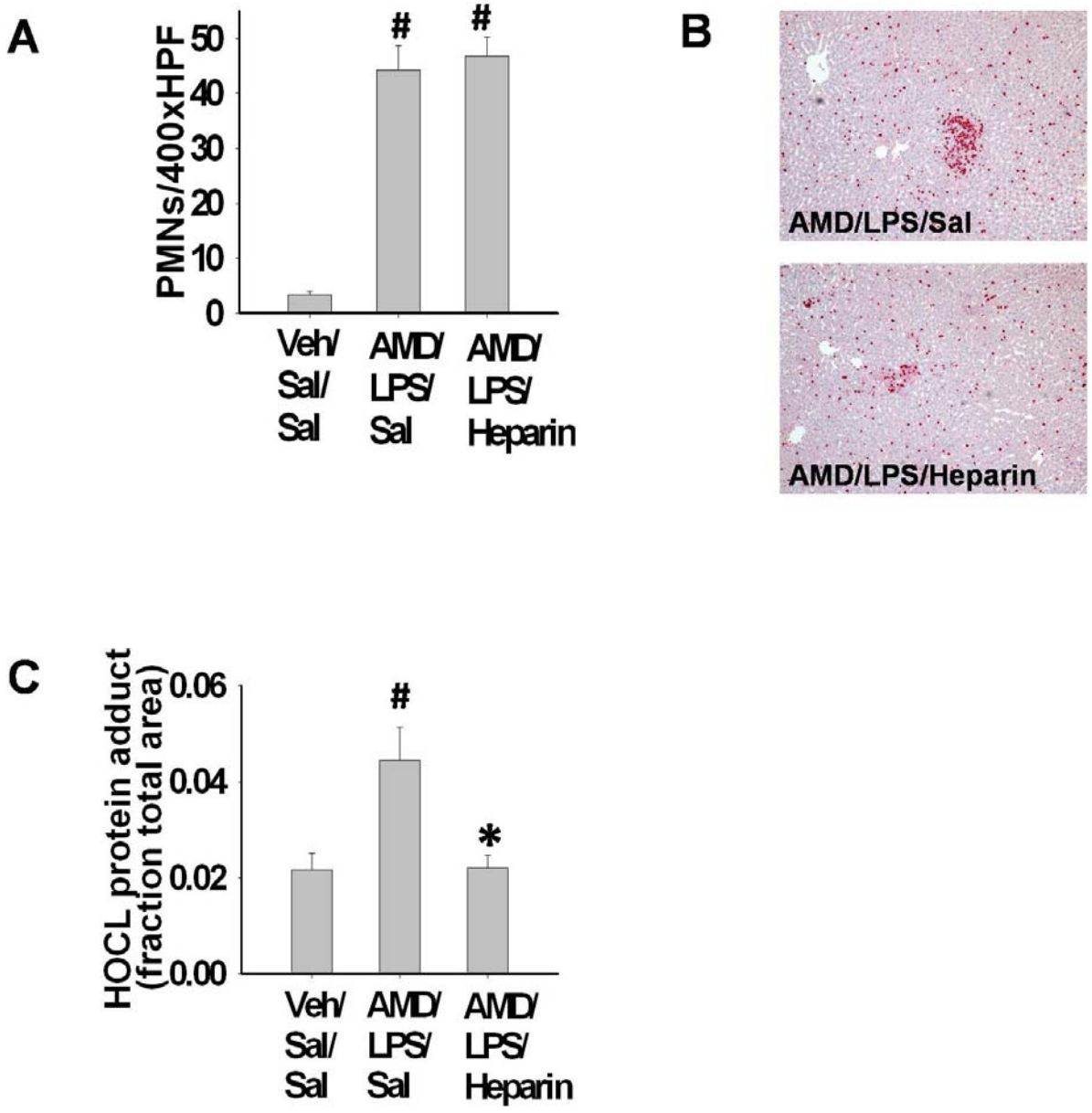

4.5 Discussion

Previous studies demonstrated that AMD/LPS-treated rats developed idiosyncrasy-like liver injury, characterized by elevated ALT, AST activities in serum and midzonal hepatocelluar necrosis, whereas AMD alone or LPS alone did not cause hepatotoxicity at the doses used in this model. The onset of liver injury was between 4h and 6h after LPS administration, and injury progressed through 10h (Lu *et al.* 2012). The present study tested the roles that the hemostatic system and PMNs play in AMD/LPS-induced liver injury in rats.

Hepatic fibrin deposition in tissues is controlled by both the coagulation system (deposition) and the fibrinolytic system (removal). LPS caused elevations in both TAT (Figure 4-1 A) and PAI-1 (Figure 4-1B), but they were not enough to result in fibrin deposition (Figure 4-2 A). AMD/LPS-induced hepatic fibrin accumulation started at 4h after LPS (Figure 4-2 A), a time at which the LPS-induced increase in PAI-1 (Figure 4-1 B) but not TAT (Figure 4-1 A) was enhanced by AMD. These results suggest that the effect of AMD on LPS-induced PAI-1 at 4h was important for the formation of hepatic fibrin after AMD/LPS cotreatment. Fibrin deposition was sustained through 10h after AMD/LPS, consistent with the sustained elevations in TAT and PAI-1.

LPS-induced coagulation activation is well characterized. Inflammatory mediators released as a consequence of LPS exposure, such as TNF, can activate TF (a primary activator of thrombin) and cause PAI-1 production by endothelial cells (Nawroth and Stern 1986; Schleef *et al.* 1988), but the mechanism by which AMD can contribute to LPS-induced thrombin and PAI-1 activation is not understood. AMD inhibited the translation and expression of TF in a mouse model of photochemical-induced carotid

artery thrombus formation (Breitenstein *et al*. 2008), so the enhancement of LPS-induced thrombin activation might be an indirect effect of AMD. Liver damage begins between 4h and 6h after LPS administration in this model, so it is possible that TF was activated as a result of sinusoidal microvascular injury. AMD has not been reported to affect PAI-1 generation directly. One mechanism by which AMD could potentiate LPS-induced PAI-1 activation is through an effect of PAI-1-inducing cytokines, e.g. TNF. AMD enhances LPS-induced TNF production in this model (Lu *et al.* 2012), and TNF can induce PAI-1 production (Nawroth and Stern 1986).

A direct consequence of fibrin deposition in the liver is disruption of sinusoidal blood flow, which can lead to hepatic hypoxia. Hypoxia can directly injure isolated hepatocytes (Khan and O'Brien 1997) or perfused livers (Lemasters *et al.* 1981). Hypoxia can also sensitize the liver or isolated hepatocytes to secondary stress, e.g. hepatotoxicants or drugs (Bacon *et al.* 1996; Sparkenbaugh *et al.* 2012), and both AMD and hypoxia can cause mitochondrial dysfunction in hepatocytes (Chandel *et al.* 2000; Spaniol *et al.* 2001). It is possible that the combination of AMD and hypoxia leads to more severe mitochondrial damage and eventually hepatocellular necrosis in AMD/LPS-cotreated animals.

Heparin is a widely used anticoagulant that inhibits thrombin activation by increasing the inhibitory effect of endogenous antithrombin III (Bjork and Lindahl 1982). Heparin administration prevented hepatic fibrin deposition (Figure 4-4 A) but only offered a 60% reduction in the AMD/LPS-induced ALT increase (Figure 4-4 B). Since a similar dose of heparin provided almost complete protection against liver damage from a larger, hepatotoxic dose of LPS in rats (Moulin *et al.* 1996). This result suggests that

coagulation activation was not solely responsible for AMD/LPS-induced liver injury and that other inflammatory factors contribute.

The influx of PMNs into the liver is mainly driven by LPS administration (Figure 4-5 A). Accumulated PMNs distributed evenly across the liver lobules of LPS-treated rats (Figure 4-5 B) and in AMD/LPS-treated rats before the onset of liver injury (data not shown). PMNs formed clusters around the necrotic foci as the liver injury progressed in AMD/LPS-cotreated rats (Figure 4-5 B). PMNs not only help to clear up injured or dying cells but also can attack hepatocytes stressed by inflammatory cytokines, because these hepatocytes express more ICAM-1 and produce greater amounts of chemokines, facilitating the recruiting and activation of PMNs (Farhood *et al.* 1995; Okaya and Lentsch 2003). NAS treatment reduced the increase in serum ALT activity by 40% in AMD/LPS-treated rats (Figure 4-7 D), suggesting that PMNs play a contributory role in the AMD/LPS-induced liver injury. Activated PMNs also contribute to tissue damage in rodent models of LPS/ranitidine- (Luyendyk *et al.* 2005), LPS/sulindac- (Zou *et al.* 2011) and LPS/trovafloxaxin- (Shaw *et al.* 2009d) induced liver injury. Together, these results suggest a commonality in the mechanism(s) by which inflammatory stress converts IDILI-associated drugs from nontoxic to hepatotoxic ones.

Accumulation of PMNs in the liver does not necessarily mean these cells participate in damaging hepatocytes. β-Integrin/ICAM-mediated transmigration of PMNs through the endothelial cell lining and subsequent adhesion to target cells are required for PMN activation and cell killing (Shappell *et al.* 1990). PMNs in LPS-treated rats, and PMNs in AMD/LPS-treated rats at 4h, were not activated (Figure 4-6 A), and injury was not observed at this time (Lu *et al.* 2012). Similar findings were observed in

acetaminophen-induced hepatocelullar injury (Lawson *et al.* 2000) and lithocholic acid-induced cholestatic injury (Fickert *et al.* 2006).

What leads to the PMN activation in AMD/LPS-cotreated animals and what is the relationship between hepatic fibrin deposition and PMN activation remain to be explored. Serine proteases released by activated PMNs can affect hepatic fibrin deposition (Deng *et al*. 2007). However, in this study, PMN activation was detected later than the appearance of hepatic fibrin deposition and hypoxia (Figure 4-2 A, Figure 4-3 A, Figure 4-6 A), and PMN depletion did not affect hepatic fibrin deposition (Figure 4-8). These results suggest that PMN activation did not initiate or contribute to hepatic fibrin deposition.

In contrast, heparin not only prevented fibrin deposition but also prevented PMN activation (Figure 4-9 C) without affecting hepatic PMN accumulation (Figure 4-9 A). These results suggested coagulation system activation contributed to PMN activation but not to tissue accumulation of these cells. One of the consequences of fibrin deposition in the microvasculature is tissue hypoxia, and hypoxia is able to induce adhesion molecules important for PMN activation (Arnould *et al.* 1993). Hypoxia can also cause necrosis of hepatocytes (Fassoulaki *et al.* 1984), which can in turn release PMN-activating chemokines, e.g. HMGB-1 (Scaffidi *et al.* 2002). It is possible that hypoxia resulting from fibrin deposition initiated hepatocellular necrosis starting 4h after LPS, and then the chemokines produced by dying hepatocytes caused activation of PMNs at a later time.

Smits et al reported that hypoxia leads to cell death of hepatocytes (Smith and Mooney 2007). This can be used to test the effects of cell death products on PMN

activation, by treating isolated PMNs with culturing medium from hypoxia-treated hepatocytes. And if medium conditioned by hypoxia-treated hepatocytes do have PMN activating effect, further studies can be performed to explore what substance released by PMN is responsible for PMN activation.

In summary, AMD enhanced LPS-induced impairment of the hemostatic system, resulting in elevated fibrin deposition and subsequent hypoxia. LPS drove PMN accumulation in the liver, but the accumulated PMNs were only activated upon exposure of the animals to AMD. These activated PMNs contributed to the progression of liver injury. Anticoagulation as well as PMN depletion reduced AMD/LPS-induced liver injury. PMN depletion did not affect hepatic fibrin deposition, whereas anticoagulation completely prevented PMN activation in the liver. These results suggest a critical interaction between the hemostatic system and PMNs in AMD/LPS-induced liver damage.

CHAPTER 5

Summary and conclusions

5.1 Summary of research findings

In this thesis project, an animal model of AMD/LPS-induced liver injury was developed, and the mechanisms of how AMD interacts with LPS resulting in hepatotoxicity were investigated. Studies in this thesis project support the hypothesis that inflammation is an important contributor to idiosyncratic drug hepatotoxicity. These studies also widened our understanding of the potential etiology of IDILIs in human patients.

First, to test the hypothesis that a concurrent inflammatory stress can interact with IDILI-inducing drugs and result in hepatotoxicity, rats were treated with nonhepatotoxic doses of AMD and with LPS to induce low-level inflammation. Liver injury was only observed in AMD/LPS-treated rats, evidenced by increase in ALT, AST, ALP and GGT activities in the serum (Figure 2-3 and 2-4), as well as hepatocellular necrosis in midzonal regions of the liver (Figure 2-5). Using AMD/LPS cotreatment as a model, roles of possible contributors to liver injury were explored.

LPS did not affect the metabolism or hepatic accumulation of AMD (Figure 2-6). AMD prolonged LPS-induced TNF elevation in serum (Figure 2-7), and TNF potentiated the cytotoxicity of both AMD and its primary metabolite, DEA (Figure 2-8). Inhibition of TNF signaling by etanercept attenuated the AMD/LPS-induced liver injury in rats (Figure 2-9).

AMD caused apoptotic cell death in Hepa1c1c7 cells, and TNF cotreatment potentiated its cytotoxicity (Figure 3-1~3-4). Activation of caspases 9 and 3/7 was observed in AMD/TNF-cotreated cells, and caspase inhibitors provided minor protection

from cytotoxicity (Figure 3-5 and 3-6). Intracellular reactive oxygen species generation (Figure 3-7) and lipid peroxidation (Figure 3-9) were observed after treatment with AMD, and these were further elevated by TNF cotreatment. Adding water-soluble antioxidants (trolox, N-acetylcysteine, glutathione or ascorbate) produced only minor attenuation of AMD/TNF-induced cytotoxicity and did not influence the effect of AMD alone (Figure 3-8). These results suggest that increase in the activation of caspases and generation of ROS only have minor contribution to the TNF's potentiation of AMD cytotoxicity. On the other hand, Toco prevented AMD toxicity and caused pronounced reduction in cytotoxicity from AMD/TNF cotreatment (Figure 3-10). Toco plus a pancaspase inhibitor completely abolished AMD/TNF-induced cytotoxicity (Figure 3-11), indicating that lipid peroxidation and caspase activation were the only two contributors to AMD/TNF-induced cytotoxicity, and that lipid peroxidation played the major role.

AMD/TNF (or AMD alone)-induced lipid peroxidation was observed in both mitochondia and lysosomes (data not shown). TNF potentiated AMD-induced mitochondrial superoxide generation and mitochondrial membrane potential (MMP) loss (data not shown). Inhibition of lipid peroxidation prevented AMD/TNF (or AMD alone)-induced MMP loss, but inhibition of lipid peroxidation did not affect AMD/TNF (or AMD alone)-induced mitochondrial superoxide generation (data not shown). These findings suggest that lipid peroxidation was downstream of mitochondrial superoxide generation.

AMD did not impair the hemostatic system by itself but significantly potentiated LPS-induced coagulation activation and fibrinolysis impairment (as marked by increased PAI-1; Figure 4-1). Increased hepatic fibrin deposition and subsequent hypoxia were observed only in AMD/LPS-treated animals (Figure 4-2 and 4-3), starting before the

onset of liver injury. Administration of heparin abolished AMD/LPS-induced hepatic fibrin deposition and attenuated AMD/LPS-induced liver damage (Figure 4-4).

LPS caused hepatic PMN accumulation by itself (Figure 4-5), but PMN activation was only observed in AMD/LPS-treated rats (Figure 4-6). Administration of NAS, which reduced the AMD/LPS-induced PMN accumulation and prevented PMN activation, partially attenuated AMD/LPS-induced liver injury in rats (Figure 4-7). PMN depletion did not affect hepatic fibrin deposition (Figure 4-8), whereas anticoagulation prevented PMN activation without affecting PMN accumulation (Figure 4-9).

In summary, TNF signaling, hemostatic system aleration and PMN activation played important roles in AMD/LPS-induced hepatocellular injury in rats. AMD enhanced LPS-induced TNF and hemostatic factor elevation in the blood. Enhanced TNF signaling potentiated the cytotoxicity of AMD though increased activation of caspases as well as increased lipid peroxidation. Increased coagulation activation and fibrinolysis impairment led to fibrin deposition and subsequent hypoxia in the liver, which not only directly damaged hepatocytes but also activated PMNs accumulated in the liver. Inhibition of TNF signaling, inhibition of coagulation or inactivation of PMNs attenuated AMD/LPS-induced liver injury in rats.

A diagram describing the above pathways involved in AMD/LPS-induced liver injury is summarized in Figure 5-1. Solid lines in the diagram are supported by experimental data in this thesis, and dashed lines are speculation based on literature reports. For example, Tukov *et al* reported that TNF contributes to coagulation activation and PMN activation in the LPS/RAN model of liver injury in rats (Tukov *et al.* 2007). Products of lipid peroxidation can induce TF (Cabre *et al.* 2004) and ICAM-

1expression (Takacs *et al.* 2001), indicating a causal relationship between lipid peroxidation and coagulation activation as well as PMN activation. Many of the AMD-induced effects on mitochondria were also observed in DEA treatment (Fromenty *et al.* 1990b), indicating that DEA is probably able to induce mitochondrial superoxide generation.

Figure 5-1 Proposed pathways to AMD/LPS-induced liver injury

See section 5.1 for detailed explanation of the pathways involved.

Figure 5-1 (cont'd)

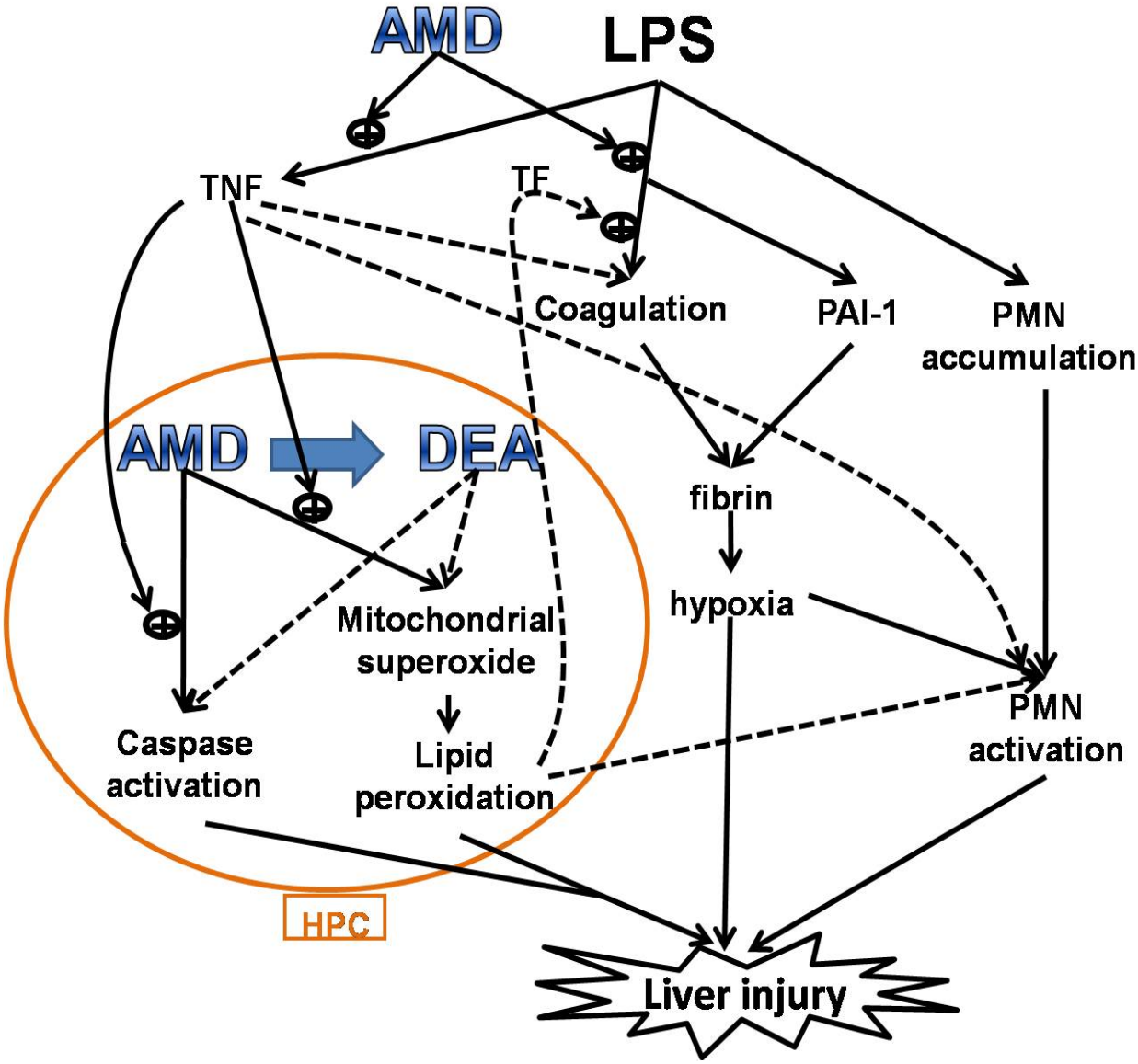

5.2 Commonalities and differences among animal models of liver injury caused by drug-inflammation interaction

Animal models supporting the inflammatory stress hypothesis for IDILIs are accumulating. IDILI-inducing drugs: chlorpromazine (CPZ), ranitidine (RAN), diclofenac (DCLF), trovafloxacin (TVX), sulindac (SLD), halothane (HAL) and amidoarone (AMD) are found to interact with modest inflammation and precipitate liver injury in laboratory rodents. The common and different characteristics of these models are summarized in Table 5-1.

Table 5-1 Commonalities and differences among animal models of IDILIs

(Y, tested to be true; N, tested, not true; blank, not tested)

Table 5-1 (cont'd)

	RAN	TVX	SLD	AMD	DCLF	CPZ	HAL	DOX
Inflammation induced by	LPS	LPS, PGN /LTA	LPS	LPS	LPS	LPS	LPS, Poly (I:C)	LPS
Route of drug administration	i.v.	p.o.	p.o.	i.p.	i.p.	i.p.	i.p.	i.p.
Number of drug administrations	1	1	2	1	1	1	1	1
Time of drug administration relative to LPS	2	-3	-15.5, 0.5	-16	2	2	-6	2
Hours after LPS before liver injury appear	6	12	12	6	6	24	15	
Enhanced TNF production	Y	Y	Y	Y			Y	Y
TNF potentiated drug cytotoxicity *in vitro*		Y	Y	Y				
TNF important for pathogenesis	Y	Y	Y	Y			Y	N
Enhanced hemostatic alteration/hypoxia	Y	Y	Y	Y				
Coagulation/hypoxia important for pathogenesis	Y	Y	Y	Y				
PMN accumulation	Y	Y	Y	Y	Y	Y	Y	
PMN activation	Y		Y	Y				
PMN activation important for pathogenesis	Y	Y	Y	Y	Y			
Hemostasis affected by TNF	Y	Y	N					
PMN activation affected byTNF	Y		Y					
Fibrin deposition affected by PMN activation	Y			N				
PMN activation affected by hemostasis	Y		Y	Y				
NK cell/IFN involved in pathogenesis		Y					Y	Y
ROS involved in pathogenesis			Y	Y				

Not only the cell wall component of gram negative bacteria, LPS, but also the main stimulatory components of gram-positive bacteria, peptidoglycan (PGN) and lipoteichoic acid (LTA), as well as the viral RNA mimetic, polyinosinic-polycytidylic acid (polyI:C) were used in these animal models to induce inflammation. Indeed, inflammation induced by a variety of stimuli from different organisms can interact with drugs to precipitate liver injury, which supports our hypothesis that inflammatory stress is a commonly shared contributor of IDILI-like liver injury in these animal models.

The timing of drug administration relative to LPS is important for the development of liver damage in these models, and this timing varies dramatically among models. For example, RAN needs to be injected 2h after LPS, whereas AMD needs to be administered 16h before LPS to achieve a maximal hepatotoxic response. The different characteristics in absorption, distribution, metabolism and clearance as well as different toxicological actions of drugs could be responsible for differences in timing requirement. For example, in human patients, the half-life of RAN is 3 hours whereas the half-life of AMD is 55 days (Juarez-Olguin *et al.* 2002; Pollak *et al.* 2000). On the other hand, the inflammatory response is also a highly organized process with every inflammatory mediator having a unique timeline for appearance and clearance. For example, LPS-induced TNF, TAT or PAI-1, each has a different starting, peaking and resolving time in the blood of the animals. Therefore, the interaction between drugs and inflammatory mediators might require a specific timing of drug and LPS administration that differs depending on the specific inflammatory factors are important in the pathogenesis of liver injury for one drug versus another.

RAN, TVX, SLD and AMD are four relatively well investigated models. Enhanced TNF production, hemostatic system alteration and PMN activation are commonly observed in these models. Inhibition of TNF signaling, coagulation and PMN activation attenuated drug/infammation-induced liver injury in each of these animal models, which demonstrates that TNF, the hemostatic system and PMNs are common players shared among drug/inflammation-induced liver injury models. Further studies revealed that these mediators interact with each other, but their interaction differs with different models. The importance and interaction of these factors in DCLF, CPZ and HAL models still need to be explored. The commonality of NK cells, IFN and ROS between drug/inflammation models needs to be further explored.

In summary, although the inflammatory stimulus, timing/routes/frequency of drug administration and the time course of liver injury progression differ among these models, several inflammatory mediators, e.g. TNF, hemostatic system and PMNs, are found to be commonly shared among several of these models. Further studies need to be performed to confirm the commonality of those less studied inflammatory mediators.

5.3 Potential future studies

In this thesis project, an animal model of AMD/LPS-induced liver injury was developed and the importance of several mediators was explored. However, the mechanisms of AMD/LPS interaction are still not completely understood. Potential directions for future studies are discussed below.

It is observed in this model that AMD potentiated the LPS-induced TNF increase in plasma, and the intracellular mechanisms by which TNF increases the cytotoxicity of AMD was also explored. However, the mechanisms by which AMD can enhance the LPS-induced TNF increase in plasma without causing TNF generation by itself remain unclear. One possibility is that AMD can affect the clearance of TNF, because the serum concentration of TNF is controlled by both the generation and the clearance. TNF is cleared from blood by binding to soluble TNF receptors (TNFRs), which are then eliminated mainly by the kidney (Bemelmans *et al.* 1993). In the murine model of TVX/TNF-induced liver injury, TVX prolonged the duration of TNF in the plasma, mainly through a decrease of TNF clearance, rather than increase of TNF production. The reduction of TNF clearance by TVX is not through a decrease in TNFRs or impairment of renal function (Shaw *et al.* 2009a).

AMD did not affect the hemostatic system by itself but was shown to potentiate LPS-induced thrombin and PAI-1 activation. The mechanisms for this phenomenon were not fully elucidated. AMD is reported to inhibit the translation and expression of TF directly (Breitenstein *et al*. 2008). No reference was found about AMD's effect on PAI-1 generation. One possibility is that AMD potentiates LPS-induced hemostatic factors through the elevation of TF- or PAI-1-inducing cytokines, e.g. TNF. This

possibility is supported by the findings in the RAN and TVX models, in which inhibition of TNF leads to decreased hemostasis. In addition, inhibition of the TNF signaling or coagulation activation each led to ~70% reduction of AMD/LPS-induced serum ALT increase, indicating that there might be at least partial interaction or casual relationship between TNF signaling and coagulation activation.

The effects of TNF on AMD-induced caspase activation and lipid peroxidation in Hepa1c1c7 cells were explored in this study, but the underlying mechanisms are not clear. The cytotoxicity of AMD is linked to its ability to cause mitochondrial abnormality, e.g. inhibition of complexes I and II-mediated respiration (Bolt *et al.* 2001), induction of mitochondrial swelling (Varbiro *et al.* 2003) and induction of permeability transition (Varbiro *et al.* 2003). Mitochondrial damage is also the bridging step between caspase 8 and caspase 9 activation in TNF-induced apoptotic signaling cascades (Wullaert *et al.* 2007). Therefore, the mitochondrion is a likely site where AMD interacts with TNF to induce downstream caspase activation and lipid peroxidation.

In summary, future studies proposed above will help to clarify how AMD prolonged LPS-induced TNF in blood, how AMD potentiated LPS induced thrombin and PAI-1 activation and how TNF increased AMD-induced lipid peroxidation. The experimental observations from Chapters 2-4 and the potential findings from the proposed future studies will help us to understand the mechanisms of this animal model of AMD/LPS-induced liver injury. Our knowledge obtained from these animal models will be of great interest in treating or preventing IDILIs in human patents.

BIBLIOGRAPHY

BIBLIOGRAPHY

1. Agoston, M., Orsi, F., Feher, E., Hagymasi, K., Orosz, Z., Blazovics, A., Feher, J., and Vereckei, A. (2003). Silymarin and vitamin E reduce amiodarone-induced lysosomal phospholipidosis in rats. *Toxicology* **190**(3), 231-241.

2. Akira, S., and Takeda, K. (2004). Toll-like receptor signalling. *Nat Rev Immunol* **4**(7), 499-511.

3. Andrade, R. J., and Tulkens, P. M. (2011). Hepatic safety of antibiotics used in primary care. *J Antimicrob. Chemother.* **66**(7), 1431-1446.

4. Arnould, T., Michiels, C., and Remacle, J. (1993). Increased PMN adherence on endothelial cells after hypoxia: involvement of PAF, CD18/CD11b, and ICAM-1. *Am J Physiol* **264**(5 Pt 1), C1102-C1110.

5. Arteel, G. E., Thurman, R. G., Yates, J. M., and Raleigh, J. A. (1995). Evidence that hypoxia markers detect oxygen gradients in liver: pimonidazole and retrograde perfusion of rat liver. *Br. J. Cancer* **72**(4), 889-895.

6. Babatin, M., Lee, S. S., and Pollak, P. T. (2008). Amiodarone hepatotoxicity. *Curr. Vasc. Pharmacol.* **6**(3), 228-236.

7. Bacon, J. A., Cramer, C. T., Petrella, D. K., Sun, E. L., and Ulrich, R. G. (1996). Potentiation of hypoxic injury in cultured rabbit hepatocytes by the quinoxalinone anxiolytic, panadiplon. *Toxicology* **108**(1-2), 9-16.

8. Balistreri, W. F., Farrell, M. K., and Bove, K. E. (1986). Lessons from the E-Ferol tragedy. *Pediatrics* **78**(3), 503-506.

9. Bargout, R., Jankov, A., Dincer, E., Wang, R., Komodromos, T., Ibarra-Sunga, O., Filippatos, G., and Uhal, B. D. (2000). Amiodarone induces apoptosis of human and rat alveolar epithelial cells in vitro. *Am. J. Physiol Lung Cell Mol. Physiol* **278**(5), L1039-L1044.

10. Barton, C. C., Ganey, P. E., and Roth, R. A. (2000). Lipopolysaccharide augments aflatoxin B(1)-induced liver injury through neutrophil-dependent and -independent mechanisms. *Toxicol. Sci.* **58**(1), 208-215.

11. Bautista, A. P. (1997). Chronic alcohol intoxication induces hepatic injury through enhanced macrophage inflammatory protein-2 production and intercellular adhesion molecule-1 expression in the liver. *Hepatology* **25**(2), 335-342.

12. Begriche, K., Igoudjil, A., Pessayre, D., and Fromenty, B. (2006). Mitochondrial dysfunction in NASH: causes, consequences and possible means to prevent it. *Mitochondrion* **6**(1), 1-28.

13. Bemelmans, M. H., Gouma, D. J., and Buurman, W. A. (1993). Influence of nephrectomy on tumor necrosis factor clearance in a murine model. *J Immunol* **150**(5), 2007-2017.

14. Benbassat, C., and Shahar, A. (1991). [Acute fulminant hepatic failure after short-term amiodarone]. *Harefuah* **121**(10), 378-380.

15. Beutler, B., and Kruys, V. (1995). Lipopolysaccharide signal transduction, regulation of tumor necrosis factor biosynthesis, and signaling by tumor necrosis factor itself. *J. Cardiovasc. Pharmacol.* **25 Suppl 2**, S1-S8.

16. Bhandari, N., Figueroa, D. J., Lawrence, J. W., and Gerhold, D. L. (2008). Phospholipidosis assay in HepG2 cells and rat or rhesus hepatocytes using phospholipid probe NBD-PE. *Assay. Drug Dev. Technol.* **6**(3), 407-419.

17. Bjork, I., and Lindahl, U. (1982). Mechanism of the anticoagulant action of heparin. *Mol Cell Biochem* **48**(3), 161-182.

18. Boelsterli, U. A., and Lim, P. L. (2007). Mitochondrial abnormalities--a link to idiosyncratic drug hepatotoxicity? *Toxicol Appl Pharmacol* **220**(1), 92-107.

19. Bolt, M. W., Card, J. W., Racz, W. J., Brien, J. F., and Massey, T. E. (2001). Disruption of mitochondrial function and cellular ATP levels by amiodarone and N-desethylamiodarone in initiation of amiodarone-induced pulmonary cytotoxicity. *J. Pharmacol. Exp. Ther.* **298**(3), 1280-1289.

20. Bonder, C. S., Ajuebor, M. N., Zbytnuik, L. D., Kubes, P., and Swain, M. G. (2004). Essential role for neutrophil recruitment to the liver in concanavalin A-induced hepatitis. *J Immunol* **172**(1), 45-53.

21. Bradham, C. A., Qian, T., Streetz, K., Trautwein, C., Brenner, D. A., and Lemasters, J. J. (1998). The mitochondrial permeability transition is required for tumor necrosis factor alpha-mediated apoptosis and cytochrome c release. *Mol. Cell Biol.* **18**(11), 6353-6364.

22. Breitenstein, A., Stampfli, S. F., Camici, G. G., Akhmedov, A., Ha, H. R., Follath, F., Bogdanova, A., Luscher, T. F., and Tanner, F. C. (2008). Amiodarone inhibits arterial thrombus formation and tissue factor translation. *Arterioscler. Thromb. Vasc Biol* **28**(12), 2231-2238.

23. Buchweitz, J. P., Ganey, P. E., Bursian, S. J., and Roth, R. A. (2002). Underlying endotoxemia augments toxic responses to chlorpromazine: is there a relationship to drug idiosyncrasy? *J. Pharmacol. Exp. Ther.* **300**(2), 460-467.

24. Cabre, A., Girona, J., Vallve, J. C., and Masana, L. (2004). Aldehydes mediate tissue factor induction: a possible mechanism linking lipid peroxidation to thrombotic events. *J Cell Physiol* **198**(2), 230-236.

25. Carr, A. (2003). Toxicity of antiretroviral therapy and implications for drug development. *Nat Rev Drug Discov* **2**(8), 624-634.

26. Chandel, N. S., Maltepe, E., Goldwasser, E., Mathieu, C. E., Simon, M. C., and Schumacker, P. T. (1998). Mitochondrial reactive oxygen species trigger hypoxia-induced transcription. *Proc. Natl. Acad. Sci. U. S. A* **95**(20), 11715-11720.

27. Chandel, N. S., McClintock, D. S., Feliciano, C. E., Wood, T. M., Melendez, J. A., Rodriguez, A. M., and Schumacker, P. T. (2000). Reactive oxygen species generated at mitochondrial complex III stabilize hypoxia-inducible factor-1alpha during hypoxia: a mechanism of O2 sensing. *J Biol Chem* **275**(33), 25130-25138.

28. Chang, C. C., Petrelli, M., Tomashefski, J. F., Jr., and McCullough, A. J. (1999). Severe intrahepatic cholestasis caused by amiodarone toxicity after withdrawal of the drug: a case report and review of the literature. *Arch Pathol Lab Med* **123**(3), 251-256.

29. Choi, I. S., Kim, B. S., Cho, K. S., Park, J. C., Jang, M. H., Shin, M. C., Jung, S. B., Chung, J. H., and Kim, C. J. (2002). Amiodarone induces apoptosis in L-132 human lung epithelial cell line. *Toxicol. Lett.* **132**(1), 47-55.

30. Chosay, J. G., Essani, N. A., Dunn, C. J., and Jaeschke, H. (1997). Neutrophil margination and extravasation in sinusoids and venules of liver during endotoxin-induced injury. *Am J Physiol* **272**(5 Pt 1), G1195-G1200.

31. Clay, K. D., Hanson, J. S., Pope, S. D., Rissmiller, R. W., Purdum, P. P., III, and Banks, P. M. (2006). Brief communication: severe hepatotoxicity of telithromycin: three case reports and literature review. *Ann Intern Med* **144**(6), 415-420.

32. Colell, A., Coll, O., Garcia-Ruiz, C., Paris, R., Tiribelli, C., Kaplowitz, N., and Fernandez-Checa, J. C. (2001). Tauroursodeoxycholic acid protects hepatocytes from ethanol-fed rats against tumor necrosis factor-induced cell death by replenishing mitochondrial glutathione. *Hepatology* **34**(5), 964-971.

33. Copple, B. L., Banes, A., Ganey, P. E., and Roth, R. A. (2002). Endothelial cell injury and fibrin deposition in rat liver after monocrotaline exposure. *Toxicol. Sci.* **65**(2), 309-318.

34. Copple, B. L., Rondelli, C. M., Maddox, J. F., Hoglen, N. C., Ganey, P. E., and Roth, R. A. (2004). Modes of cell death in rat liver after monocrotaline exposure. *Toxicol. Sci.* **77**(1), 172-182.

35. Corda, S., Laplace, C., Vicaut, E., and Duranteau, J. (2001). Rapid reactive oxygen species production by mitochondria in endothelial cells exposed to

tumor necrosis factor-alpha is mediated by ceramide. *Am. J. Respir. Cell Mol. Biol.* **24**(6), 762-768.

36. Corpechot, C., Barbu, V., Wendum, D., Kinnman, N., Rey, C., Poupon, R., Housset, C., and Rosmorduc, O. (2002). Hypoxia-induced VEGF and collagen I expressions are associated with angiogenesis and fibrogenesis in experimental cirrhosis. *Hepatology* **35**(5), 1010-1021.

37. Curzio, M., Esterbauer, H., Di, M. C., Cecchini, G., and Dianzani, M. U. (1986). Chemotactic activity of the lipid peroxidation product 4-hydroxynonenal and homologous hydroxyalkenals. *Biol Chem Hoppe Seyler* **367**(4), 321-329.

38. Das, A., and Mukhopadhyay, S. (2011). The evil axis of obesity, inflammation and type-2 diabetes. *Endocr Metab Immune Disord Drug Targets* **11**(1), 23-31.

39. De Marzo, A. M., Platz, E. A., Sutcliffe, S., Xu, J., Gronberg, H., Drake, C. G., Nakai, Y., Isaacs, W. B., and Nelson, W. G. (2007). Inflammation in prostate carcinogenesis. *Nat Rev Cancer* **7**(4), 256-269.

40. Deng, X., Luyendyk, J. P., Zou, W., Lu, J., Malle, E., Ganey, P. E., and Roth, R. A. (2007). Neutrophil interaction with the hemostatic system contributes to liver injury in rats cotreated with lipopolysaccharide and ranitidine. *J. Pharmacol. Exp. Ther.* **322**(2), 852-861.

41. Deng, X., Stachlewitz, R. F., Liguori, M. J., Blomme, E. A., Waring, J. F., Luyendyk, J. P., Maddox, J. F., Ganey, P. E., and Roth, R. A. (2006). Modest inflammation enhances diclofenac hepatotoxicity in rats: role of neutrophils and bacterial translocation. *J. Pharmacol. Exp. Ther.* **319**(3), 1191-1199.

42. Deschamps, D., DeBeco, V., Fisch, C., Fromenty, B., Guillouzo, A., and Pessayre, D. (1994). Inhibition by perhexiline of oxidative phosphorylation and the beta-oxidation of fatty acids: possible role in pseudoalcoholic liver lesions. *Hepatology* **19**(4), 948-961.

43. Doval, H. C., Nul, D. R., Grancelli, H. O., Perrone, S. V., Bortman, G. R., and Curiel, R. (1994). Randomised trial of low-dose amiodarone in severe congestive heart failure. Grupo de Estudio de la Sobrevida en la Insuficiencia Cardiaca en Argentina (GESICA). *Lancet* **344**(8921), 493-498.

44. Dugan, C. M., MacDonald, A. E., Roth, R. A., and Ganey, P. E. (2010). A mouse model of severe halothane hepatitis based on human risk factors. *J. Pharmacol. Exp. Ther.* **333**(2), 364-372.

45. Elsherbiny, M. E., El-Kadi, A. O., and Brocks, D. R. (2008). The metabolism of amiodarone by various CYP isoenzymes of human and rat, and the inhibitory influence of ketoconazole. *J. Pharm. Pharm. Sci.* **11**(1), 147-159.

46. Farhood, A., McGuire, G. M., Manning, A. M., Miyasaka, M., Smith, C. W., and Jaeschke, H. (1995). Intercellular adhesion molecule 1 (ICAM-1) expression and its role in neutrophil-induced ischemia-reperfusion injury in rat liver. *J Leukoc Biol* **57**(3), 368-374.

47. Fassoulaki, A., Eger, E. I., Johnson, B. H., Ferrell, L. D., Smuckler, E. A., Harper, M. H., Eger, R. R., and Cahalan, M. K. (1984). Brief periods of hypoxia can produce hepatic injury in rats. *Anesth Analg* **63**(10), 885-887.

48. Feissner, R. F., Skalska, J., Gaum, W. E., and Sheu, S. S. (2009). Crosstalk signaling between mitochondrial Ca2+ and ROS. *Front Biosci.* **14**, 1197-1218.

49. Feng, J. Y., Johnson, A. A., Johnson, K. A., and Anderson, K. S. (2001). Insights into the molecular mechanism of mitochondrial toxicity by AIDS drugs. *J Biol Chem* **276**(26), 23832-23837.

50. Fickert, P., Fuchsbichler, A., Marschall, H. U., Wagner, M., Zollner, G., Krause, R., Zatloukal, K., Jaeschke, H., Denk, H., and Trauner, M. (2006). Lithocholic acid feeding induces segmental bile duct obstruction and destructive cholangitis in mice. *Am J Pathol* **168**(2), 410-422.

51. Fischl, M. A., Dickinson, G. M., and La, V. L. (1988). Safety and efficacy of sulfamethoxazole and trimethoprim chemoprophylaxis for Pneumocystis carinii pneumonia in AIDS. *JAMA* **259**(8), 1185-1189.

52. Fransen, L., Van der, H. J., Ruysschaert, R., and Fiers, W. (1986). Recombinant tumor necrosis factor: its effect and its synergism with interferon-gamma on a variety of normal and transformed human cell lines. *Eur. J. Cancer Clin. Oncol.* **22**(4), 419-426.

53. Fromenty, B., Fisch, C., Berson, A., Letteron, P., Larrey, D., and Pessayre, D. (1990a). Dual effect of amiodarone on mitochondrial respiration. Initial protonophoric uncoupling effect followed by inhibition of the respiratory chain at the levels of complex I and complex II. *J. Pharmacol. Exp. Ther.* **255**(3), 1377-1384.

54. Fromenty, B., Fisch, C., Labbe, G., Degott, C., Deschamps, D., Berson, A., Letteron, P., and Pessayre, D. (1990b). Amiodarone inhibits the mitochondrial beta-oxidation of fatty acids and produces microvesicular steatosis of the liver in mice. *J. Pharmacol. Exp. Ther.* **255**(3), 1371-1376.

55. Fuhrmann, V., Jager, B., Zubkova, A., and Drolz, A. (2010). Hypoxic hepatitis - epidemiology, pathophysiology and clinical management. *Wien. Klin. Wochenschr.* **122**(5-6), 129-139.

56. Futamura, Y. (1996). Effect of amiodarone on cytokine release and on enzyme activities of mouse alveolar macrophages, bone marrow macrophages, and blood monocytes. *J. Toxicol. Sci.* **21**(2), 125-134.

57. Ganey, P. E., Barton, Y. W., Kinser, S., Sneed, R. A., Barton, C. C., and Roth, R. A. (2001). Involvement of cyclooxygenase-2 in the potentiation of allyl alcohol-induced liver injury by bacterial lipopolysaccharide. *Toxicol. Appl. Pharmacol.* **174**(2), 113-121.

58. Ganey, P. E., Luyendyk, J. P., Maddox, J. F., and Roth, R. A. (2004). Adverse hepatic drug reactions: inflammatory episodes as consequence and contributor. *Chem. Biol. Interact.* **150**(1), 35-51.

59. Gardiner, K. R., Halliday, M. I., Barclay, G. R., Milne, L., Brown, D., Stephens, S., Maxwell, R. J., and Rowlands, B. J. (1995). Significance of systemic endotoxaemia in inflammatory bowel disease. *Gut* **36**(6), 897-901.

60. Gill, J., Heel, R. C., and Fitton, A. (1992). Amiodarone. An overview of its pharmacological properties, and review of its therapeutic use in cardiac arrhythmias. *Drugs* **43**(1), 69-110.

61. Graham, D. J., Green, L., Senior, J. R., and Nourjah, P. (2003). Troglitazone-induced liver failure: a case study. *Am J Med* **114**(4), 299-306.

62. Greenfield, E. A., Nguyen, K. A., and Kuchroo, V. K. (1998). CD28/B7 costimulation: a review. *Crit Rev Immunol* **18**(5), 389-418.

63. Gross, S. A., Bandyopadhyay, S., Klaunig, J. E., and Somani, P. (1989). Amiodarone and desethylamiodarone toxicity in isolated hepatocytes in culture. *Proc. Soc. Exp. Biol. Med.* **190**(2), 163-169.

64. Gudz, T. I., Tserng, K. Y., and Hoppel, C. L. (1997). Direct inhibition of mitochondrial respiratory chain complex III by cell-permeable ceramide. *J Biol Chem* **272**(39), 24154-24158.

65. Gujral, J. S., Liu, J., Farhood, A., Hinson, J. A., and Jaeschke, H. (2004). Functional importance of ICAM-1 in the mechanism of neutrophil-induced liver injury in bile duct-ligated mice. *Am J Physiol Gastrointest Liver Physiol* **286**(3), G499-G507.

66. Ha, H. R., Bigler, L., Binder, M., Kozlik, P., Stieger, B., Hesse, M., Altorfer, H. R., and Follath, F. (2001). Metabolism of amiodarone (part I): identification of a new hydroxylated metabolite of amiodarone. *Drug Metab Dispos* **29**(2), 152-158.

67. Ha, H. R., Bigler, L., Wendt, B., Maggiorini, M., and Follath, F. (2005). Identification and quantitation of novel metabolites of amiodarone in plasma of treated patients. *Eur. J. Pharm. Sci.* **24**(4), 271-279.

68. Haasio, K., Koponen, A., Penttila, K. E., and Nissinen, E. (2002). Effects of entacapone and tolcapone on mitochondrial membrane potential. *Eur J Pharmacol* **453**(1), 21-26.

69. Harris, L., Hind, C. R., McKenna, W. J., Savage, C., Krikler, S. J., Storey, G. C., and Holt, D. W. (1983). Renal elimination of amiodarone and its desethyl metabolite. *Postgrad Med J* **59**(693), 440-442.

70. Hassan, F., Morikawa, A., Islam, S., Tumurkhuu, G., Dagvadorj, J., Koide, N., Naiki, Y., Mori, I., Yoshida, T., and Yokochi, T. (2008). Lipopolysaccharide augments the in vivo lethal action of doxorubicin against mice via hepatic damage. *Clin Exp Immunol* **151**(2), 334-340.

71. Hatano, E., Bradham, C. A., Stark, A., Iimuro, Y., Lemasters, J. J., and Brenner, D. A. (2000). The mitochondrial permeability transition augments Fas-induced apoptosis in mouse hepatocytes. *J. Biol. Chem.* **275**(16), 11814-11823.

72. Hentze, H., Latta, M., Kunstle, G., Dhakshinamoorthy, S., Ng, P. Y., Porter, A. G., and Wendel, A. (2004). Topoisomerase inhibitor camptothecin sensitizes mouse hepatocytes in vitro and in vivo to TNF-mediated apoptosis. *Hepatology* **39**(5), 1311-1320.

73. Hewett, J. A., and Roth, R. A. (1993). Hepatic and extrahepatic pathobiology of bacterial lipopolysaccharides. *Pharmacol Rev* **45**(4), 382-411.

74. Hewett, J. A., Schultze, A. E., VanCise, S., and Roth, R. A. (1992). Neutrophil depletion protects against liver injury from bacterial endotoxin. *Lab Invest* **66**(3), 347-361.

75. Higuchi, M., Proske, R. J., and Yeh, E. T. (1998). Inhibition of mitochondrial respiratory chain complex I by TNF results in cytochrome c release, membrane permeability transition, and apoptosis. *Oncogene* **17**(19), 2515-2524.

76. Isomoto, S., Kawakami, A., Arakaki, T., Yamashita, S., Yano, K., and Ono, K. (2006). Effects of antiarrhythmic drugs on apoptotic pathways in H9c2 cardiac cells. *J. Pharmacol. Sci.* **101**(4), 318-324.

77. Jaeschke, H., Farhood, A., and Smith, C. W. (1991). Neutrophil-induced liver cell injury in endotoxin shock is a CD11b/CD18-dependent mechanism. *Am J Physiol* **261**(6 Pt 1), G1051-G1056.

78. Jaeschke, H., Farhood, A., and Smith, C. W. (1990). Neutrophils contribute to ischemia/reperfusion injury in rat liver in vivo. *FASEB J* **4**(15), 3355-3359.

79. Jones, B. E., Lo, C. R., Liu, H., Srinivasan, A., Streetz, K., Valentino, K. L., and Czaja, M. J. (2000). Hepatocytes sensitized to tumor necrosis factor-alpha cytotoxicity undergo apoptosis through caspase-dependent and caspase-independent pathways. *J. Biol. Chem.* **275**(1), 705-712.

80. Jones, B. E., Lo, C. R., Srinivasan, A., Valentino, K. L., and Czaja, M. J. (1999b). Ceramide induces caspase-independent apoptosis in rat hepatocytes sensitized by inhibition of RNA synthesis. *Hepatology* **30**(1), 215-222.

81. Jones, B. E., Lo, C. R., Srinivasan, A., Valentino, K. L., and Czaja, M. J. (1999a). Ceramide induces caspase-independent apoptosis in rat hepatocytes sensitized by inhibition of RNA synthesis. *Hepatology* **30**(1), 215-222.

82. Jones, K. H., and Senft, J. A. (1985). An improved method to determine cell viability by simultaneous staining with fluorescein diacetate-propidium iodide. *J. Histochem. Cytochem.* **33**(1), 77-79.

83. Juarez-Olguin, H., Flores, J., Perez, G., Hernandez, G., Flores, C., Guille, A., Camacho, A., Toledo, A., Carrasco, M., and Lares, I. (2002). Bioavailability of ranitidine in healthy Mexican volunteers: effect of food. *Proc West Pharmacol Soc.* **45**, 156-158.

84. Kaplowitz, N. (2005). Idiosyncratic drug hepatotoxicity. *Nat. Rev. Drug Discov.* **4**(6), 489-499.

85. Kaufmann, P., Torok, M., Hanni, A., Roberts, P., Gasser, R., and Krahenbuhl, S. (2005). Mechanisms of benzarone and benzbromarone-induced hepatic toxicity. *Hepatology* **41**(4), 925-935.

86. Khan, S., and O'Brien, P. J. (1997). Rapid and specific efflux of glutathione before hepatocyte injury induced by hypoxia. *Biochem Biophys Res Commun* **238**(2), 320-322.

87. Khutornenko, A. A., Roudko, V. V., Chernyak, B. V., Vartapetian, A. B., Chumakov, P. M., and Evstafieva, A. G. (2010). Pyrimidine biosynthesis links mitochondrial respiration to the p53 pathway. *Proc Natl Acad Sci U S A* **107**(29), 12828-12833.

88. Kinser, S., Sneed, R., Roth, R., and Ganey, P. (2004). Neutrophils contribute to endotoxin enhancement of allyl alcohol hepatotoxicity. *J. Toxicol. Environ. Health A* **67**(12), 911-928.

89. Konrad, D., Rudich, A., Bilan, P. J., Patel, N., Richardson, C., Witters, L. A., and Klip, A. (2005). Troglitazone causes acute mitochondrial membrane depolarisation and an AMPK-mediated increase in glucose phosphorylation in muscle cells. *Diabetologia* **48**(5), 954-966.

90. Koopman, G., Reutelingsperger, C. P., Kuijten, G. A., Keehnen, R. M., Pals, S. T., and van Oers, M. H. (1994). Annexin V for flow cytometric detection of phosphatidylserine expression on B cells undergoing apoptosis. *Blood* **84**(5), 1415-1420.

91. Landsteiner, K., and Jacobs, J. (1935). STUDIES ON THE SENSITIZATION OF ANIMALS WITH SIMPLE CHEMICAL COMPOUNDS. *J Exp Med* **61**(5), 643-656.

92. Lasser, K. E., Allen, P. D., Woolhandler, S. J., Himmelstein, D. U., Wolfe, S. M., and Bor, D. H. (2002). Timing of new black box warnings and withdrawals for prescription medications. *JAMA* **287**(17), 2215-2220.

93. Lawson, J. A., Farhood, A., Hopper, R. D., Bajt, M. L., and Jaeschke, H. (2000). The hepatic inflammatory response after acetaminophen overdose: role of neutrophils. *Toxicol Sci* **54**(2), 509-516.

94. Lazarou, J., Pomeranz, B. H., and Corey, P. N. (1998). Incidence of adverse drug reactions in hospitalized patients: a meta-analysis of prospective studies. *JAMA* **279**(15), 1200-1205.

95. Leist, M., Gantner, F., Bohlinger, I., Germann, P. G., Tiegs, G., and Wendel, A. (1994). Murine hepatocyte apoptosis induced in vitro and in vivo by TNF-alpha requires transcriptional arrest. *J. Immunol.* **153**(4), 1778-1788.

96. Lemasters, J. J., Ji, S., and Thurman, R. G. (1981). Centrilobular injury following hypoxia in isolated, perfused rat liver. *Science* **213**(4508), 661-663.

97. Lepper, P. M., Held, T. K., Schneider, E. M., Bolke, E., Gerlach, H., and Trautmann, M. (2002). Clinical implications of antibiotic-induced endotoxin release in septic shock. *Intensive Care Med* **28**(7), 824-833.

98. Levi, M., Keller, T. T., van, G. E., and ten, C. H. (2003). Infection and inflammation and the coagulation system. *Cardiovasc Res* **60**(1), 26-39.

99. Lewis, J. H., Ranard, R. C., Caruso, A., Jackson, L. K., Mullick, F., Ishak, K. G., Seeff, L. B., and Zimmerman, H. J. (1989). Amiodarone hepatotoxicity: prevalence and clinicopathologic correlations among 104 patients. *Hepatology* **9**(5), 679-685.

100. Lorch, V., Murphy, D., Hoersten, L. R., Harris, E., Fitzgerald, J., and Sinha, S. N. (1985). Unusual syndrome among premature infants: association with a new intravenous vitamin E product. *Pediatrics* **75**(3), 598-602.

101. Lu, J., Jones, A. D., Harkema, J. R., Roth, R. A., and Ganey, P. E. (2012). Amiodarone Exposure During Modest Inflammation Induces Idiosyncrasy-like Liver Injury in Rats: Role of Tumor Necrosis Factor-alpha. *Toxicol. Sci.* **125**(1), 126-133.

102. Luyendyk, J. P., Maddox, J. F., Cosma, G. N., Ganey, P. E., Cockerell, G. L., and Roth, R. A. (2003). Ranitidine treatment during a modest inflammatory response precipitates idiosyncrasy-like liver injury in rats. *J. Pharmacol. Exp. Ther.* **307**(1), 9-16.

103. Luyendyk, J. P., Maddox, J. F., Green, C. D., Ganey, P. E., and Roth, R. A. (2004). Role of hepatic fibrin in idiosyncrasy-like liver injury from lipopolysaccharide-ranitidine coexposure in rats. *Hepatology* **40**(6), 1342-1351.

104. Luyendyk, J. P., Shaw, P. J., Green, C. D., Maddox, J. F., Ganey, P. E., and Roth, R. A. (2005). Coagulation-mediated hypoxia and neutrophil-dependent hepatic injury in rats given lipopolysaccharide and ranitidine. *J. Pharmacol. Exp. Ther.* **314**(3), 1023-1031.

105. Luyendyk, J. P., Shores, K. C., Ganey, P. E., and Roth, R. A. (2002). Bacterial lipopolysaccharide exposure alters aflatoxin B(1) hepatotoxicity: benchmark dose analysis for markers of liver injury. *Toxicol. Sci.* **68**(1), 220-225.

106. Malle, E., Hazell, L., Stocker, R., Sattler, W., Esterbauer, H., and Waeg, G. (1995). Immunologic detection and measurement of hypochlorite-modified LDL with specific monoclonal antibodies. *Arterioscler. Thromb. Vasc. Biol.* **15**(7), 982-989.

107. Melnik, G., Schwesinger, W. H., Teng, R., Dogolo, L. C., and Vincent, J. (1998). Hepatobiliary elimination of trovafloxacin and metabolites following single oral doses in healthy volunteers. *Eur J Clin Microbiol. Infect Dis* **17**(6), 424-426.

108. Mencin, A., Kluwe, J., and Schwabe, R. F. (2009). Toll-like receptors as targets in chronic liver diseases. *Gut* **58**(5), 704-720.

109. Metushi, I. G., Cai, P., Zhu, X., Nakagawa, T., and Uetrecht, J. P. (2011). A fresh look at the mechanism of isoniazid-induced hepatotoxicity. *Clin Pharmacol Ther* **89**(6), 911-914.

110. Moulin, F., Pearson, J. M., Schultze, A. E., Scott, M. A., Schwartz, K. A., Davis, J. M., Ganey, P. E., and Roth, R. A. (1996). Thrombin is a distal mediator of lipopolysaccharide-induced liver injury in the rat. *J Surg Res* **65**(2), 149-158.

111. Mulder, J. E., Brien, J. F., Racz, W. J., Takahashi, T., and Massey, T. E. (2011). Mechanisms of amiodarone and desethylamiodarone cytotoxicity in nontransformed human peripheral lung epithelial cells. *J. Pharmacol. Exp. Ther.* **336**(2), 551-559.

112. Nawroth, P. P., and Stern, D. M. (1986). Modulation of endothelial cell hemostatic properties by tumor necrosis factor. *J Exp Med* **163**(3), 740-745.

113. Nicoletti, I., Migliorati, G., Pagliacci, M. C., Grignani, F., and Riccardi, C. (1991). A rapid and simple method for measuring thymocyte apoptosis by propidium iodide staining and flow cytometry. *J. Immunol. Methods* **139**(2), 271-279.

114. Njoku, D. B., Greenberg, R. S., Bourdi, M., Borkowf, C. B., Dake, E. M., Martin, J. L., and Pohl, L. R. (2002). Autoantibodies associated with volatile anesthetic hepatitis found in the sera of a large cohort of pediatric anesthesiologists. *Anesth Analg* **94**(2), 243-9, table.

115. O'Sullivan, J. J., McCarthy, P. T., and Wren, C. (1995). Differences in amiodarone, digoxin, flecainide and sotalol concentrations between

antemortem serum and femoral postmortem blood. *Hum. Exp. Toxicol.* **14**(7), 605-608.

116. Ohno, M., Yamaguchi, I., Yamamoto, I., Fukuda, T., Yokota, S., Maekura, R., Ito, M., Yamamoto, Y., Ogura, T., Maeda, K., Komuta, K., Igarashi, T., and Azuma, J. (2000). Slow N-acetyltransferase 2 genotype affects the incidence of isoniazid and rifampicin-induced hepatotoxicity. *Int J Tuberc Lung Dis* **4**(3), 256-261.

117. Ohyama, K., Nakajima, M., Nakamura, S., Shimada, N., Yamazaki, H., and Yokoi, T. (2000). A significant role of human cytochrome P450 2C8 in amiodarone N-deethylation: an approach to predict the contribution with relative activity factor. *Drug Metab Dispos* **28**(11), 1303-1310.

118. Okaya, T., and Lentsch, A. B. (2003). Cytokine cascades and the hepatic inflammatory response to ischemia and reperfusion. *J Invest Surg* **16**(3), 141-147.

119. Piccoli, C., Quarato, G., Ripoli, M., D'Aprile, A., Scrima, R., Cela, O., Boffoli, D., Moradpour, D., and Capitanio, N. (2009). HCV infection induces mitochondrial bioenergetic unbalance: causes and effects. *Biochim Biophys Acta* **1787**(5), 539-546.

120. Pilgrim, J. L., Gerostamoulos, D., and Drummer, O. H. (2011). Review: Pharmacogenetic aspects of the effect of cytochrome P450 polymorphisms on serotonergic drug metabolism, response, interactions, and adverse effects. *Forensic Sci Med Pathol* **7**(2), 162-184.

121. Pollak, P. T., Bouillon, T., and Shafer, S. L. (2000). Population pharmacokinetics of long-term oral amiodarone therapy. *Clin. Pharmacol. Ther.* **67**(6), 642-652.

122. Pollak, P. T., and Shafer, S. L. (2004). Use of population modeling to define rational monitoring of amiodarone hepatic effects. *Clin. Pharmacol. Ther.* **75**(4), 342-351.

123. Pollak, P. T., and You, Y. D. (2003). Monitoring of hepatic function during amiodarone therapy. *Am. J. Cardiol.* **91**(5), 613-616.

124. Pourbaix, S., Berger, Y., Desager, J. P., Pacco, M., and Harvengt, C. (1985). Absolute bioavailability of amiodarone in normal subjects. *Clin Pharmacol Ther* **37**(2), 118-123.

125. Pullen, H., Wright, N., and Murdoch, J. M. (1967). Hypersensitivity reactions to antibacterial drugs in infectious mononucleosis. *Lancet* **2**(7527), 1176-1178.

126. Punithavathi, D., Venkatesan, N., and Babu, M. (2003). Protective effects of curcumin against amiodarone-induced pulmonary fibrosis in rats. *Br. J. Pharmacol.* **139**(7), 1342-1350.

127. Ratz Bravo, A. E., Drewe, J., Schlienger, R. G., Krahenbuhl, S., Pargger, H., and Ummenhofer, W. (2005). Hepatotoxicity during rapid intravenous loading with amiodarone: Description of three cases and review of the literature. *Crit Care Med. %2005. Jan. ;33. (1):128. -34.* **discussion**.

128. Reinhart, P. G., and Gairola, C. G. (1997). Amiodarone-induced pulmonary toxicity in Fischer rats: release of tumor necrosis factor alpha and transforming growth factor beta by pulmonary alveolar macrophages. *J. Toxicol. Environ. Health* **52**(4), 353-365.

129. Rivera, A., Jr., Abdo, K. M., Bucher, J. R., Leininger, J. R., Montgomery, C. A., and Roberts, R. J. (1990). Toxicity studies of intravenous vitamin E in newborn rabbits. *Dev. Pharmacol Ther* **14**(4), 231-237.

130. Roth, R. A., Harkema, J. R., Pestka, J. P., and Ganey, P. E. (1997). Is exposure to bacterial endotoxin a determinant of susceptibility to intoxication from xenobiotic agents? *Toxicol Appl Pharmacol* **147**(2), 300-311.

131. Roth, R. A., Luyendyk, J. P., Maddox, J. F., and Ganey, P. E. (2003). Inflammation and drug idiosyncrasy--is there a connection? *J. Pharmacol. Exp. Ther.* **307**(1), 1-8.

132. Rothwell, C., McGuire, E. J., Altrogge, D. M., Masuda, H., and de, l., I (2002). Chronic toxicity in monkeys with the thiazolidinedione antidiabetic agent troglitazone. *J Toxicol Sci* **27**(1), 35-47.

133. Rotmensch, H. H., Belhassen, B., Swanson, B. N., Shoshani, D., Spielman, S. R., Greenspon, A. J., Greenspan, A. M., Vlasses, P. H., and Horowitz, L. N. (1984). Steady-state serum amiodarone concentrations: relationships with antiarrhythmic efficacy and toxicity. *Ann. Intern. Med.* **101**(4), 462-469.

134. Scaffidi, P., Misteli, T., and Bianchi, M. E. (2002). Release of chromatin protein HMGB1 by necrotic cells triggers inflammation. *Nature* **418**(6894), 191-195.

135. Schleef, R. R., Bevilacqua, M. P., Sawdey, M., Gimbrone, M. A., Jr., and Loskutoff, D. J. (1988). Cytokine activation of vascular endothelium. Effects on tissue-type plasminogen activator and type 1 plasminogen activator inhibitor. *J Biol Chem* **263**(12), 5797-5803.

136. Semenza, G. L. (2004). Hydroxylation of HIF-1: oxygen sensing at the molecular level. *Physiology (Bethesda)* **19**, 176-182.

137. Sewer, M. B., Koop, D. R., and Morgan, E. T. (1997). Differential inductive and suppressive effects of endotoxin and particulate irritants on hepatic and renal cytochrome P-450 expression. *J. Pharmacol. Exp. Ther.* **280**(3), 1445-1454.

138. Shappell, S. B., Toman, C., Anderson, D. C., Taylor, A. A., Entman, M. L., and Smith, C. W. (1990). Mac-1 (CD11b/CD18) mediates adherence-dependent hydrogen peroxide production by human and canine neutrophils. *J Immunol* **144**(7), 2702-2711.

139. Shaw, P. J., Beggs, K. M., Sparkenbaugh, E. M., Dugan, C. M., Ganey, P. E., and Roth, R. A. (2009a). Trovafloxacin enhances TNF-induced inflammatory stress and cell death signaling and reduces TNF clearance in a murine model of idiosyncratic hepatotoxicity. *Toxicol. Sci.* **111**(2), 288-301.

140. Shaw, P. J., Fullerton, A. M., Scott, M. A., Ganey, P. E., and Roth, R. A. (2009b). The role of the hemostatic system in murine liver injury induced by coexposure to lipopolysaccharide and trovafloxacin, a drug with idiosyncratic liability. *Toxicol. Appl. Pharmacol.* **236**(3), 293-300.

141. Shaw, P. J., Ganey, P. E., and Roth, R. A. (2009c). Tumor necrosis factor alpha is a proximal mediator of synergistic hepatotoxicity from trovafloxacin/lipopolysaccharide coexposure. *J. Pharmacol. Exp. Ther.* **328**(1), 62-68.

142. Shaw, P. J., Ganey, P. E., and Roth, R. A. (2010). Idiosyncratic drug-induced liver injury and the role of inflammatory stress with an emphasis on an animal model of trovafloxacin hepatotoxicity. *Toxicol Sci* **118**(1), 7-18.

143. Shaw, P. J., Ganey, P. E., and Roth, R. A. (2009d). Trovafloxacin enhances the inflammatory response to a Gram-negative or a Gram-positive bacterial stimulus, resulting in neutrophil-dependent liver injury in mice. *J. Pharmacol. Exp. Ther.* **330**(1), 72-78.

144. Shaw, P. J., Hopfensperger, M. J., Ganey, P. E., and Roth, R. A. (2007). Lipopolysaccharide and trovafloxacin coexposure in mice causes idiosyncrasy-like liver injury dependent on tumor necrosis factor-alpha. *Toxicol. Sci.* **100**(1), 259-266.

145. Shayeganpour, A., Hamdy, D. A., and Brocks, D. R. (2008). Pharmacokinetics of desethylamiodarone in the rat after its administration as the preformed metabolite, and after administration of amiodarone. *Biopharm. Drug Dispos.* **29**(3), 159-166.

146. Shenton, J. M., Chen, J., and Uetrecht, J. P. (2004). Animal models of idiosyncratic drug reactions. *Chem Biol Interact* **150**(1), 53-70.

147. Shojiro I, Atsushi K, Akira O, Shunichi Y, and Katsusuke Y. Antiarrhythmic Amiodarone Mediates Apoptotic Cell Death of HepG2 Hepatoblastoma Cells

through the Mitochondrial Pathway. 49, 13-17. 2004.
Ref Type: Generic

148. Singh, B. N. (1996). Antiarrhythmic actions of amiodarone: a profile of a paradoxical agent. *Am. J. Cardiol. %1996. Aug. 29. ;78. (4A.):41. -53.*(4A:41-53).

149. Smith, M. K., and Mooney, D. J. (2007). Hypoxia leads to necrotic hepatocyte death. *J Biomed. Mater. Res A* **80**(3), 520-529.

150. Snipes, M. B., Barnett, A. L., Harkema, J. R., Hotchkiss, J. A., Rebar, A. H., and Reddick, L. J. (1995). Specific biological effects of an anti-rat PMN antiserum intraperitoneally infected into f344/n rats. *Vet. Clin. Pathol.* **24**(1), 11-17.

151. Spaniol, M., Bracher, R., Ha, H. R., Follath, F., and Krahenbuhl, S. (2001). Toxicity of amiodarone and amiodarone analogues on isolated rat liver mitochondria. *J. Hepatol.* **35**(5), 628-636.

152. Sparkenbaugh, E. M., Ganey, P. E., and Roth, R. A. (2012). Hypoxia sensitization of hepatocytes to neutrophil elastase-mediated cell death depends on MAPKs and HIF-1alpha. *Am J Physiol Gastrointest Liver Physiol*.

153. Sparkenbaugh, E. M., Saini, Y., Greenwood, K. K., LaPres, J. J., Luyendyk, J. P., Copple, B. L., Maddox, J. F., Ganey, P. E., and Roth, R. A. (2011). The role of hypoxia-inducible factor-1alpha in acetaminophen hepatotoxicity. *J Pharmacol Exp Ther* **338**(2), 492-502.

154. Stadler, K., Ha, H. R., Ciminale, V., Spirli, C., Saletti, G., Schiavon, M., Bruttomesso, D., Bigler, L., Follath, F., Pettenazzo, A., and Baritussio, A. (2008). Amiodarone alters late endosomes and inhibits SARS coronavirus infection at a post-endosomal level. *Am. J. Respir. Cell Mol. Biol.* **39**(2), 142-149.

155. Takacs, P., Kauma, S. W., Sholley, M. M., Walsh, S. W., Dinsmoor, M. J., and Green, K. (2001). Increased circulating lipid peroxides in severe preeclampsia activate NF-kappaB and upregulate ICAM-1 in vascular endothelial cells. *FASEB J* **15**(2), 279-281.

156. Talajic, M., DeRoode, M. R., and Nattel, S. (1987). Comparative electrophysiologic effects of intravenous amiodarone and desethylamiodarone in dogs: evidence for clinically relevant activity of the metabolite. *Circulation* **75**(1), 265-271.

157. Teoh, N., Field, J., Sutton, J., and Farrell, G. (2004). Dual role of tumor necrosis factor-alpha in hepatic ischemia-reperfusion injury: studies in tumor necrosis factor-alpha gene knockout mice. *Hepatology* **39**(2), 412-421.

158. Traber, M. G. (2007). Vitamin E regulatory mechanisms. *Annu. Rev. Nutr.* **27**, 347-362.

159. Trachootham, D., Lu, W., Ogasawara, M. A., Nilsa, R. D., and Huang, P. (2008). Redox regulation of cell survival. *Antioxid Redox Signal* **10**(8), 1343-1374.

160. Trivier, J. M., Libersa, C., Belloc, C., and Lhermitte, M. (1993). Amiodarone N-deethylation in human liver microsomes: involvement of cytochrome P450 3A enzymes (first report). *Life Sci* **52**(10), L91-L96.

161. Tukov, F. F., Luyendyk, J. P., Ganey, P. E., and Roth, R. A. (2007). The role of tumor necrosis factor alpha in lipopolysaccharide/ranitidine-induced inflammatory liver injury. *Toxicol. Sci.* **100**(1), 267-280.

162. Uetrecht, J. (2007). Idiosyncratic drug reactions: current understanding. *Annu. Rev. Pharmacol. Toxicol.* **47**, 513-539.

163. Vanhorebeek, I., De, V. R., Mesotten, D., Wouters, P. J., De Wolf-Peeters, C., and Van den, B. G. (2005). Protection of hepatocyte mitochondrial ultrastructure and function by strict blood glucose control with insulin in critically ill patients. *Lancet* **365**(9453), 53-59.

164. Varbiro, G., Toth, A., Tapodi, A., Veres, B., Sumegi, B., and Gallyas, F., Jr. (2003). Concentration dependent mitochondrial effect of amiodarone. *Biochem. Pharmacol.* **65**(7), 1115-1128.

165. Waldhauser, K. M., Torok, M., Ha, H. R., Thomet, U., Konrad, D., Brecht, K., Follath, F., and Krahenbuhl, S. (2006). Hepatocellular toxicity and pharmacological effect of amiodarone and amiodarone derivatives. *J. Pharmacol. Exp. Ther.* **319**(3), 1413-1423.

166. Walgren, J. L., Mitchell, M. D., and Thompson, D. C. (2005). Role of metabolism in drug-induced idiosyncratic hepatotoxicity. *Crit Rev Toxicol* **35**(4), 325-361.

167. Waring, J. F., Liguori, M. J., Luyendyk, J. P., Maddox, J. F., Ganey, P. E., Stachlewitz, R. F., North, C., Blomme, E. A., and Roth, R. A. (2006). Microarray analysis of lipopolysaccharide potentiation of trovafloxacin-induced liver injury in rats suggests a role for proinflammatory chemokines and neutrophils. *J. Pharmacol. Exp. Ther.* **316**(3), 1080-1087.

168. Willerson, J. T., and Ridker, P. M. (2004). Inflammation as a cardiovascular risk factor. *Circulation* **109**(21 Suppl 1), II2-10.

169. Wullaert, A., van, L. G., Heyninck, K., and Beyaert, R. (2007). Hepatic tumor necrosis factor signaling and nuclear factor-kappaB: effects on liver homeostasis and beyond. *Endocr. Rev.* **28**(4), 365-386.

170. Wyllie, A. H. (1980). Glucocorticoid-induced thymocyte apoptosis is associated with endogenous endonuclease activation. *Nature* **284**(5756), 555-556.

171. Yano, T., Itoh, Y., Yamada, M., Egashira, N., and Oishi, R. (2008). Combined treatment with L-carnitine and a pan-caspase inhibitor effectively reverses amiodarone-induced injury in cultured human lung epithelial cells. *Apoptosis.* **13**(4), 543-552.

172. Yee, S. B., Hanumegowda, U. M., Hotchkiss, J. A., Ganey, P. E., and Roth, R. A. (2003). Role of neutrophils in the synergistic liver injury from monocrotaline and bacterial lipopolysaccharide exposure. *Toxicol. Sci.* **72**(1), 43-56.

173. Yin, M., Wheeler, M. D., Kono, H., Bradford, B. U., Gallucci, R. M., Luster, M. I., and Thurman, R. G. (1999). Essential role of tumor necrosis factor alpha in alcohol-induced liver injury in mice. *Gastroenterology* **117**(4), 942-952.

174. Young, R. A., and Mehendale, H. M. (1989). Effects of short-term and long-term administration of amiodarone on hepatobiliary function in male rats. *J. Appl. Toxicol.* **9**(6), 407-412.

175. Zou, W., Beggs, K. M., Sparkenbaugh, E. M., Jones, A. D., Younis, H. S., Roth, R. A., and Ganey, P. E. (2009a). Sulindac metabolism and synergy with tumor necrosis factor-alpha in a drug-inflammation interaction model of idiosyncratic liver injury. *J. Pharmacol. Exp. Ther.* **331**(1), 114-121.

176. Zou, W., Devi, S. S., Sparkenbaugh, E., Younis, H. S., Roth, R. A., and Ganey, P. E. (2009b). Hepatotoxic interaction of sulindac with lipopolysaccharide: role of the hemostatic system. *Toxicol. Sci.* **108**(1), 184-193.

177. Zou, W., Roth, R. A., Younis, H. S., Malle, E., and Ganey, P. E. (2011). Neutrophil-cytokine interactions in a rat model of sulindac-induced idiosyncratic liver injury. *Toxicology* **290**(2-3), 278-285.